Blood-surface Interaction: Improving the Assessment of Blood Compatible Biomaterials to Mitigate the Intrinsic Pathway Activation

Kyunghoon Kim

A dissertation

submitted in partial fulfillment of the requirements for the degree of

Doctor of Philosophy

University of Washington

2024

Reading Committee:

Buddy D. Ratner, Chair

Lara J. Gamble

Hongxia Fu

Program Authorized to Offer Degree:

Bioengineering

University of Washington

Abstract

Blood-surface Interaction: Improving the Assessment of Blood Compatible Biomaterials to Mitigate the Intrinsic Pathway Activation

Kyunghoon Kim

Chair of the Supervisory Committee:

Buddy D. Ratner

Department of Bioengineering

Blood-compatible surfaces are essential for advancing blood-contacting medical devices to prevent complications, enhance therapeutic outcomes, and reduce post-care costs. This dissertation evaluates the blood compatibility of diverse polymer surfaces, including commercial fluoropolymers, plasma-polymerized fluoropolymers, medical polymers, and zwitterionic polymers. The primary scope of studies focuses on the intrinsic pathway of coagulation, which is a dominant thrombus formation mechanism in low-shear hemodynamic flow conditions. Through comprehensive assessment of Factor XII adsorption/activation, thrombin generation, and fibrin clot formation, we demonstrate that zwitterionic poly(carboxybetaine) copolymer surfaces exhibit superior blood compatibility, while plasma-polymerized hexafluoropropylene (ppC_3F_6) shows the second-best performance. These materials achieve their enhanced blood compatibility through distinct mechanisms: zwitterionic polymers prevent protein fouling through a strong hydration layer, particularly preventing Factor XII adsorption and subsequent activation, while ppC_3F_6 surfaces demonstrate unique protein tight-binding properties that promote stable albumin retention and reduce Factor XIIa activity. The ultralow protein fouling property of zwitterionic polymer

effectively prevents the initiation of the intrinsic coagulation pathway by creating a barrier against Factor XII adsorption and activation. Conversely, ppC_3F_6 exhibits remarkable protein tight-binding characteristics that maintain a stable albumin passivation layer resistant to displacement by larger thrombogenic proteins such as FXII or fibrinogen, while simultaneously reducing Factor XIIa activity through tight surface binding that diminishes the bioactivity of adsorbed Factor XII. These findings suggest two promising but mechanistically distinct approaches to achieving enhanced blood compatibility: prevention of protein adsorption through surface hydration, and protein tight binding that promotes beneficial interactions while minimizing thrombogenic responses.

Keywords*:* intrinsic pathway, blood compatibility, zwitterionic polymer, RFGD plasma-polymerized polymer, fluoropolymer, Factor XII, thrombin, fibrin clot

Dedicated to God in Heaven,

In honor of Major Young-Gul Kim

My beloved grandmother, Soon-bae Lee

All my family

Acknowledgements

First of all, I would like to thank God in heaven. I have no doubt that You always have my back and prepare the path of my life behind the scenes. Through faith, I am always confident and rigorous in everything I do. The vision You rooted in me during my time in the USA will guide the mission of my life.

I would like to express my deepest gratitude to my PhD advisor, Dr. Buddy Ratner. I am certain that no better mentor exists in this world. Your vision, not only as a scientist but as a human being who explores and enjoys the joys, adventures, and pursuits of happiness in life, has been an incredible inspiration to me. I deeply cherish our time in Kona playing guitar together—sharing a hobby with my advisor has been a tremendous blessing. I'll always be excited to join your summer and holiday parties, guitar in hand, ready to play.

I am also profoundly grateful to my committee members, Drs. Lara Gamble, Hongxia Fu, and Wendy Thomas. Your insightful advice has significantly enhanced my scientific perspective and improved the quality of my data and analyses. I consider myself incredibly fortunate to have had you on my committee. I have carefully recorded your comments and suggestions in a notebook, and they will undoubtedly shape my future studies. A special thanks to Dr. Shaoyi Jiang for his invaluable advice and mentorship during the early stages of my PhD journey.

To all past and present members of the Ratner Lab: Sharon, Winston, and Felix—thank you for your unwavering support throughout my PhD. Without your advice and assistance, I could not have completed this project. Runbang, David, Le, Lars, Marvin, Irini, Ian, Louis, and Xiaojie—your shared knowledge and expertise were immensely helpful, and the friendships we built over the years have meant so much to me. Julia and Prabhleen, thank you for being such wonderful labmates and friends. Your kindness and support were a constant source of comfort.

Sherry and Kan, I feel truly fortunate to have had you in my life. Our late-night conversations, covering everything from art, music, science, philosophy, and history to love and life itself, enriched my PhD experience in ways I never imagined. Thanks to you, I grew to love this city, Seattle, and I'll always treasure our memories in the beautiful state of Washington.

The "Dum Spiro Spero" spirit runs deep in my family. My grandfather, Major Young-Geol Kim, former CEO of Eastern Light, has been a powerful influence, inspiring me to move forward without hesitation. His life as a soldier and entrepreneur has served as a guiding example. Though he is in heaven now, I continue to feel his blessing and protection. My grandmother, Soon-Bae Lee, has been a driving force, pushing me to pursue higher achievements with relentless determination. Her love and care throughout my life have taught me the true meaning of love.

To my father, Dr. Seonghwan Kim, the first PhD in our family tree: you have instilled in me a sense of nobility and critical thinking. The values and life lessons you imparted during my childhood have become the foundation of my philosophy as a Christian, scholar, and scientist. You are my ultimate role model, the source of my passion and grit. To my mother, Mija, you are my greatest inspiration. Much of my character reflects yours, particularly our shared determination to

persevere and achieve what we believe is true, under God's guidance. Having parents with whom I can discuss anything is a tremendous blessing.

To my sister, I wish you all the happiness in the world. Your warmth and encouragement have been a great source of solace during my hardships. To my brother, I remember how we promised each other as kids to make our family great again. We've come so far, and now is the perfect time to move forward together.

I'd also like to thank my friends in the Korean community here in Seattle: Jaehyung, Justin, Yujung, Junghyun, Changho, Jooyoung, Namu, Yonghoon, Joonyong, Iris, Jongseob, and Yongtae. Your support and the many nights we spent discussing life, philosophy, happiness, vision, politics, and science have helped me grow immensely. You have been not only friends but also great teachers to me.

To my church community at CCS Adelpos, especially Nana, Michelle, Angie, Daniel, and Tiffany: thank you for being my fortress of faith and for praying for me. Your encouragement and fellowship strengthened my faith and gave me the resilience to endure tough times.

I cannot forget my dear friends, Soocheol and Seonghwan. Our daily chats have been a constant source of encouragement, even when we didn't discuss the challenges we faced. You are both friends I trust deeply and for life. Thank you for always being there for me.

To my musical friends—Robert, Alestair, Andy, Jim M, Jim P, Don, and Kelly: thank you for being part of such an incredible band. At the final stage of my PhD, our weekend performances at Park Lane Kirkland and Thruline Coffee were a true source of refreshment. Your guidance pushed me out of my comfort zone and helped me grow. I hope we can continue to make music together for years to come.

Finally, I would like to express my gratitude to Dr. Chris Neils, who greatly inspired me to refine my teaching philosophy and vision for guiding students. I also thank Flora (Fang-Hua) Hu and Tran Luu for being exceptional TAs when I was navigating the challenges of teaching ENGR115. Your support helped me elevate my class and teaching approach.

To Dr. Kyoung G. Lee and Dr. Tae Seok Seo, my academic mentors during my early research years: I deeply appreciate your enduring support and willingness to guide me in becoming a better researcher and scientist.

Two quotes that I like the most throughout my PhD will be a good ending of this acknowledgement:

"The cure to boredom is curiosity. There is no cure for curiosity"

by Dorothy Parker (was told by Buddy Ratner)

"There is no easy PhD. You can't be an exception"

by Dr. Seonghwan Kim

Contents

List of Figures

Supplementary Figures

List of Schemes

List of Tables

Chapter 1. Overview of Blood Compatible Biomaterials

This chapter will introduce the basic concepts and perspectives of blood compatibility, to provide an overview of several subjects that play key roles in all the studies conducted for this dissertation.

1.1. History of Blood Compatibility

Early Developments: Initial Concepts and Trial Phases

The exploration of blood compatibility began in earnest during the mid-20th century, coinciding with the advent of medical devices like artificial heart valves and dialysis machines. These early implementations were primarily constructed from metals such as stainless steel and polymers like polyurethane and polymethyl methacrylate [1]. While mechanically robust, these materials often provoked severe thrombotic events and immune responses when exposed to blood. Initial studies highlighted a critical gap: the understanding of the interactions between blood and material surfaces was insufficient.

The first decade of research centered around observational data that pointed to the rapid adsorption of plasma proteins as the initial event in blood-surface interaction[2], [3]. It was quickly established that fibrinogen, a key plasma protein, played a significant role in subsequent platelet adhesion and activation—a discovery that linked surface chemistry directly to thrombogenesis. However, these insights were rudimentary, and the mechanisms underlying protein-surface interactions remained elusive.

The 1960s-1970s: Laying the Foundation for Surface Interaction Studies

The 1960s marked a pivotal era where the correlation between surface wettability and protein adsorption began to take shape. Experiments revealed that hydrophobic surfaces tended to promote greater protein adsorption compared to hydrophilic ones. This understanding provided the groundwork for tailoring surface properties to mitigate thrombogenic reactions. By adjusting the balance between hydrophilic and hydrophobic moieties on the surface, researchers aimed to control protein adsorption profiles.

1980s: A Shift Toward Strategic Surface Modification

The 1980s heralded significant strides in the intentional design of blood-contacting surfaces. Numerous pioneering efforts pushed the boundaries by exploring how surface modification could be used to influence protein adsorption and subsequent cellular interactions. Techniques such as plasma polymerization and chemical grafting became tools of choice for altering surface properties while preserving the bulk characteristics of the underlying material.

These works emphasized that blood compatibility should not merely aim for biological inertness but should strategically promote controlled biological interactions. This shift in perspective was encapsulated in call for a "paradigm shift" in biomaterials science. There was an argue that many of the biomaterials used up until that point had been optimized through trial and error rather than designed to meet precise biological objectives.

1990s-2000s: Technological Advancements and In-depth Analysis

The advent of sophisticated surface analysis tools such as Electron Spectroscopy for Chemical Analysis (ESCA, XPS) and time-of-flight secondary ion mass spectrometry (TOF-SIMS) revolutionized the study of blood compatibility. These tools allowed researchers to quantify the

types and arrangements of molecules adsorbed to biomaterial surfaces, providing unprecedented insights into how specific surface chemistries influenced protein behavior and platelet interactions

During this period, the strategic introduction of hydrophilic and low-fouling polymers, such as polyethylene oxide (PEO), demonstrated how surface modifications could minimize nonspecific protein adsorption and reduce platelet adhesion. This was a critical step forward in developing surfaces that could sustain contact with blood without provoking thrombosis.

Modern Perspectives: Smart Surfaces and Future Directions

Entering the 21st century, the concept of blood compatibility evolved further to include smart and responsive surfaces that could adapt to physiological conditions. Materials such as poly(N-isopropylacrylamide) (pNIPAM), which exhibit temperature-sensitive changes in hydrophobicity and hydrophilicity, emerged as practical solutions for controlling protein adsorption and cellular responses.

The deeper integration of molecular-scale design principles has set the stage for contemporary and future biomaterials that not only mitigate unwanted reactions but actively foster desired biological outcomes. The focus has expanded from merely preventing thrombosis to fine-tuning interactions with immune cells, particularly macrophages, to control inflammation and promote healing.

The history of blood compatibility is a testament to the journey from empirical experimentation to the precise engineering of material surfaces. With continuous advances in analytical tools and a nuanced understanding of biological responses, future blood-contacting biomaterials are poised to provide more predictable, tailored outcomes in medical applications.

1.2. Blood Compatibility: Where We Are

The progression of blood compatibility research in our group traces a rich lineage from Dr. Allan Hoffman's pioneering work on Dacron Grafts [4], [5] (**Figure 1**) through Dr. Buddy Ratner's contributions [6], [7], [8], [9] to our present investigations. Despite more than five decades of intensive research efforts, three fundamental challenges persist in the field. First, we lack universal consensus on blood compatibility criteria due to the complex nature of blood-material interactions. Second, truly ideal blood-compatible biomaterials remain elusive, with even the most advanced materials showing limitations in long-term applications. Third, standardized comprehensive testing protocols have yet to be established, making cross-study comparisons challenging.

The ongoing debate over optimal surface properties particularly illustrates these challenges, especially regarding hydrophobic versus hydrophilic surfaces. Each surface type demonstrates distinct advantages through different mechanisms: hydrophilic surfaces generate protective hydration layers that physically prevent protein and cell adhesion through thermodynamic and kinetic barriers. In contrast, hydrophobic surfaces, particularly fluorinated ones, demonstrate improved compatibility through low surface energy and selective protein binding that can promote beneficial protein conformations while reducing thrombogenic responses. This dichotomy in surface properties highlights the complexity of blood-material interactions and suggests that multiple strategies may be necessary for different medical applications. The success of fluorinated surfaces, despite their hydrophobic nature, particularly challenges conventional wisdom about surface-blood interactions and emphasizes the need for deeper understanding of underlying molecular mechanisms.

1.3. Blood Coagulation Cascades

The blood coagulation cascade [10], [11], [12], [13]represents a complex and finely balanced system designed to prevent blood loss while maintaining fluidity in the vasculature. This cascade involves a network of enzymatic reactions that result in the formation of a stable fibrin clot at the site of vascular injury. It is a key element in hemostasis, integrating multiple pathways that are activated under specific physiological or pathological conditions. Understanding the nuances of these cascades is critical for designing biomaterials that interact safely with blood.

Overview of Coagulation Pathways

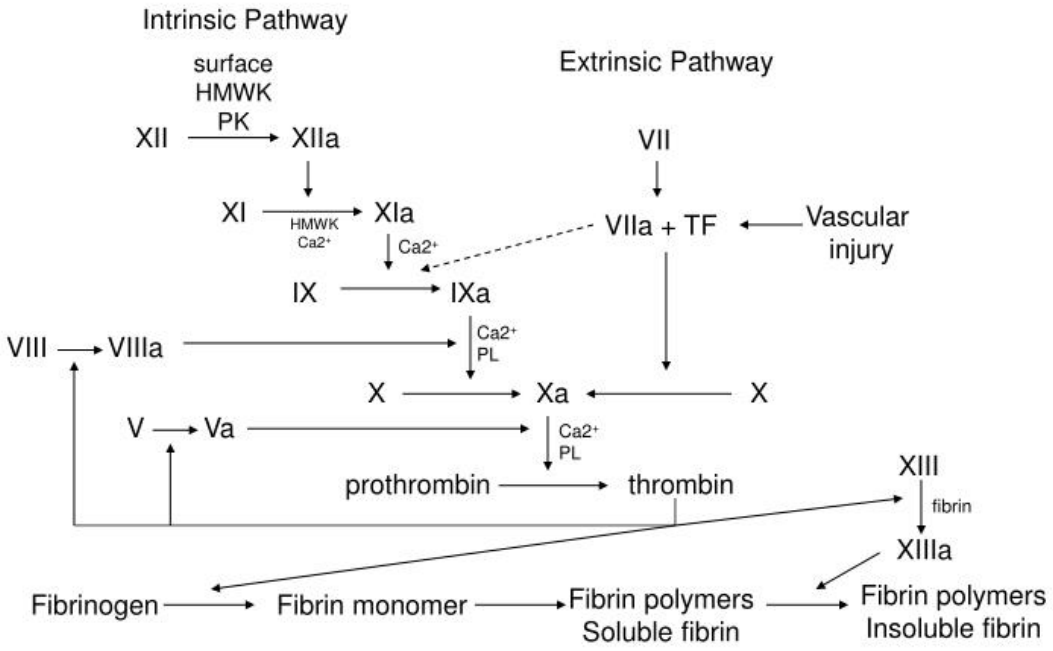

Scheme 1. Blood Coagulation Pathway Schemes

(**Scheme 1**) The coagulation process is traditionally divided into three interconnected pathways: the intrinsic, extrinsic, and common pathways. Each pathway plays a distinct role in amplifying the coagulation response, and their convergence ultimately results in the transformation of soluble fibrinogen into an insoluble fibrin mesh, forming the structural basis of a clot.

Intrinsic Pathway

Intrinsic pathway, also known as the contact activation pathway, is triggered by damage to the endothelial surface or the exposure of blood to negatively charged surfaces[11], [14], [15], [16], [17], [18]. The intrinsic pathway begins with the activation of Factor XII (FXII, Hageman factor), which sequentially activates Factor XI, IX, and, in conjunction with Factor VIIIa, Factor X. The significance of this pathway in blood-material interactions is profound, as the initial activation can occur due to direct contact with foreign materials. The primary scope of this dissertation is focused on this intrinsic pathway activation.

Extrinsic Pathway

The extrinsic pathway[19], or tissue factor pathway, is initiated by tissue factor (TF), a protein exposed when vascular integrity is compromised. TF forms a complex with Factor VIIa, rapidly activating Factor X. This pathway is responsible for the initial and rapid response to tissue injury, setting off a chain reaction that boosts thrombin generation.

Common Pathway

Both the intrinsic and extrinsic pathways converge at the activation of Factor X. Once activated, Factor Xa forms a complex with Factor Va and calcium ions, converting prothrombin to thrombin. Thrombin acts as a key enzyme that catalyzes the conversion of fibrinogen to fibrin monomers, which are then cross-linked by Factor XIIIa to form a stable clot.

The Role of Thrombin and Its Regulation

Thrombin[20], [21] is the central enzyme in the coagulation cascade, playing a dual role as both a pro-coagulant and an anticoagulant. While its primary function is to convert fibrinogen to fibrin,

thrombin also activates platelets, amplifies the cascade by feedback activation of Factors V, VIII, and XI, and interacts with regulatory proteins such as thrombomodulin to modulate its activity.

Regulatory mechanisms are vital to maintain balance in coagulation and prevent pathologies such as excessive clotting (thrombosis) or uncontrolled bleeding (hemorrhage). Antithrombin III and protein C are key inhibitors in this system; antithrombin III neutralizes thrombin and other serine proteases, while protein C, when activated by thrombin-thrombomodulin complex, inactivates Factors Va and VIIIa.

Intrinsic Pathway Activation by Biomaterials

When blood encounters artificial surfaces, particularly those that lack endothelial properties, the intrinsic pathway can be triggered. The exposure of blood to biomaterial surfaces often results in the adsorption of plasma proteins, such as fibrinogen and high-molecular-weight kininogen, which facilitate the activation of Factor XII[22], [23], [24]. This process, if unregulated, can lead to unwanted thrombosis and limit the use of certain biomaterials.

There has been emphasis that the chemical composition and surface properties of biomaterials—such as hydrophilicity, charge, and roughness—play crucial roles in how they interact with blood. Surface modifications, such as incorporating hydrophilic or zwitterionic coatings, have been shown to reduce protein adsorption and subsequent Factor XII activation, thereby mitigating the intrinsic pathway's contribution to thrombogenesis.

Clinical and Biomaterial Implications

Understanding the coagulation cascades in detail is imperative for the development of blood-contacting medical devices. Devices such as vascular grafts, stents, and extracorporeal circuits need to be designed with consideration for minimizing unintended coagulation pathway activation

. Recent advancements in biomaterial science have focused on surface engineering that mimics endothelial cell functionality, incorporating anticoagulant molecules like heparin or designing non-thrombogenic polymer layers.

For instance, plasma treatments and polymer grafting techniques have been explored to enhance the blood compatibility of materials by reducing protein adsorption and platelet adhesion. Moreover, smart biomaterials that respond to environmental changes, such as pH or temperature, are being investigated as potential solutions for dynamic regulation of coagulation activity.

To summarize, the blood coagulation cascade is a multifaceted system that ensures hemostasis but poses challenges when it interacts with artificial surfaces. Innovations in biomaterial design and a deeper understanding of the molecular mechanisms involved in coagulation have paved the way for developing surfaces that minimize undesired activation of coagulation pathways. Moving forward, interdisciplinary approaches that incorporate molecular biology, surface chemistry, and hemostasis research are essential for advancing blood-compatible biomaterials that meet the high standards of clinical safety and efficacy.

Remarks: Center for Dialysis Innovation (CDI)

In 2017, as the collective effort between University of Washington School of Medicine and College of Engineering, the Center for Dialysis Innovation (CDI) was found to serve as a central research hub for scientists, engineers, and clinicians dedicated to bringing up the innovative solution for the end-stage renal disease (ESRD) patients who are under hemodialysis treatment. It aimed to embody a multidisciplinary approach to revolutionize dialysis technology and patient care. Its

mission is to go beyond incremental improvements and reimagine dialysis technology to substantially enhance patients' quality of life while improving clinical outcomes. This ambition reflects a deep commitment to cutting-edge research that integrates biomedical engineering, nephrology, materials science, and patient advocacy.

The University of Washington holds a distinguished place in medical history as the birthplace of long-term dialysis. Since the 1960s, Seattle has been a focal point for groundbreaking efforts in renal care, marked by collaborative initiatives that brought together nephrologists, engineers, and researchers to pioneer chronic dialysis treatments. These early efforts laid the foundation for continuous advancements in the field and cemented UW's role as a leader in nephrology and medical innovation.

The establishment of CDI was a natural extension of this legacy. Recognizing that while existing dialysis technology had greatly extended the lives of patients, the associated health risks, complications, and reduced quality of life called for a transformative approach, UW founded CDI to focus on holistic and patient-centric innovations. The center embodies the ethos of UW's collaborative spirit and commitment to pushing the boundaries of medical research.

Key Research Focuses and Innovations

The research conducted at CDI spans various domains, all aimed at developing next-generation dialysis solutions. Key areas of focus include:

Development of Blood compatible Surfaces: Investigating advanced materials that minimize blood-material interactions is essential for reducing clotting and infection rates in dialysis systems. This involves creating innovative coatings and modifying surfaces to improve blood compatibility and device lifespan.

Portable and Wearable Dialysis Devices: CDI aims to reduce the burden on patients by developing more portable dialysis options, including wearable devices that provide continuous, lower-intensity dialysis, closely mimicking natural kidney function.

Dialyzer Membrane Innovations: The center explores novel membrane technologies to enhance solute clearance while maintaining high biocompatibility. This research seeks to optimize the selective permeability of membranes, improving the efficiency of waste removal.

Artificial Kidney Prototypes: One of CDI's most ambitious projects involves the development of an artificial kidney. This device integrates advanced filtration technology and bioengineered components to offer a long-term, implantable solution that reduces reliance on external dialysis equipment.

Collaborative Efforts and Multidisciplinary Approach

The CDI exemplifies a collaborative research model that harnesses expertise from nephrology, chemical engineering, biochemistry, and materials science. This multidisciplinary approach enables comprehensive problem-solving and the incorporation of cutting-edge techniques such as nanotechnology and advanced polymer science.

The roots of such collaboration date back to the 1960s, when UW teams first came together to tackle the challenges of chronic kidney disease. This tradition continues at CDI, which fosters partnerships not only within UW but also with national and international research centers, creating a global network aimed at accelerating discovery and innovation.

Efforts Toward Patient-Centered Innovation

Central to CDI’s philosophy is a patient-first approach. The center actively engages with dialysis patients and healthcare providers to gather feedback and input that guide research directions. This ensures that developed technologies not only meet clinical objectives but also align with patients' real-world needs and preferences.

Outreach initiatives, including educational programs and public seminars, raise awareness of kidney disease and inform the community about emerging dialysis technologies. These efforts bridge the gap between research, clinical implementation, and patient experience, reinforcing the center’s commitment to comprehensive care.

To summarize, the Center for Dialysis Innovation at the University of Washington is a testament to the university’s longstanding leadership in renal research. Building upon UW’s historic role as the birthplace of long-term dialysis and its decades of dedicated work since the 1960s, CDI continues this legacy through its commitment to transformative research aimed at improving patient outcomes. By integrating multidisciplinary expertise and fostering a patient-centered approach, CDI is poised to redefine dialysis care and offer hope for a better quality of life for individuals with ESRD.

1.4. Blood Protein Adsorption and the Vroman Effect

Blood protein adsorption to biomaterial surfaces is an essential determinant of subsequent biological responses, including platelet adhesion, activation of coagulation pathways, and immune reactions. This initial interaction is rapid and dynamic, setting the stage for a cascade of cellular and molecular events that can lead to thrombosis or biocompatibility. Central to understanding these interactions is the Vroman effect, which describes the competitive adsorption of plasma

proteins over time. Among the significant players in this process is Factor XII, a key protein in initiating the intrinsic pathway of coagulation.

The Initial Phase of Protein Adsorption

When blood contacts a biomaterial surface, proteins rapidly adsorb due to differences in surface energy, hydrophilicity/hydrophobicity, charge, and topography. This initial layer of adsorbed proteins serves as a dynamic interface that mediates cellular and molecular interactions. Key proteins include fibrinogen, albumin, high-molecular-weight kininogen, and Factor XII.

Factor XII, or Hageman factor, is particularly noteworthy because its activation on negatively charged or hydrophobic surfaces can trigger the intrinsic pathway of coagulation. Upon contact with a surface, Factor XII undergoes conformational changes that lead to its autoactivation. This activation sets off a chain reaction involving Factor XI, Factor IX, and subsequent clotting factors, culminating in the generation of thrombin and the formation of a fibrin clot.

Mechanisms Underlying Protein Adsorption

The adsorption of proteins is influenced by their molecular structure, surface chemistry, and interaction forces such as electrostatic interactions, hydrogen bonding, and van der Waals forces. Upon binding to a surface, proteins like fibrinogen and Factor XII may undergo conformational changes that expose reactive sites. For example, Factor XII's interaction with hydrophobic or charged surfaces can enhance its activation, leading to a pro-coagulant state.

The Vroman Effect: Competitive Adsorption Dynamics

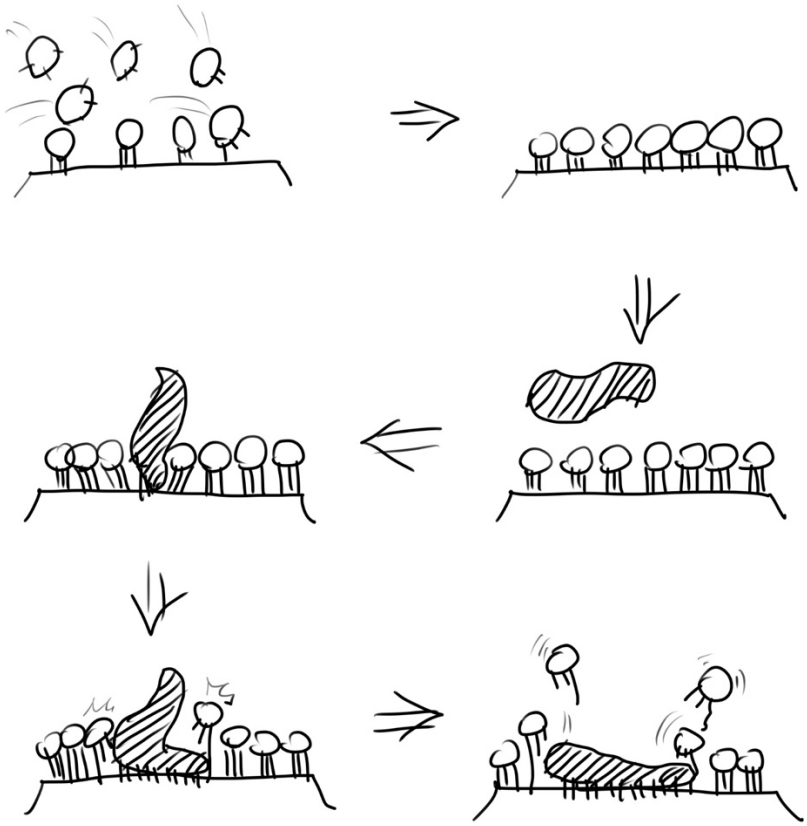

Scheme 2. The illustration of Vroman Effect*. Along with the order guided by arrows, small protein with higher mobility arrives at the surface earlier, then form a layer. Later, larger protein arrives and displaces the already-adsorbed proteins by forming higher number of bindings, and more surface-protein interactions.*

Leo Vroman's studies [25], [26] in the 1960s shed light on the competitive nature of protein adsorption over time. The Vroman effect (**Scheme 2**) describes how proteins with high plasma concentrations and low molecular weights, such as albumin, initially dominate the adsorption process due to their rapid diffusion[25], [26], [27], [28]. However, over time, these proteins are displaced by others with greater surface affinities but lower diffusion rates, such as higher-molecular-weight proteins like Factor XII and fibrinogen.

This temporal hierarchy is significant in understanding blood-material interactions. While albumin adsorption may initially provide a passivating layer[29], [30], [31], [32], [33], [34], [35], [36], [37],

the displacement by fibrinogen and Factor XII can lead to pro-thrombogenic outcomes. Factor XII's activation is particularly relevant as it serves as a trigger for the intrinsic pathway, which can amplify the coagulation response when blood interacts with artificial surfaces.

Factors Influencing the Vroman Effect and Factor XII Activation

Several properties of biomaterials affect the sequence and stability of protein adsorption, including the following:

Surface Energy and Chemistry: High-energy surfaces tend to initially attract proteins more readily. However, as equilibrium is approached, proteins like Factor XII with higher affinities for charged or rough surfaces may displace others.

Surface Hydrophilicity/Hydrophobicity: Hydrophobic surfaces tend to promote the adsorption of fibrinogen and Factor XII, whereas hydrophilic surfaces may favor non-thrombogenic proteins like albumin.

Surface Modifications: Engineering surfaces with hydrophilic or zwitterionic coatings can inhibit the adsorption and subsequent activation of pro-coagulant proteins such as Factor XII. Coatings like polyethylene glycol (PEG) create a hydration barrier that resists protein interaction and minimizes the Vroman effect.

Clinical and Design Implications

A comprehensive understanding of the Vroman effect and the activation of Factor XII is vital for designing blood-compatible biomaterials. Surfaces that promote stable adsorption of passivating proteins like albumin and minimize the displacement by fibrinogen and Factor XII are key to

reducing thrombotic risks. Moreover, developing surfaces that mimic endothelial cell properties, such as heparin-like molecules or negatively charged groups, can modulate the activation of Factor XII and maintain a non-thrombogenic state.

The strategic engineering of biomaterials to control protein adsorption and minimize unwanted activation of coagulation factors, including Factor XII, continues to be a focus in biomaterial research. Smart coatings and surface treatments that dynamically respond to physiological conditions show promise in achieving this goal.

To summarize, protein adsorption and the competitive dynamics explained by the Vroman effect, including the role of Factor XII activation, are critical in determining the blood compatibility of biomaterials. Understanding and modulating these interactions through surface chemistry and engineering can lead to improved blood-contacting devices with minimized thrombotic risks. This insight forms the basis for ongoing innovation in creating safer, more effective biomaterials.

1.5. Promising Biomaterials for Blood-contacting Surface: Fluoropolymer and Zwitterionic Polymer

The design of blood-contacting surfaces that minimize thrombogenicity and prevent undesirable biological responses has been a cornerstone of biomaterials research[11], [38], [39], [40]. In recent years, significant attention has been directed towards developing materials that reduce protein adsorption, platelet activation, and subsequent thrombus formation. Among these, fluoropolymers and zwitterionic polymers have emerged as promising candidates due to their unique surface properties and biocompatibility.

1.5.1. Fluoropolymers: Unique Properties and Applications

Fluoropolymers, such as polytetrafluoroethylene (PTFE) and polyvinylidene fluoride (PVDF), are synthetic polymers characterized by their carbon-fluorine bonds, which confer exceptional chemical resistance, low surface energy, and hydrophobicity. The inherent properties of fluoropolymers make them attractive for use in blood-contacting applications.

Mechanisms of Blood Compatibility

Low Surface Energy: The low surface energy of fluoropolymers leads to minimal protein adsorption. This property reduces the initial interaction between blood proteins and the surface, which is essential for preventing subsequent platelet adhesion and activation.

Non-stick Properties: The hydrophobic nature of fluoropolymers discourages protein unfolding, a phenomenon that can expose hidden binding sites, such as those in fibrinogen, that promote platelet activation.

Despite their advantages, fluoropolymers can sometimes promote nonspecific adsorption of certain proteins, which may limit their application without further surface modification. Strategies such as plasma treatment and the addition of hydrophilic coatings have been employed to enhance their blood compatibility.

Applications in Medical Devices: Fluoropolymers are widely used in vascular grafts, catheters, and blood filtration devices due to their stability and low reactivity. Coatings based on PTFE are particularly noted for reducing friction and maintaining smooth blood flow in cardiovascular applications.

1.5.2. Zwitterionic Polymers: Biomimetic and Anti-fouling Surfaces

Zwitterionic polymers represent a newer class of biomaterials that mimic the zwitterionic nature of cell membranes, presenting both positive and negative charges in close proximity. This structure leads to highly hydrated surfaces, which resist protein adsorption through strong electrostatic and hydration interactions.

Mechanisms of Blood Compatibility:

Hydration Layer: Zwitterionic surfaces create a dense, tightly bound layer of water molecules. This hydration layer acts as a physical and energetic barrier, preventing protein adsorption and cellular interactions.

Charge Neutrality: The presence of both positive and negative charges creates a net neutral surface that mimics the phosphatidylcholine head groups in cell membranes. This structural mimicry minimizes undesirable protein-surface interactions.

Representative zwitterionic polymers & Applications

Poly(carboxybetaine) (pCB) and Poly(sulfobetaine) (pSB) have emerged as leading zwitterionic polymers, demonstrating superior resistance to protein fouling in both in vitro and in vivo studies. This exceptional performance establishes them as ideal candidates for blood-contacting applications, and they form the focus of blood compatibility studies in this dissertation. In medical device applications, zwitterionic polymers are increasingly being implemented in catheters, stents, and extracorporeal circulation devices. Their ability to maintain non-thrombogenic surfaces has significantly enhanced device performance and safety profiles. Recent advances have expanded

their application to microfluidic devices and biosensors, where precise control over blood interactions is critical.

Comparative Advantages and Challenges

Both fluoropolymers and zwitterionic polymers offer distinct benefits and limitations. Fluoropolymers excel in durability, chemical resistance, and low friction, making them particularly suitable for long-term implants. However, their hydrophobic nature can occasionally trigger protein adsorption. Conversely, zwitterionic polymers provide exceptional anti-fouling properties through their hydration capacity but may lack the mechanical strength required for certain high-load applications.

Future Directions and Summary

Current research focuses on developing hybrid materials that combine the robust mechanical properties of fluoropolymers with the biocompatible and anti-fouling characteristics of zwitterionic polymers. Surface engineering techniques, including plasma-assisted deposition and graft polymerization, are being employed to create multifunctional coatings that leverage the strengths of both material types. These advances in fluoropolymer and zwitterionic polymer technology represent significant progress in blood-contacting biomaterial design, offering distinct pathways to mitigate thrombogenicity and enhance medical device performance.

1.6. Radio Frequency Glow Discharge (RFGD) Plasma Deposition

The field of blood-compatible surface engineering has significantly benefited from advances in surface modification technologies, with radio frequency glow discharge plasma deposition emerging as a pivotal method. This technique provides reliable and versatile surface modification of biomaterials, enhancing their suitability for blood-contacting applications. The significance of RFGD plasma deposition extends from its fundamental principles through its historical development to its unique properties, particularly in modifying fluoropolymers and hydrophilic polymers like hydroxyethyl methacrylate (HEMA).

Our group's early research demonstrated the effectiveness of RFGD plasma-deposited fluoropolymer coatings (**Figure 1**) [5]. Notably, Dacron grafts modified with RFGD plasma deposition showed exceptional performance in baboon shunt models, while untreated Dacron grafts exhibited significant surface thrombus formation. This pioneering work established the foundation for subsequent developments in plasma-based surface modification strategies.

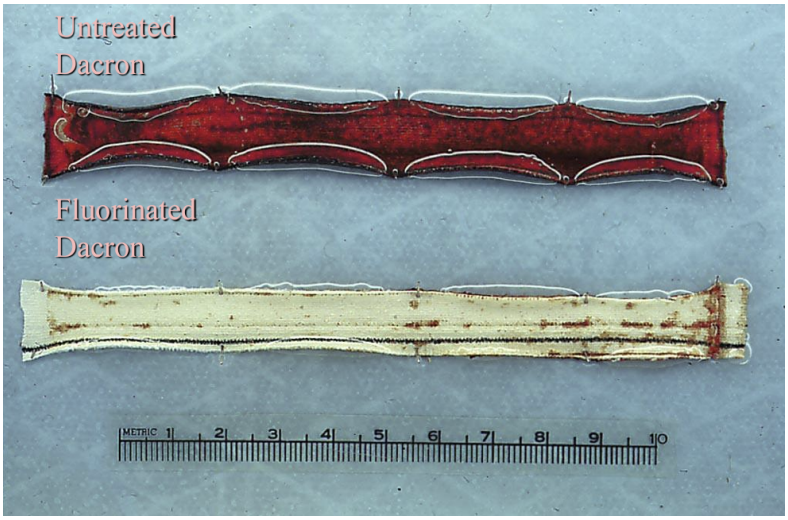

Figure 1. Comparison of two Dacron vascular graft recovered from baboon study. *Top: untreated Dacron graft. Bottom: RFGD fluorinated Dacron graft[5]*

Principles of RFGD Plasma Deposition

RFGD plasma deposition involves generating a plasma by applying a radio frequency (RF) electric field to a low-pressure gas. This plasma consists of a mix of ions, radicals, electrons, and neutral species. These reactive particles interact with the substrate, enabling chemical reactions that result in a thin film being deposited. The process can modify the surface without altering the bulk properties of the material, making it ideal for biomedical applications.

Mechanics of Deposition

Ionization and Excitation: RF energy accelerates electrons, causing collisions that ionize gas molecules and create reactive species.

Film Formation: These species polymerize on the substrate, creating a uniform, conformal coating that can incorporate various functional groups.

History of RFGD Plasma Deposition in the Medical Device Industry

The use of RFGD plasma deposition in surface modification dates to the 1960s and 1970s when it was first employed in the electronics industry for coating and etching[41], [42], [43], [44], [45]. By the late 20th century, it gained prominence in the medical field as a method to modify biomaterials to improve blood compatibility and reduce fouling. Early pioneers, including Buddy D. Ratner, recognized its potential for altering surface chemistry to influence protein adsorption and cellular interactions.

The transition from basic coatings to advanced, functional surfaces was driven by the need to mitigate issues such as thrombosis and immune reactions. RFGD plasma deposition proved to be

a reliable method for creating anti-thrombogenic and biocompatible surfaces on various substrates, including polymers and metals.

Unique Properties of RFGD Plasma-Deposited Surfaces and Their Advantages

RFGD plasma deposition offers several distinct properties and benefits. First, the technique produces coatings that adhere uniformly to complex geometries without compromising the underlying bulk properties. Second, it supports the deposition of a wide range of chemistries, from hydrophilic to hydrophobic, and allows the incorporation of functional groups. These attributes make RFGD plasma deposition especially useful for enhancing the performance of blood-contacting medical devices.

RFGD Plasma-Deposited Fluoropolymer Surfaces

Fluoropolymers deposited via RFGD plasma are valued for their low surface energy and chemical inertness. Plasma deposition allows these materials to maintain their inherent non-stick properties while introducing subtle surface modifications that enhance blood compatibility. Such coatings are known to limit protein unfolding and subsequent platelet activation, making them highly effective for use in vascular grafts, stents, and catheters. Fluoropolymer coating offers long-term durability and low friction, ideal for high-performance medical devices. Plasma deposition allows these coatings to incorporate additional functionality without altering the bulk material.

To summarize, RFGD plasma deposition has proven critical for enhancing biomaterial surface interactions with blood. The technique's ability to create uniform, functional films on complex substrates has secured its position in medical device development. While plasma-deposited HEMA coatings provide hydration and biocompatibility [46], [47], [48], fluoropolymer coatings contribute low surface energy and resistance to protein adsorption. The enduring relevance of RFGD plasma deposition stems from its adaptability, cost-effectiveness, and proven reliability in creating blood-compatible surfaces for diverse biomedical applications[31], [49], [50], [51], [52], [53] .

1.7. Hypotheses

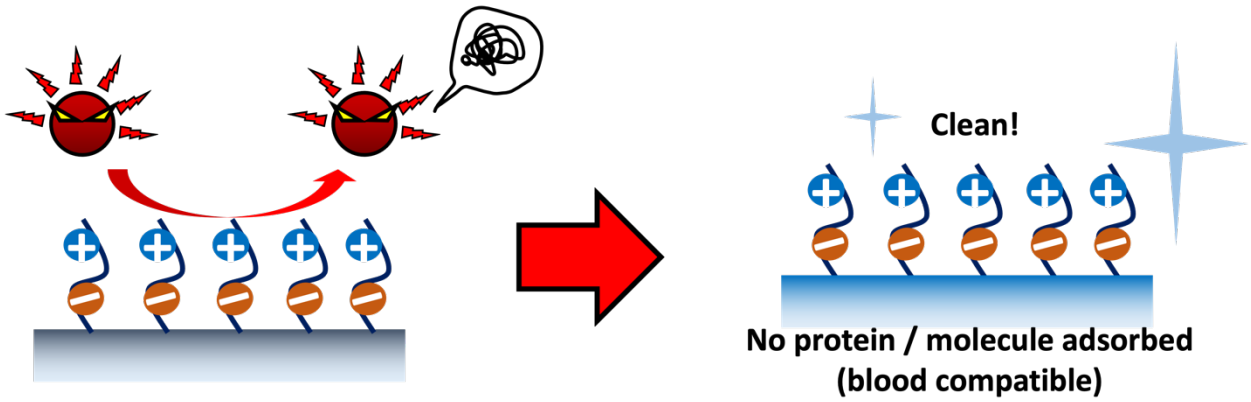

Scheme 3. ***Illustration of hypothesis 1***. *The zwitterionic polymer surface repels all the protein/cell adhesion, which promotes 'cleanliness' of surface without any unwanted and nonspecific interaction between surface-blood.*

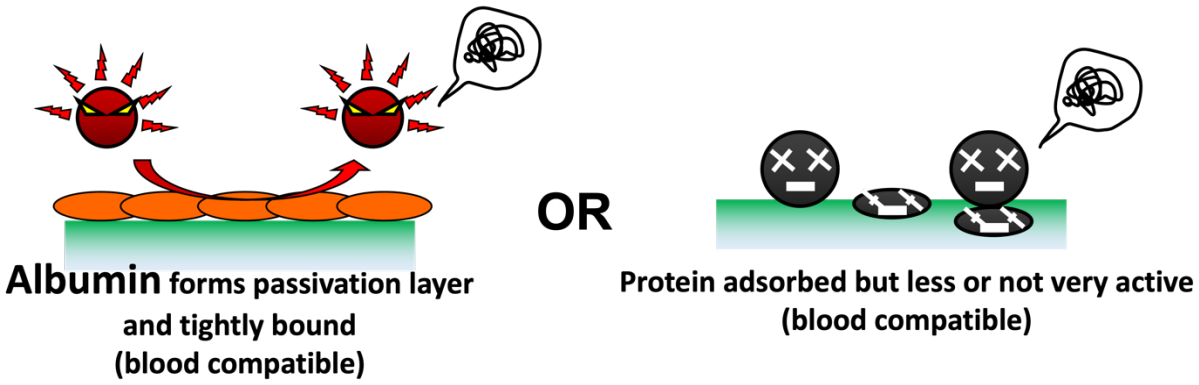

Scheme 4. ***Illustration of hypothesis 2***. *Albumin tight-binding forms passivation layer to prevent the unwanted protein adsorption, or the tight binding inactivates the activity of thrombogenic protein*

The primary scope and hypotheses of this dissertation address two key aspects: First, we examine how protein antifouling properties of zwitterionic polymers may enhance surface blood compatibility by preventing Factor XII protein fouling that triggers intrinsic pathway activation (**Scheme 3**). Second, we investigate how protein tight-binding may improve blood compatibility through an alternative mechanism – namely, how albumin tight binding forms a passivation layer to prevent unwanted protein-surface interactions, or how increased binding tightness affects protein activity at the surface (**Scheme 4**). Through these investigations, we aim to demonstrate how protein antifouling, tight-binding induced inactivation, and albumin-preferential binding can prevent the cascade of protein-protein interactions that trigger coagulation. We anticipate superior performance from zwitterionic polymer surfaces, while the second hypothesis may be validated through the unique protein-surface interactions observed with ppC_3F_6 surfaces.

Chapter 2. Materials Preparation

2.1. Methods

2.1.1. Preparation of commercial polymeric surfaces

Surface	Preparation	Condition	Concentration	ETC
PE	Extract from bulk PTFE film	-	-	-
PTFE	Extract from bulk PTFE film	-	-	-
PVDF	Spin casting	2500 rpm	2.3 wt% in DMF	Dry under N2
PVDF-HFP	Spin casting	2500 rpm	2.6 wt% in DMF	Dry under N2
ppC_3F_6-1	RFGD	20 min, in-glow	10.1 sccm HFP	Stored in Ar
ppC_3F_6-2	RFGD	40 min, downstream	10.1 sccm HFP	Stored in Ar
ppC_3F_6-3	RFGD	180 min, downstream	10.1 sccm HFP	Stored in Ar
pCBAA	UV crosslinking	-	5 wt% in DI water	Dry in fume hood
PU	Spin casting	2500 rpm	1 wt% in DMF	Dry under N2
PVC	Spin casting	2500 rpm	3 wt% in DMF	Dry under N2
PSf	Spin casting	2500 rpm	4 wt% in DMF	Dry under N2
PC	Spin casting	2500 rpm	3 wt% in DCM	Dry under N2
PS	Spin casting	2500 rpm	1 wt% in DMSO	Dry under N2

Table 1. Overview of all the surfaces' preparation and conditions used in the studies

Table 1 presents the biomaterial surfaces evaluated in this dissertation. Sample preparation proceeded as follows: The NIH-manufactured high-quality polyethylene (PE) was used as a reference material. A 8 mm (for radiolabeled protein adsorption assay) and 15 mm (for any other blood compatibility assays discussed in this dissertation) disc-shaped samples were extracted by using biopsy punch from the thin bulk film of PE sheets. Polyurethane (PU), polycarbonate (PC),

polysulfone (PSf), poly(vinyl)chloride (PVC) were prepared by dissolving commercial products of each polymer into methylene chloride. PU tubing, PC lab plasticware, PSf pellet (sigma-aldrich), and PVC tubing were dissolved in methylene chloride with the 2.5 wt% of concentration, sonicated for 30 min, and heated for 2 hours at 80C. After being dissolved, 200 ul of each polymer solution were dropped onto the 8 mm and 15 mm glass coverslips (ProSciTech), spin casted at 2500 RPM for 30 seconds, dried under nitrogen atmosphere overnight. The spin-casted polymer was coated on both sides of glass coverslip. Poly(vinylidene)fluoride (PVDF), and poly(vinylidene)fluoride-hexafluoropropylene copolymer (PVDF-HFP) (both purchased from Sigma-Aldrich) pellets were dissolved in dimethylformamide (DMF) by 2.3 wt% and 2.6 wt%, respectively. Identical to the organic commercial controls, the 200 ul of each polymer solution was dropped onto the glass coverslips, and spin casted both sides at 2500 RPM for 30 seconds, dried under nitrogen atmosphere overnight. Skived polytetrafluoroethylene (PTFE) bulk film was purchased from ePlastics (San Diego, CA, United States), and 8 mm and 15 mm disc-shaped samples were extracted by using biopsy punch from the bulk film.

2.1.2. Preparation of RFGD plasma polymerized surfaces

ppC_3F_6 surfaces were prepared with the custom-built plasma reactor (**Figure 2**) using radio frequency glow discharge (RFGD) plasma deposition, modified from previous studies [49], [50], [54], [55], [56], [57], [58], with varying conditions. Before plasma polymerization, a Pyrex glass reactor was cleaned by air etching for 2 hours at a power of 40W and in-reactor pressure of 300 mTorr. All the samples were cleaned prior to being loaded into the reactor. Samples were loaded at the in-glow and downstream positions (**Scheme 5**), and a vacuum was applied. Loaded samples

were etched first with Ar with a pressure of 150 mTorr, gas supply rate of 62.1 cm, and the power of 40W (forward) and 3W (reverse) for 5 minutes to activate the surface for the following deposition steps. Methane adhesion layer deposition was followed by a pressure of 200 mTorr, a gas supply rate of 3.0 cm, and a power of 120W (forward) and 5W (reverse) for 5 minutes. Hexafluoropropylene (C_3F_6) (PCR, Gainesville, FL) adhesion layer deposition was carried out with the pressure of 150 mTorr, gas supply rate of 10.1 sccm, and the power of 60W (forward) and 3W (reverse), for 1 minute. Characteristic C3F6 surface deposition was performed with the pressure of 150 mTorr, gas supply rate of 10.1 sccm, and the power of 20W (forward) and 3W (reverse), for 1) 20 minutes in the glow, 2) 60 minutes at the downstream, and 3) 180 minutes at the downstream. All the samples were sealed with a nitrogen atmosphere.

Scheme 5 is an illustration of how the RFGD plasma-polymerized surface is created. The monomer HFP gas molecule is ionized by plasma, generating reactive C-Fx species. The generated reactive species are being reacted randomly, creates a deposited layer on the substrate surface. The functional group exposed could be highly varied depending on the condition—location and deposition time this case—but the fixed condition generates consistent surface chemistries proven by ESCA analysis.

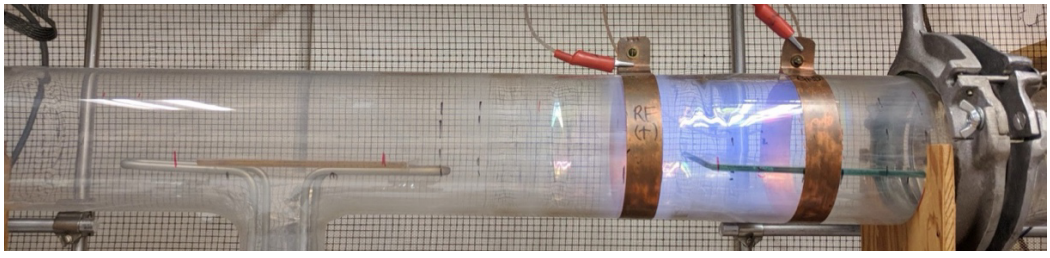

***Figure 2**. Picture of our group's custom-built RFGD plasma deposition reactor. Monomer inflow feeding is from right to left*

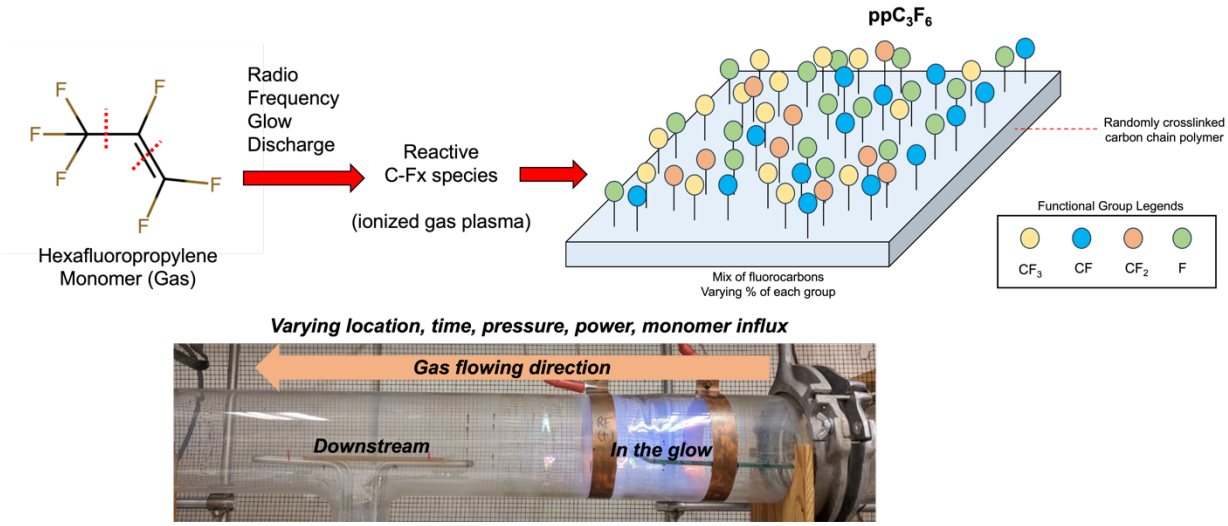

Scheme 5. *The description of RFGD plasma polymerization process and the reactor*

2.1.3. Preparation of zwitterionic surfaces

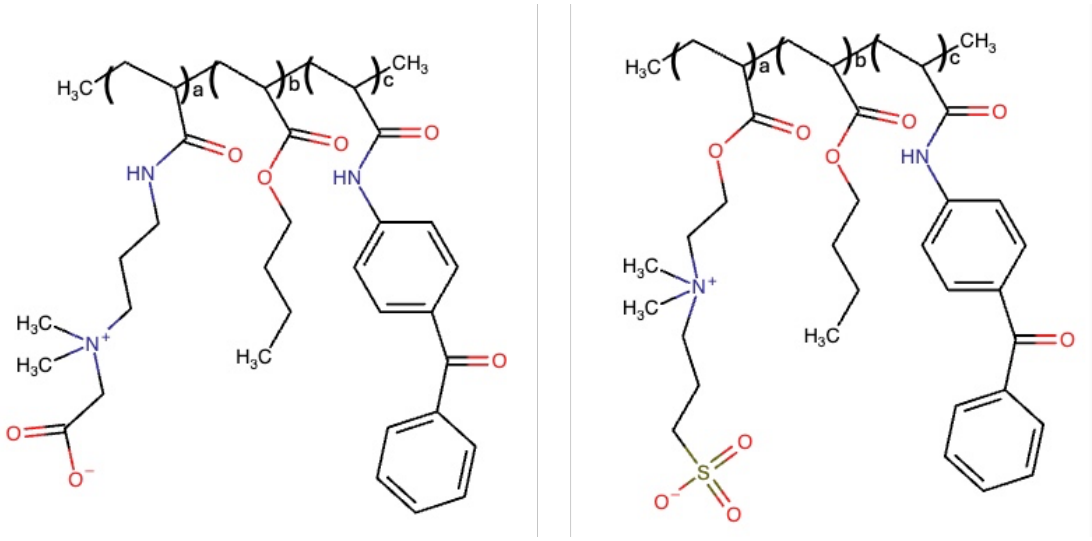

Scheme 6. Chemical structure of two zwitterionic polymer. Carboxybetaine-based copolymer pCBAA-2-BMA-BPAA (left), and sulfobetaine-based copolymer pSBMA-BMA-BPAA (right)

The photoreactive biocompatible poly(carboxybetaine)-based triblock copolymer[59], [60], [61], poly(CBAA-r-BMA-r-BPAA)* and poly(sulfobetaine)-based triblock copolymer (poly(SBMA-r-

BMA-r-BPAA)** chemical structure is shown in **Scheme *6***. They were synthesized by a thermally initiated free-radical polymerization with optimized molar ratio and molecular weight [60]. CBAA and BPAA monomers were pre-synthesized using a method reported previously [59], [60], and BMA was purchased from commercial sources (TCI Chemicals, Portland, OR). CBAA-1: BMA: BPAA molar ratio was 70:20:10 mol %, and less than 1% of AiBN was used as a thermal initiator. The final product was retrieved as a fine white powder [59], [60], [61], [62], [63].

*(*this triblock copolymer is abbreviated as pCBAA, and ** for pSBMA in this dissertation)*

pCBAA copolymer was dissolved in DI water with 5 wt % with sonication for 2 hours. Then, the solution was filtered using a PTFE syringe filter. The polystyrene surface (disc or non-treated 24-well plates) was immersed with the filtered pCBAA solution and incubated at room temperature for 30 minutes. After incubation, the pCBAA solution was gently removed from the polystyrene surface and dried under the fume hood for 2 hours. UV illumination was followed to initiate the photoinduced cross-linking of polymer, allowing BPAA moiety to react with the polystyrene surface. The surface was hydrated right before use. Poly(SBMA-BMA-BPAA) copolymer was prepared in an identical condition and method, only by replacing pCBAA monomer with pSBMA monomer.

2.1.4. Electron Spectroscopy for Chemical Analysis (ESCA, XPS)

We evaluated all test surfaces for elemental composition, surface chemistry, coating uniformity, and stability using electron spectroscopy for chemical analysis at the Molecular Analysis Facility of NESAC/BIO, University of Washington, employing a Kratos AXIS Ultra DLD XPS instrument. High-resolution C1s spectra collection occurred at a 55° take-off angle, with results shown in

Figure 3 and fluorocarbon ratio analysis (CF_2:CF_3) presented in Figure 7. We referenced binding energies to the standard C-H peak at 285.0 eV and CF_2 peak at 292.0 eV.

2.1.5. Human Plasma

We utilized citrated human plasma from BloodWorks (Seattle, WA), implementing a carefully controlled thawing protocol. The process began with transfer from -80°C storage to -20°C for 8 hours, followed by 4°C overnight storage, and concluded with 40-minute equilibration in a 37°C water bath. All experiments employed fresh frozen plasma from BloodWorks.

2.2. Results and Discussion

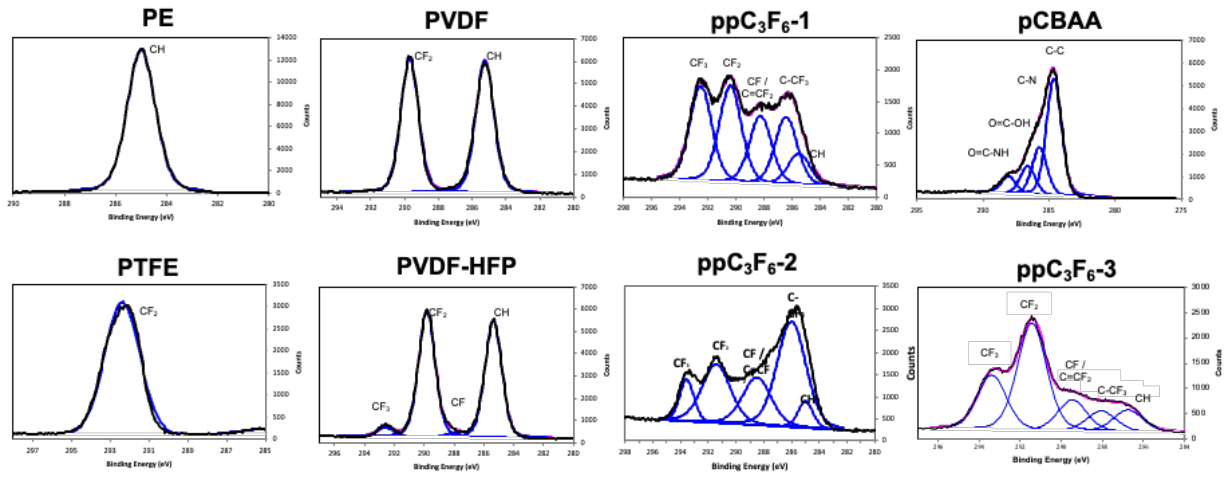

Figure 3. *High-resolution Carbon C1s spectra from ESCA*

ESCA/XPS survey scans were conducted to verify the chemical compositions of the fluoropolymer films' uniformity and assess their integrity following delamination testing (**see supplement section**). Characteristic high-resolution carbon C1s spectra is described in **Figure 3**. PE, PTFE,

PVDF and PVDF-HFP had a matching spectra and composition with the reference, as they are commercially available. For PTFE, PVDF, PVDF-HFP, only carbon and fluorine were detected. The spin-casted PVDF and PVDF-HFP is retaining its high-quality coating with no remaining DMF solvent present at the surface. The absence of silicon peak from the glass substrate indirectly proves that the coating thickness is larger than 10 nm.

For the C1s spectra of ppC_3F_6 surfaces, the CF_2 percentage increases as the downstream deposition time prolonged. The ppC_3F_6-3 shows highest CF_2 ratio among ppC_3F_6 surfaces. For these surface chemistries, we assigned fluorocarbon peaks to the references: CF_3 and CF_2 peaks are defined at 293.9 and 292.0 eV, respectively, while the C-F/C=CFx and C-CFx peaks are slightly broader at 289.9 and 287.8 eV, respectively. C1s spectra of pCBAA zwitterionic polymer was identical to that of the literature [60].

2.3. Summary

In this chapter, all the materials tested are characterized. The ESCA provides elemental composition and C1s spectra for understanding of varying surface chemistries. The preparation of surfaces with varying fluorocarbon ratio is the one of primary intention of this study to understand how different fluorocarbon chemistry interact with blood proteins, affecting the thrombogenicity.

Chapter 3. Intrinsic Study

3.1. Outline & Fundamentals

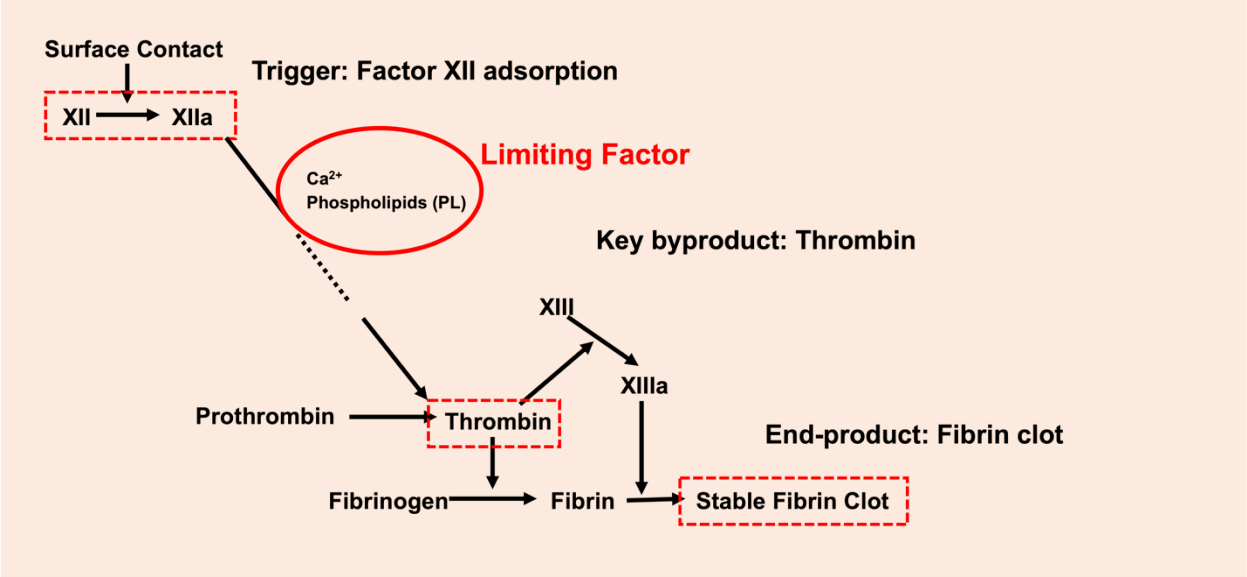

Scheme 7. Illustration of the approach for intrinsic pathway study*. Three dashed box indicates primary points to be discussed in following chapters. Calcium and phospholipids are utilized as limiting factor to control the pathway progression.*

Blood compatibility studies in this chapter has been built upon the understanding of intrinsic coagulation pathway from an engineering perspective (**Scheme 7**). We examined thrombin generation, fibrin clot formation, and FXII adsorption and activation to develop a comprehensive understanding of blood compatibility. Calcium and phospholipids serve as limiting factors, as their presence proves crucial in sequential downstream activation of the blood coagulation cascade. We consider the addition of calcium and phospholipids as the actual 'initiation' of activation, marking our initial timepoint.

3.2. Thrombin generation assay

3.2.1. Methods

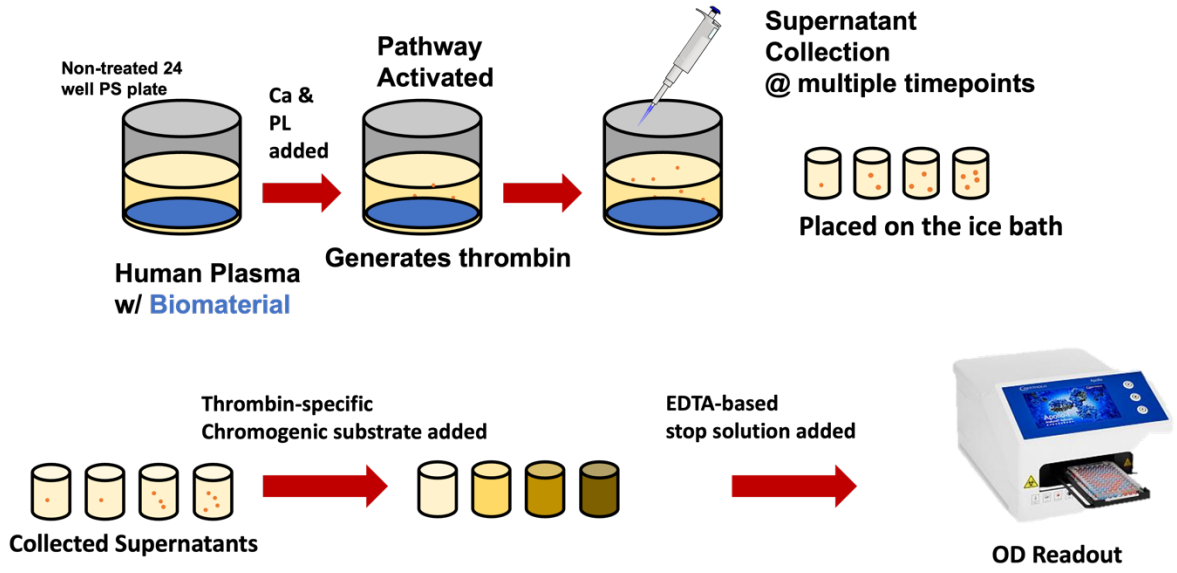

Scheme 8. Illustration of thrombin generation assay.

(**Scheme 8**) We modified the thrombin generation assay from previous studies (Oeveren et al.[64], [65], [66], and Cao et al[55], [56], and [67], [68]). The downstream sequential activation of the intrinsic pathway following FXII adsorption and activation requires calcium and phospholipid. Before introducing plasma to the samples, we added calcium chloride and magnesium chloride stock solutions to establish physiologically relevant conditions, achieving final concentrations of 2.5 mM calcium and 1 mM magnesium. We also included phospholipid to facilitate activation.

We added recalcified human plasma to samples and incubated the plate at 37°C for 20 minutes, with mixing every 5 minutes. During incubation, we prepared buffer solution (HaemoScan, Groningen, Netherlands) in 1.5 ml centrifuge tubes (490 µL) and placed them in an ice bath. We also added 90 µL of buffer solution to 96-well plates maintained at 37°C.

Sample collection occurred at multiple timepoints (1, 3, 5, 15, and 30 minutes), with immediate 490 μL buffer dilution and cooling in an ice bath with gentle resuspension. We transferred 10 μL of each mixture to 96-well plates, added thrombin-specific chromogenic substrate, and incubated at 37°C for 30 minutes. EDTA-based stop solution terminated the reactions, followed by optical density measurement at 405 nm using a plate reader.

All statistical analyses employed One-way ANOVA with Tukey HSD test, using significance levels of * ($p<0.05$), ** ($p<0.01$), *** ($p<0.001$), and **** ($p<0.0001$).

3.2.2. Results

Thrombin Generation

Figure 4 illustrates the temporal evolution of thrombin generation on various biomaterial surfaces at 1, 3, 5, 15, and 30 minutes. Glass demonstrated the highest thrombogenicity, generating approximately 700 mU/ml/cm² by 30 minutes, with a marked increase between 5 and 15 minutes. This rapid thrombin generation indicates strong pro-thrombotic properties. PE and PTFE also showed significant thrombin generation, though lower than glass. PTFE reached approximately 400 mU/ml/cm² by 30 minutes, while PE achieved approximately 350 mU/ml/cm². PVDF and PVDF-HFP generated moderate thrombin levels, reaching around 200 mU/ml/cm² for PVDF-HFP and 250 mU/ml/cm² for PVDF by 30 minutes. The ppC_3F_6 variants (ppC_3F_6-1, ppC_3F_6-2, and ppC_3F_6-3) exhibited reduced thrombin generation compared to conventional materials, with final concentrations between 100 and 180 mU/ml/cm² (ppC_3F_6-3 showing the lowest values in the ppC_3F_6 group), suggesting that RFGD plasma polymerization treatment effectively reduces thrombogenicity. The zwitterionic polymer pCBAA demonstrated superior anti-thrombogenic

properties, maintaining thrombin generation below 50 mU/ml/cm² throughout the 30-minute period, with minimal and steady increases over time.

Thrombin Generation Rate

Figure 5 presents thrombin generation rates for each surface, calculated across successive time intervals (0-1 min, 1-3 min, 3-5 min, 5-15 min, and 15-30 min). Glass exhibited the highest generation rates across all intervals, particularly during early phases (0-1 min and 1-3 min), indicating immediate and strong thrombin activation upon contact. PE and PTFE also showed high initial rates, especially during the 1-3 minute interval, though their rates decreased more steadily than glass over time. Notably, PTFE demonstrated a unique ~2.3-fold increase between 15 and 30 minutes, while other materials showed less than 1-fold increments. PVDF and PVDF-HFP displayed moderate rates sustained throughout the 30-minute period, with PVDF ultimately achieving cumulative thrombin generation similar to PTFE. The ppC_3F_6 surfaces maintained relatively low rates across all intervals, particularly ppC_3F_6-3, suggesting reduced thrombogenicity potentially due to surface properties imparted by RFGD plasma polymerization. pCBAA consistently demonstrated the lowest rates, remaining nearly constant and minimal throughout, indicating strong resistance to thrombin activation.

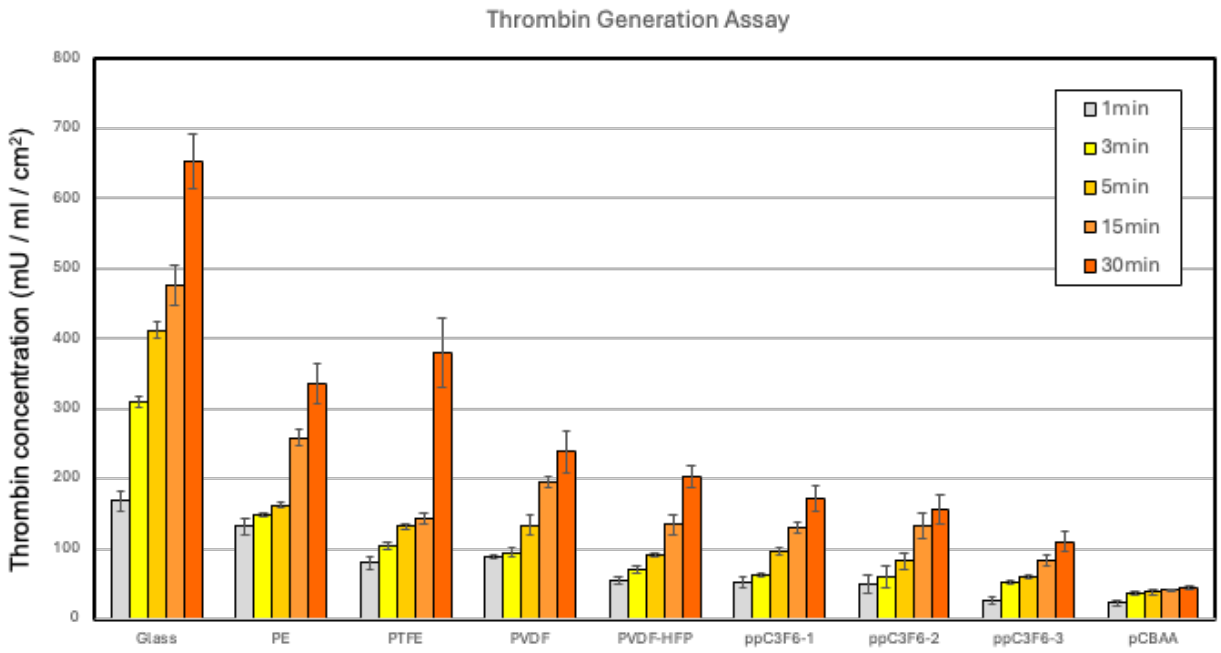

Figure 4. Thrombin Generation on Biomaterial Surfaces Over Time in 1% Human Plasma

Thrombin concentration (mU/ml/cm²) generated on each biomaterial surface, measured at 1, 3, 5, 15, and 30 minutes. Glass and PE showed rapid thrombin generation, indicating high thrombogenic risk, while pCBAA exhibited the lowest thrombin generation rate, demonstrating strong anti-thrombogenic behavior.

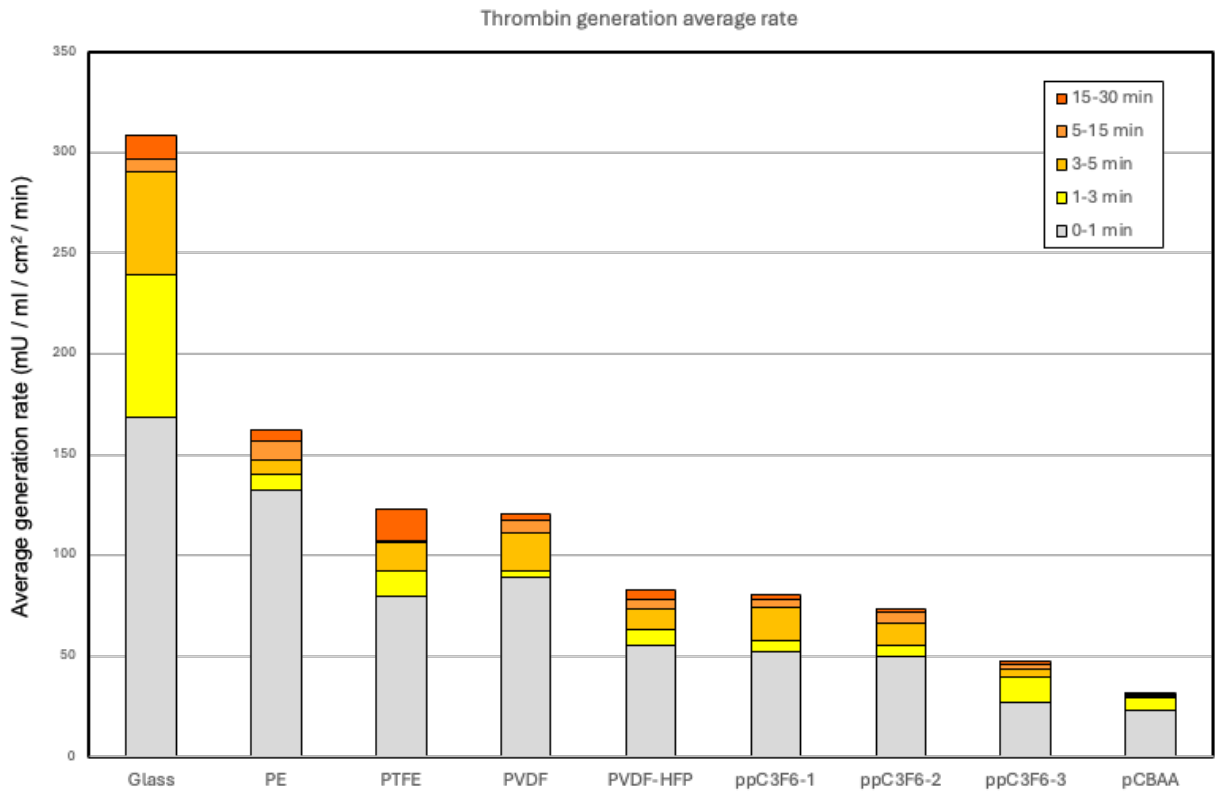

Figure 5. Thrombin Generation Rate Across Time Points on Biomaterial Surfaces

Rate of thrombin generation over sequential time intervals for each surface. Glass exhibited the highest rate in early intervals, while PTFE showed a delayed increase in thrombin generation, suggesting potential thrombogenic risk over extended exposure. pCBAA maintained the lowest thrombin generation rate, underscoring its blood compatibility.

3.3.3. Discussion

Thrombin Generation as an Indicator of Thrombogenic Potential

The thrombin generation results across various biomaterials reveal the different propensities of these surfaces to initiate and sustain thrombotic activity, which is crucial in assessing their suitability for blood-contacting applications. Thrombin is a central enzyme in the coagulation cascade, catalyzing fibrin formation and furtherly promoting platelet aggregation. High thrombin

generation on a surface suggests a high thrombogenic potential, leading to an increased risk of clot formation. Glass is a known positive control of blood compatibility study, and a classical activator of the intrinsic pathway. The fact that glass exhibited the highest thrombin concentration and generation rate, especially in the early time points, is presumably coming from the high initial FXII adsorption and activation. Overall, the rapid and substantial thrombin generation indicates that such a surface strongly activates the coagulation cascade, likely due to its high-fouling or improved activity of FXII, considering FXII is being attracted by negatively charged surface, which means glass may attract a lot of FXII. Thus, high initial and cumulative thrombin levels on glass suggest that this material would likely induce acute thrombosis in blood-contacting applications.

Thrombotic Risk of PE and PTFE

PE and PTFE, hydrophobic surfaces with lower surface energy than glass, also generated relatively high thrombin levels, though at lower concentrations than glass. Their relatively high initial thrombin generation rate suggests that these materials support early-phase thrombotic activation, likely through hydrophobic interactions with plasma proteins, which can lead to structural changes in proteins that activate the clotting cascade. Over time, however, the rate of thrombin generation on these materials slowed, indicating that while they may not sustain thrombin generation as strongly as glass, they still pose a moderate thrombogenic risk.

These results suggest that unmodified PE and PTFE surfaces may not be ideal for long-term blood-contacting applications due to their tendency to promote early thrombin activation, even though the PTFE is being used in clinical application for the vascular graft or bypass. For these materials to be used safely in medical devices such as catheters or blood filtration membranes, additional surface treatments—such as engineered hydrophilic coatings or plasma modifications—may be required to reduce their thrombogenicity.

Moderate Thrombin Generation on PVDF and PVDF-HFP

PVDF and PVDF-HFP generated intermediate levels of thrombin compared to glass, PE, and PTFE, indicating moderate thrombogenic potential. These surfaces maintained relatively steady thrombin generation rates over time, without the sharp increase seen on glass or PE. This moderate response suggests that PVDF-based materials may be suitable for applications where some level of thrombin formation can be tolerated, such as in controlled anticoagulant environments or short-term blood-contacting applications.

The moderate thrombogenicity of PVDF and PVDF-HFP also opens possibilities for selective applications where anticoagulants or surface modifications could further reduce their thrombotic activity. This characteristic positions them as flexible options for short-term blood-contacting devices, although their use in long-term implants would likely require surface modifications to improve blood compatibility.

Reduced Thrombin Generation on RFGD Plasma-Polymerized ppC_3F_6 Surfaces

The RFGD plasma-polymerized ppC_3F_6 surfaces (ppC_3F_6-1, ppC_3F_6-2, and ppC_3F_6-3) displayed reduced thrombin generation compared to glass, PE, PTFE, PVDF, and PVDF-HFP, demonstrating a moderate anti-thrombogenic effect. The RFGD plasma polymerization process likely modifies the surface energy and introduces functional groups that either resist protein adsorption or maintain proteins in conformations that do not promote coagulation. By reducing both the amount of thrombin generated and the thrombin generation rate, ppC_3F_6 surfaces present a balanced anti-thrombogenic profile.

The moderate thrombin generation on ppC_3F_6 suggests that these surfaces could be beneficial in applications where controlled thrombotic responses are desirable or where a moderate anti-

thrombogenic effect suffices. Examples include extracorporeal circuits or devices used for short-term blood contact, where the device's moderate thrombotic response can be managed with standard anticoagulation protocols. The results also indicate that further optimization of the RFGD process could enhance the anti-thrombogenic properties of ppC_3F_6, making it an even more viable option for blood-contacting devices.

Superior Anti-Thrombogenic Performance of Zwitterionic pCBAA

Among all the materials tested, pCBAA demonstrated the lowest levels of thrombin generation and the slowest rate of thrombin formation, underscoring its excellent anti-thrombogenic properties. The zwitterionic nature of pCBAA creates a hydration layer on the surface that minimizes protein-surface interactions, thereby reducing the adsorption and conformational changes of proteins that could trigger the coagulation cascade. The exceptionally low thrombin activity on pCBAA indicates that this material could significantly lower thrombotic risk when used in blood-contacting applications.

The ability of pCBAA to resist thrombin generation so effectively makes it ideal for applications that demand minimal coagulation, such as in vascular grafts, stents, or long-term blood-contacting implants where even low levels of thrombin formation could pose serious risks. By maintaining low thrombin generation rates throughout all measured time intervals, pCBAA provides a stable, biocompatible interface that could reduce the need for systemic anticoagulation therapy in patients, thereby minimizing potential side effects and improving patient outcomes.

Implications for Biomaterial Selection and Future Directions

The findings from this study highlight important considerations for biomaterial selection in blood-contacting applications:

Glass demonstrated high thrombin generation and the fastest rate, which aligns with the intended employment of glass as a positive control. Glass is a classical activator of the intrinsic pathway.

PE and PTFE demonstrated relatively high thrombotic risks, suggesting that their direct use in blood-contacting applications would likely trigger coagulation responses. For these materials to be viable, surface modifications or coatings to reduce protein adsorption and thrombin generation would be essential. With relatively moderate thrombin generation, PVDF and PVDF-HFP could be considered for short-term blood-contacting applications or in settings where thrombotic responses can be controlled pharmacologically. Further research into surface modifications for PVDF-based materials could enhance their blood compatibility, potentially expanding their use in more demanding blood-contact environments. The moderate anti-thrombogenic effect of ppC_3F_6 surfaces suggests that RFGD plasma-polymerized materials could serve as a middle-ground solution, balancing selective protein interactions with reduced thrombin generation. Further refinement of the RFGD process could optimize ppC_3F_6 for broader blood-contact applications.

The strong anti-thrombogenic profile of **pCBAA,** with minimal thrombin generation, marks it as the most promising candidate for applications requiring minimal coagulation risk. Its ability to suppress both protein adsorption and thrombin activation makes it ideal for long-term implants and devices that benefit from a stable, low-thrombogenic interface.

To summarize, this study demonstrates that different biomaterial surfaces exhibit distinct levels of thrombogenic potential, as reflected by thrombin generation and activation rates. PE, and PTFE present relatively high thrombogenic risks, while PVDF and PVDF-HFP show relatively moderate thrombin activity. RFGD plasma-polymerized ppC_3F_6 surfaces reduced thrombin generation moderately, making them viable for selective applications. The zwitterionic polymer pCBAA, with its strong anti-thrombogenic profile, emerges as the most promising candidate for blood-contacting

devices that require minimal coagulation activation. These findings underscore the value of tailored surface engineering to develop blood compatible materials optimized for specific clinical applications.

3.3. Fibrin clot formation time assay

3.3.1. Methods

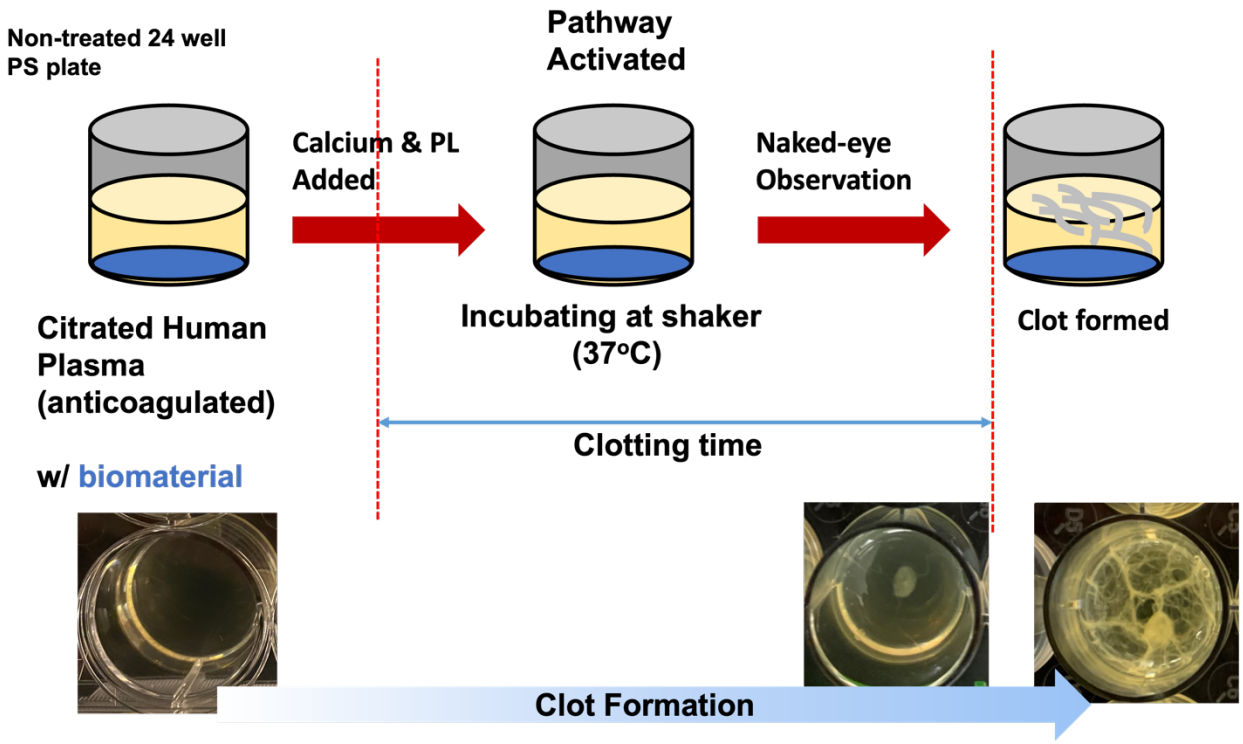

Scheme 9. Illustration of fibrin clot formation time assay.

Following **Scheme 9**, we modified the clot formation time assay from previous work in our group[55], [56]. We placed samples in 24-well non-treated polystyrene plates and equilibrated them with PBS for 2 hours. After PBS removal, we added calcium (2.5 mM) and magnesium (1 mM) to citrated human plasma to restore coagulation capacity. After adding this recalcified plasma to samples, we sealed plates with PCR film and placed them on an orbital shaker (120 rpm) at 37°C. We defined clot formation time as either visible white clot formation or significant plasma mobility reduction due to gelation from multiple micro-embolisms, accounting for donor-specific variations. Gelation assessment relied on either opacity changes or sudden decreases in fluid

viscosity, indicated by plasma assuming a jelly-like consistency resistant to movement even at plate tilts exceeding 45 degrees.

3.3.2. Results

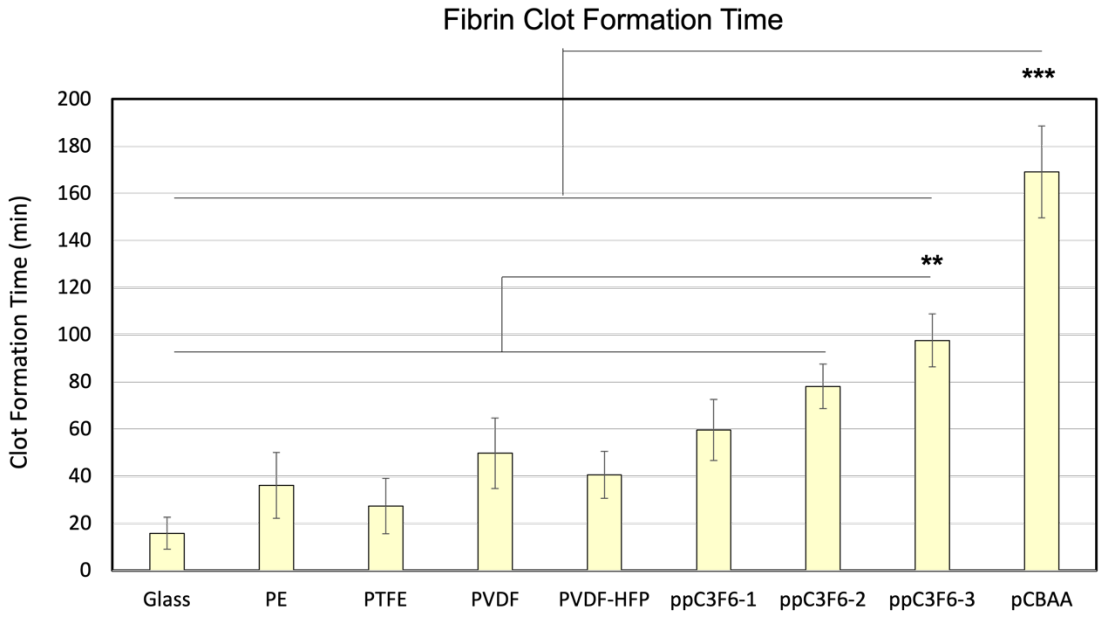

Figure 6. Fibrin Clot Formation Time on Biomaterial Surfaces

Time required for fibrin clot formation on each surface, with longer times indicating better anti-thrombogenic properties. pCBAA exhibited the longest clot formation time, suggesting strong resistance to clot formation, while glass displayed the shortest time, indicating a high tendency to promote clotting.

Fibrin Clot Formation Time

Figure 6 presents fibrin clot formation times for each biomaterial surface, with longer times indicating superior anti-thrombogenic properties. Glass exhibited the shortest clot formation time, approximately 20 minutes, demonstrating high thrombogenicity and confirming its suitability as a positive control. PE and PTFE showed marginally longer times, reaching 15-25 minutes, indicating

moderate thrombogenic risk despite slight improvement over glass. PVDF and PVDF-HFP demonstrated intermediate performance with clot formation times of approximately 40 minutes, suggesting improved resistance compared to glass, PE, and PTFE. Among ppC_3F_6 surfaces, we observed progressive improvement in anti-thrombogenic behavior: ppC_3F_6-1 delayed clotting to around 60 minutes, ppC_3F_6-2 to 80 minutes, and ppC_3F_6-3 extended the time to approximately 100 minutes. pCBAA achieved the longest clot formation time, approaching 180 minutes, indicating exceptional resistance to fibrin clot formation.

3.3.3. Discussion

The fibrin clot formation assay results highlight significant variations in the thrombogenic potential of each biomaterial surface. **Glass** exhibited the shortest clot formation time, which is loyal to its role as a classical activator of intrinsic pathway, which promote protein adsorption and activation of the coagulation cascade. **PE** and **PTFE** also demonstrated short clot formation times, though slightly longer than glass, suggesting that these surfaces still facilitate coagulation but may delay clot initiation to some extent compared to glass. The relatively quick clot formation on PE and PTFE indicates that these surfaces are not ideal for blood-contacting applications without further anti-thrombogenic modifications, as they could promote undesired clot formation in clinical settings. **PVDF** and **PVDF-HFP** showed intermediate clot formation times of around 40–50 minutes, indicating improved anti-thrombogenic behavior compared to glass, PE, and PTFE. The longer clotting times on PVDF-based surfaces suggest that these materials may possess surface characteristics that reduce protein activation and delay coagulation. However, while PVDF and PVDF-HFP offer moderate resistance to clot formation, their performance is still not sufficient

for applications requiring strong anti-thrombogenic properties, such as long-term implants. These materials may be more suitable for devices used in short-term blood-contacting applications or could be improved through additional surface modifications.

Improved Anti-Thrombogenic Performance of ppC₃F₆ Surfaces

The ppC₃F₆ surfaces showed progressively longer clot formation times within the group, with ppC₃F₆-1 clotting around 60 minutes, ppC₃F₆-2 around 80 minutes, and ppC₃F₆-3 reaching approximately 100 minutes. This trend suggests that subtle variations in the RFGD plasma polymerization process can influence the surface properties of ppC₃F₆, affecting its interaction with plasma proteins and clot formation.

The relatively long clotting times on ppC₃F₆ surfaces indicate that these materials have moderate to strong anti-thrombogenic properties, likely due to specific surface chemistries or topographies created by the plasma treatment. Among the ppC₃F₆ variants, ppC₃F₆-3 showed the longest clot formation time, suggesting that this specific RFGD treatment produces the effective anti-thrombogenic surface within the group. This enhanced clotting resistance on ppC₃F₆ surfaces, especially ppC₃F₆-3, makes them promising candidates for applications where moderate anti-thrombogenic performance is required, such as in short-term blood-contacting devices.

Strong Anti-Thrombogenic Properties of Zwitterionic pCBAA

pCBAA exhibited the longest clot formation time, approaching 180 minutes, indicating a very strong resistance to clot formation. The zwitterionic nature of pCBAA generates a hydration layer to present anti-fouling at the protein-surface interactions, preventing protein adsorption and activation required for clotting. This extended clot formation time confirms pCBAA's excellent anti-thrombogenic properties, making it highly suitable for long-term blood-contacting

applications where minimal thrombogenicity is essential, such as vascular grafts, stents, and implants.

Potential clue of CF_2-CF_3

Figure 7 reveals a potential correlation between CF_2:CF_3 ratio and clot formation time, chosen for analysis because clot formation time serves as a realistic indicator of blood compatibility in the intrinsic pathway. This observation builds on Dr. Allan Hoffman's earlier work regarding CF_3 number effects[5]. Among various fluorocarbon ratios examined (CF:CF_2, CF:CF_3, CF_2:CF_3), only CF_2:CF_3 demonstrated correlation with extended clot formation time. However, this relationship applies exclusively to plasma-polymerized surfaces; PTFE (100% CF_2) and PVDF-HFP (high CF_2:CF_3 ratio) do not follow this trend despite their fluorocarbon compositions (**Figure 6**).

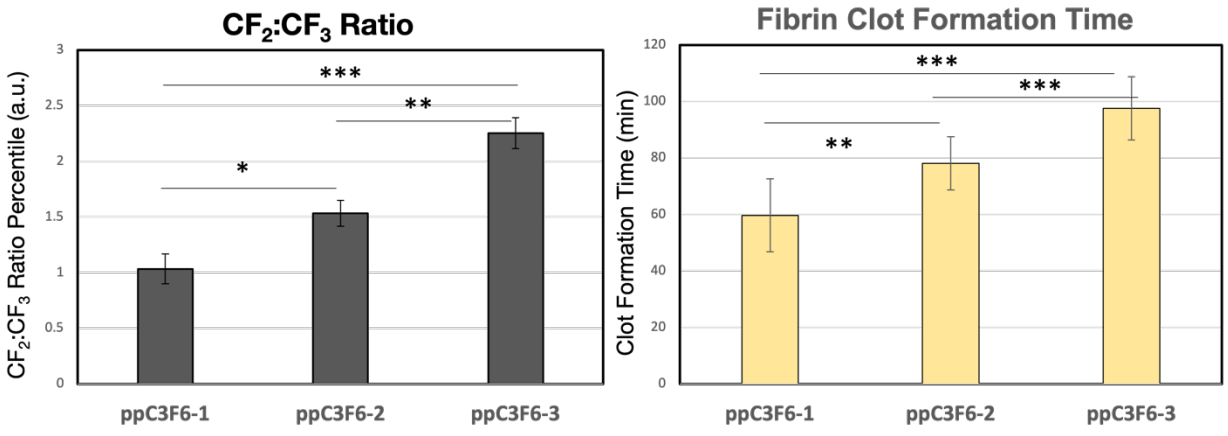

Figure 7. CF_2:CF_3 ratio and Fibrin Clot Formation Time of three ppC_3F_6 surfaces

Materials	Fluorocarbon Ratio (%)			
	Hydrocarbon	CF	CF2	CF3
LDPE	100	-	-	-
PTFE	-	-	100	-
PVDF	50.0 ± 1.4		50.0 ± 1.4	
PVDF-HFP	46.0 ± 0.4	2.0 ± 0.1	49.0 ± 0.3	3.0 ± 0.1
ppC_3F_6-1	6.4 ± 1.1	25.6 ± 0.8	34.6 ± 1.4	33.3 ± 0.3
ppC_3F_6-2	10.0 ± 1.5	14.4 ± 2.1	43.0 ± 2.6	31.6 ± 1.1
ppC_3F_6-3	9.8 ± 1.2	8.3 ± 1.5	48.5 ± 2.1	21.8 ± 1.3

Table 2. Fluorocarbon group ratio of surfaces

3.4. FXII bioactivity assay

3.4.1. Radiolabeled FXII adsorption assay

3.4.1.1. Methods

Factor XII and albumin iodination

We radiolabeled human FXII protein (Prolytix, Essex Junction, VT) using the iodine monochloride method [69]. We began by adding 1 mCi of Iodine-125 radionuclide to 0.5 ml 2X borate buffered solution, followed by 0.5 ml of ICl/NaCl mixture (4:1 ratio) for FXII. We optimized the ICl/NaCl mixture molar ratio to maximize protein iodination yield. For albumin (Sigma-Aldrich, St. Louis, MO), we employed the same method but with a modified ICl/NaCl mixture ratio of 3:1 [31], [70], [71] .

The procedure continued with addition of 0.5 ml of FXII (40 μg/ml) in 1X borate buffered solution (pH 8.0), performing the radiolabeling reaction on ice for 20 minutes to tag tyrosine residues with iodine-125 isotope. We purified the radiolabeled FXII solution through size-exclusion chromatography, collecting 40 fractions of 0.5 ml solution to evaluate iodination efficiency. After pooling labeled protein peak fractions, we performed a second chromatographic purification. For albumin labeling, we followed identical procedures using 0.5 ml of 10 mg/ml albumin solution.

Radiolabeled FXII and albumin adsorption

Prior to protein adsorption assays, we preincubated all samples with cPBS solution containing 10 mM NaI (cPBSzI) for 1 hour. We conducted adsorption assays under three conditions using 1% plasma concentrations: single FXII solution in cPBSzI, binary FXII/albumin solution in cPBSzI, and human plasma diluted with Tyrode's buffer. We prepared "hot protein" solutions by adding radiolabeled protein to achieve approximately 100 CPM/ng activity. After 2-hour surface exposure, we performed triple rinses with cPBSzI to remove unbound proteins. We measured sample radioactivity for 1 minute alongside protein standards using a Perkin-Elmer gamma counter (Wizard 2 automatic gamma counter 2470), reporting adsorption data in ng/cm².

For retention studies, we immersed samples in 2% sodium dodecyl sulfate solution for 12 hours, followed by triple cPBSzI rinses. We conducted radioactivity measurements as in the adsorption study, reporting retention data in ng/cm². We calculated retention percentiles by dividing retention by adsorption and multiplying by 100.

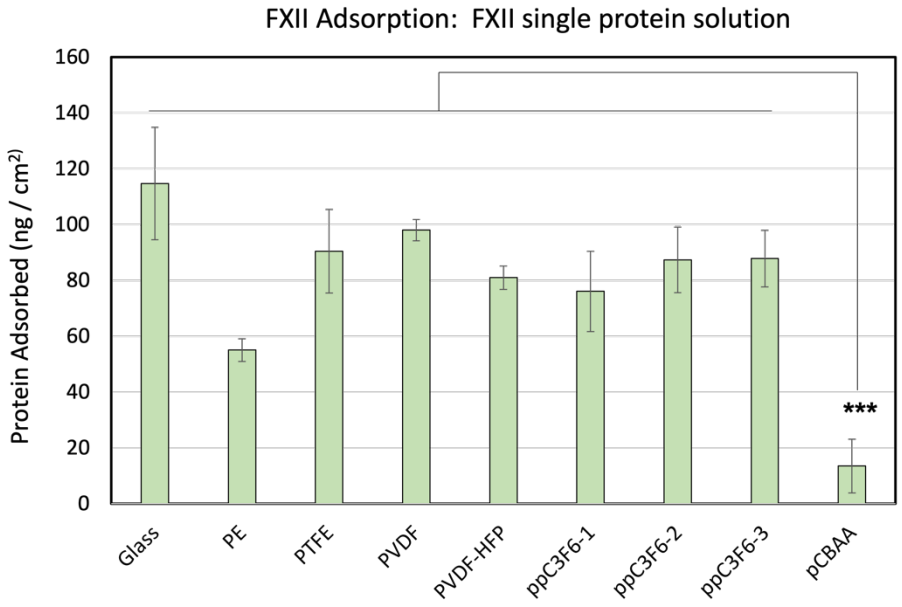

Figure 8. FXII Adsorption on Various Biomaterials in Single-Protein PBS Solution

FXII adsorption levels on biomaterial surfaces after incubation in a single-protein PBS solution. The Y-axis represents the amount of FXII adsorbed (ng/cm²) on each surface.

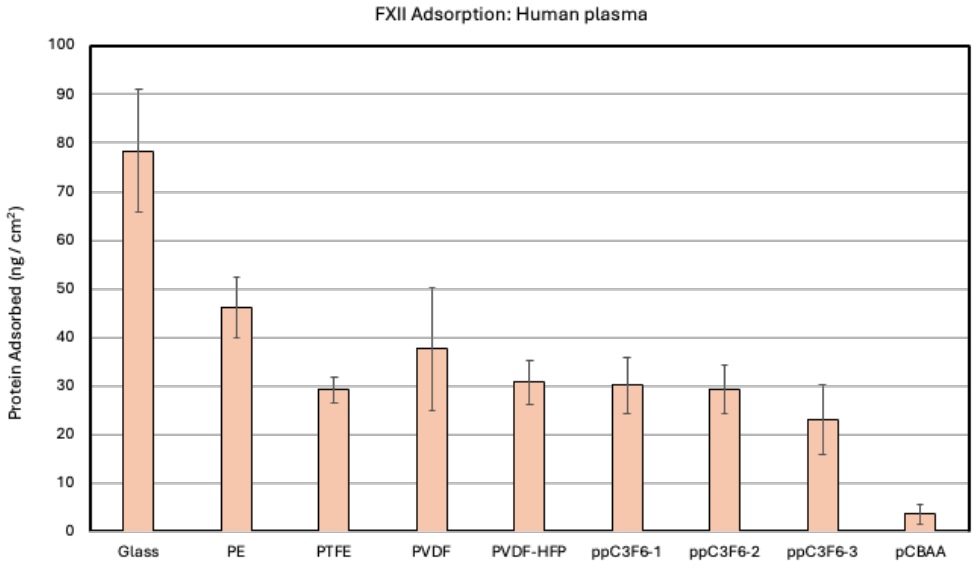

Figure 9. FXII Adsorption on Various Biomaterials in 1% Human Plasma

FXII adsorption levels on biomaterial surfaces after incubation in a competitive environment (1% human plasma). FXII adsorption decreased across all surfaces due to the presence of multiple competing plasma proteins.

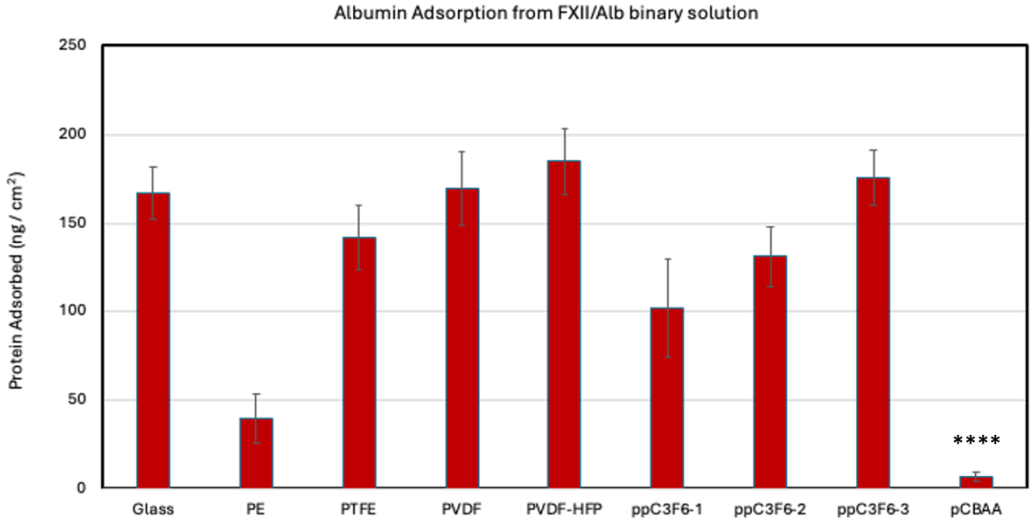

Figure 10. Albumin Adsorption in FXII/Albumin Binary Solution

Albumin adsorption on various biomaterial surfaces from a binary protein solution containing FXII and albumin, showing each surface's albumin-binding affinity in a competitive setting.

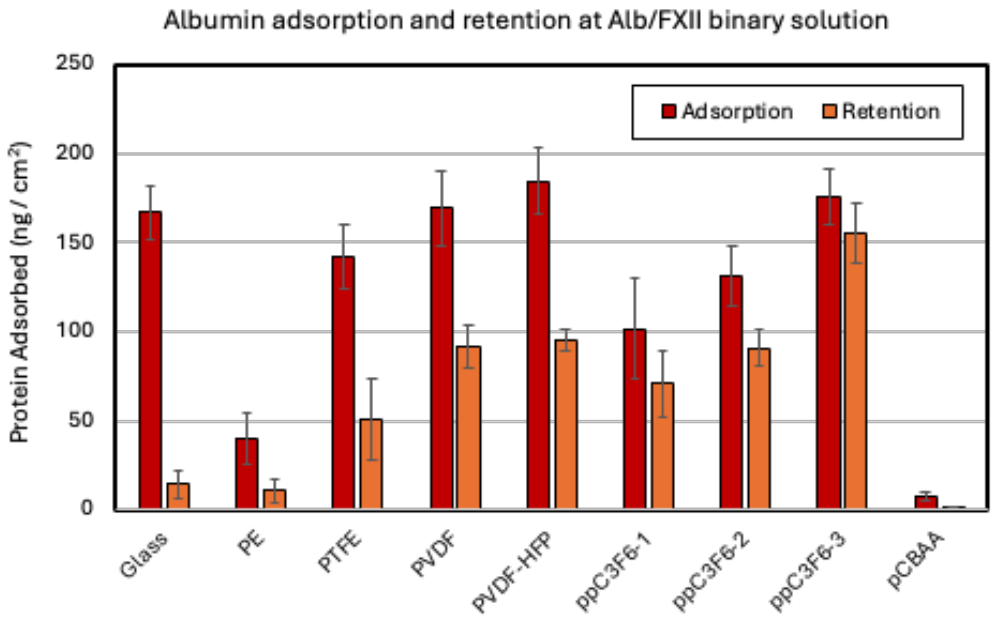

Figure 11. Albumin Adsorption and Retention on Biomaterial Surfaces in Binary Solution

Initial albumin adsorption (red bars) and retention (orange bars) after a 24-hour rinse in 2% SDS buffer, measuring binding stability.

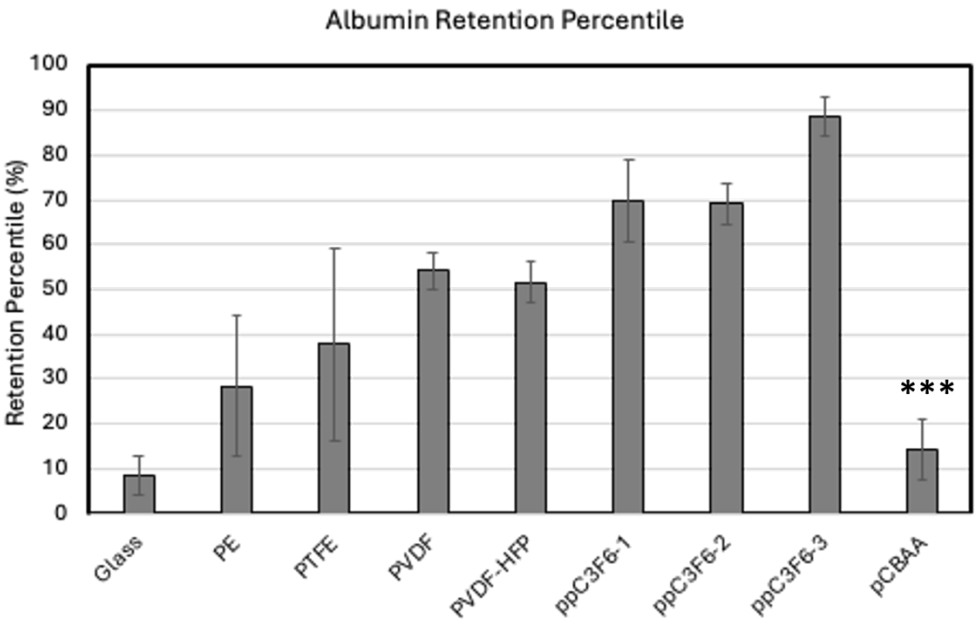

Figure 12. Albumin Retention Percentage on Biomaterial Surfaces

Albumin retention as a percentage of initial adsorption, reflecting binding stability post-rinse.

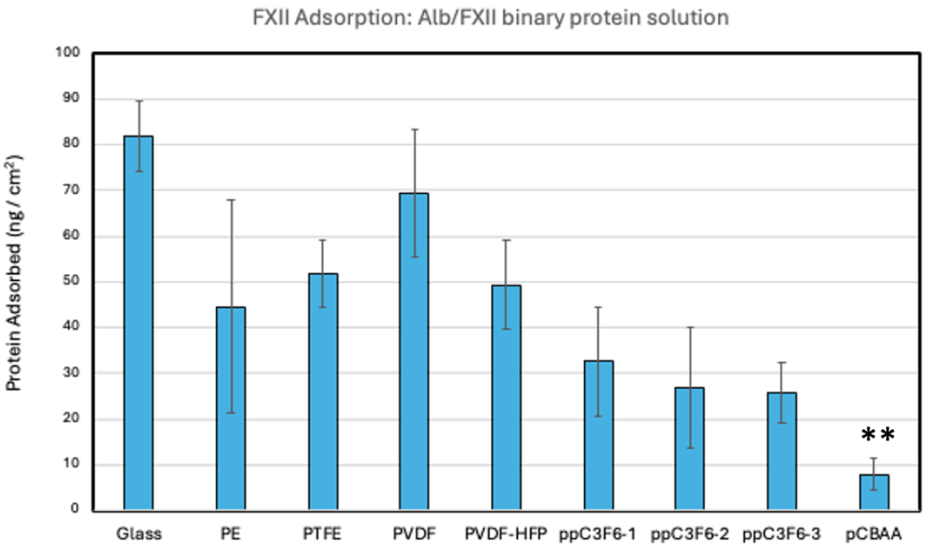

Figure 13. FXII Adsorption in FXII/Albumin Binary Solution

FXII adsorption on biomaterial surfaces in the FXII/Albumin binary solution, demonstrating the competition between FXII and albumin for surface binding.

3.4.1.2. Results

FXII Adsorption in Single-Protein PBS Buffer Solution

Figure 8 demonstrates FXII adsorption patterns across biomaterial surfaces in single-protein solution conditions. Glass surfaces exhibited the highest FXII adsorption, exceeding 120 ng/cm², indicating strong binding affinity and significant FXII promotion. PE demonstrated relatively low adsorption (~55 ng/cm²), suggesting moderate FXII binding resistance attributable to its hydrophobic nature. PTFE and PVDF showed moderate adsorption levels (80-100 ng/cm²), indicating FXII binding capacity below that of glass. PVDF-HFP exhibited slightly reduced adsorption compared to PTFE and PVDF, suggesting modest reduction in FXII affinity. The ppC_3F_6 variants showed moderate FXII adsorption ranging from 70 to 90 ng/cm², with similar values across variants indicating that RFGD plasma polymerization does not dramatically alter FXII binding in single-protein conditions. The zwitterionic polymer pCBAA achieved the lowest FXII adsorption (~10 ng/cm²), demonstrating superior anti-fouling properties that effectively prevent FXII attachment.

FXII Adsorption in 1% Human Plasma Solution

Figure 9 illustrates FXII adsorption on each surface in a 1% human plasma diluted with Tyrode's buffer, introducing competitive adsorption from various plasma proteins. **Glass** maintained the highest FXII adsorption (~80 ng/cm²), though lower than in PBS, indicating its affinity for FXII remains high even in a competitive environment, working as a positive control.

PE and PTFE showed relatively moderate FXII adsorption levels (around 30–45 ng/cm²), suggesting they retain some affinity for FXII despite the presence of other proteins. PVDF also

displayed moderate FXII adsorption (~40 ng/cm²), similar to PE and PTFE, indicating some resistance to competition but with sufficient FXII binding. PVDF-HFP showed slightly lower FXII adsorption than PVDF, indicating moderate resistance to competitive binding. Among the ppC_3F_6 surfaces, ppC_3F_6-1 and ppC_3F_6-2 displayed slightly lower FXII adsorption (~30 ng/cm²), while ppC_3F_6-3 had a bit lower level (~20 ng/cm²) compared to other ppC_3F_6s, indicating modest variation within the group of ppC_3F_6s. pCBAA exhibited the lowest FXII adsorption (~5 ng/cm²), confirming its anti-fouling properties by preventing FXII attachment even in a competitive protein environment.

Albumin Adsorption in Binary Protein Solution (Competitive Adsorption with FXII)

Figure 10 shows albumin adsorption in a albumin and FXII binary protein solution (in PBS) containing both albumin and FXII, providing insights into albumin binding selectivity on each surface. Glass, PTFE, and PVDF displayed high albumin adsorption levels (150–200 ng/cm²), indicating strong albumin binding affinity. The high adsorption suggests these surfaces allow albumin attachment, even in the presence of FXII. PE showed relatively low albumin adsorption (~50 ng/cm²), indicating weaker albumin binding likely due to its hydrophobic surface. PVDF-HFP exhibited relatively high albumin adsorption (~180 ng/cm²), indicating a still significant affinity for albumin. Among the ppC_3F_6 surfaces, all three variants (ppC_3F_6-1, ppC_3F_6-2, and ppC_3F_6-3) exhibited moderate to high albumin adsorption (~100, ~140, ~180 ng/cm², respectively to ppC_3F_6-1, 2, 3). This suggests that ppC_3F_6-3 surface effectively promote albumin binding even in competitive conditions. pCBAA showed minimal albumin adsorption (~5 ng/cm²), consistent with its strong anti-fouling properties that prevent protein attachment.

Albumin Retention percentage

Figure 11 examines albumin adsorption and retention in binary protein solutions containing albumin and FXII. The retention percentile calculation (100*[retention]/[adsorption]) appears in Figure 12, highlighting albumin binding stability on each surface. Glass showed minimal retention (~10%), indicating predominantly weak, reversible albumin binding. PE and PTFE achieved moderate retention (30-40%), demonstrating intermediate binding strength that maintained some albumin after rinsing. PVDF and PVDF-HFP showed enhanced retention (50-60%), indicating improved binding stability compared to glass, PE, and PTFE. Among ppC_3F_6 surfaces, ppC_3F_6-1 and ppC_3F_6-2 exhibited high retention (~70%), while ppC_3F_6-3 achieved the highest retention (>70%), demonstrating exceptional albumin tight-binding stability. These high retention values indicate formation of durable albumin layers on ppC_3F_6 surfaces. pCBAA showed low retention values similar to glass but through a different mechanism, reinforcing its anti-fouling properties that prevent stable albumin binding.

FXII Adsorption in Binary Protein Solution (Competitive Adsorption with Albumin)

Figure 13 illustrates FXII adsorption in a binary protein solution where albumin is also present, showing the competitive adsorption behavior of FXII on each surface. Glass and PVDF displayed the highest FXII adsorption (~70–80 ng/cm²), indicating a strong binding affinity for FXII, even in the presence of competing albumin. This suggests that these surfaces favor FXII binding and may promote thrombotic activity. PTFE and PE demonstrated relatively lower FXII adsorption levels (~45–50 ng/cm²), indicating moderate FXII binding in a competitive setting. This suggests

that while they allow FXII adsorption, the level is reduced compared to PVDF and glass. PVDF-HFP higher FXII adsorption (~70 ng/cm²), suggesting low resistance to FXII binding in the presence of albumin. Among the ppC_3F_6 surfaces, ppC_3F_6-2 and ppC_3F_6-3 showed similar, low FXII adsorption (~20–30 ng/cm²), while ppC_3F_6-1 showed slightly higher FXII adsorption (~35 ng/cm²). This variation suggests that the ppC_3F_6 surfaces allow some FXII binding but may selectively promote albumin adsorption, blocking FXII attachment to an extent. pCBAA exhibited the lowest FXII adsorption (~8 ng/cm²), further demonstrating its resistance to protein adsorption in competitive conditions, consistent with its strong anti-fouling properties.

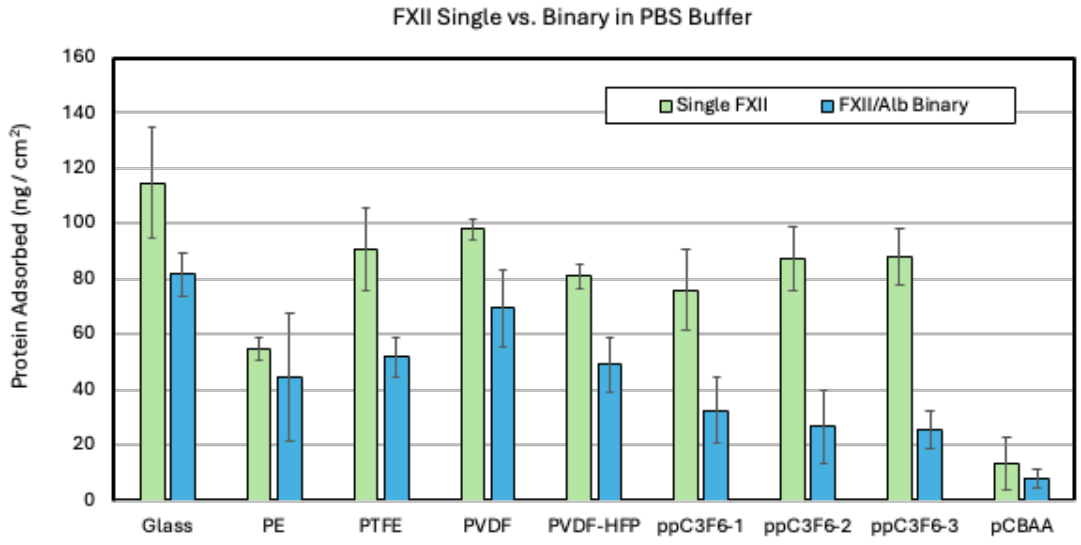

Figure 14. Comparison of FXII Adsorption on Biomaterials in Single-Protein vs. Binary Solutions

Comparison of FXII adsorption in single-protein PBS solution (figure 7) and FXII/Albumin binary solution (figure 12), showing the effect of competitive albumin presence on FXII adsorption. FXII adsorption was reduced on most surfaces in the binary solution, particularly on ppC_3F_6 surfaces, suggesting a shift toward albumin preference.

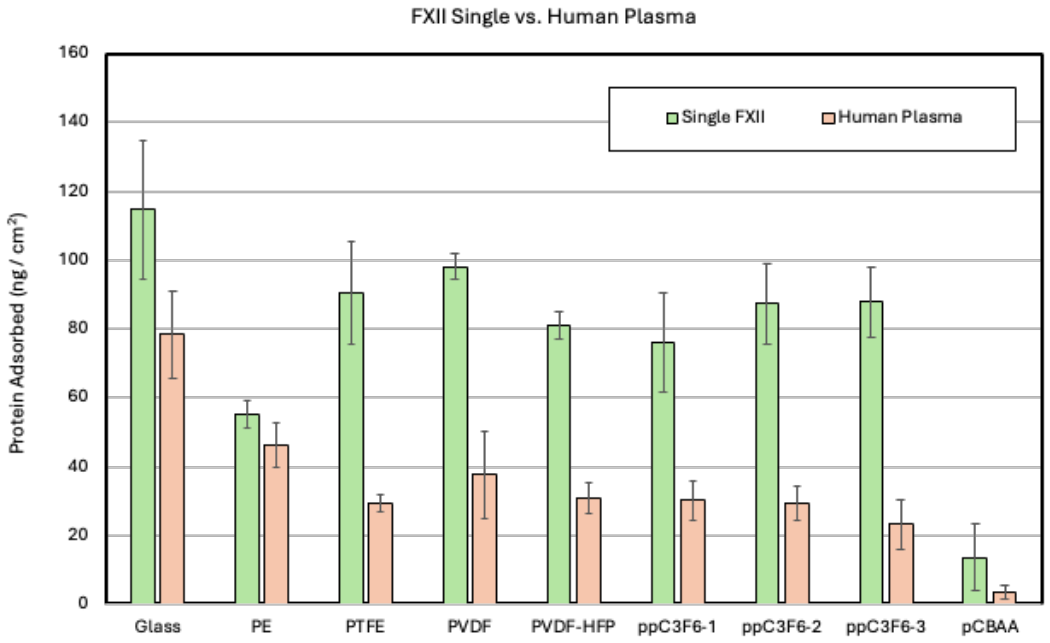

Figure 15. Comparison of FXII Adsorption on Biomaterials in Single-Protein vs. Plasma Environments

Comparison of FXII adsorption from single-protein PBS solution (from Figure 7) and 1% human plasma (from Figure 8), showing the impact of complex protein competition. FXII adsorption decreased significantly in plasma across most surfaces, with pCBAA maintaining minimal FXII binding in both conditions.

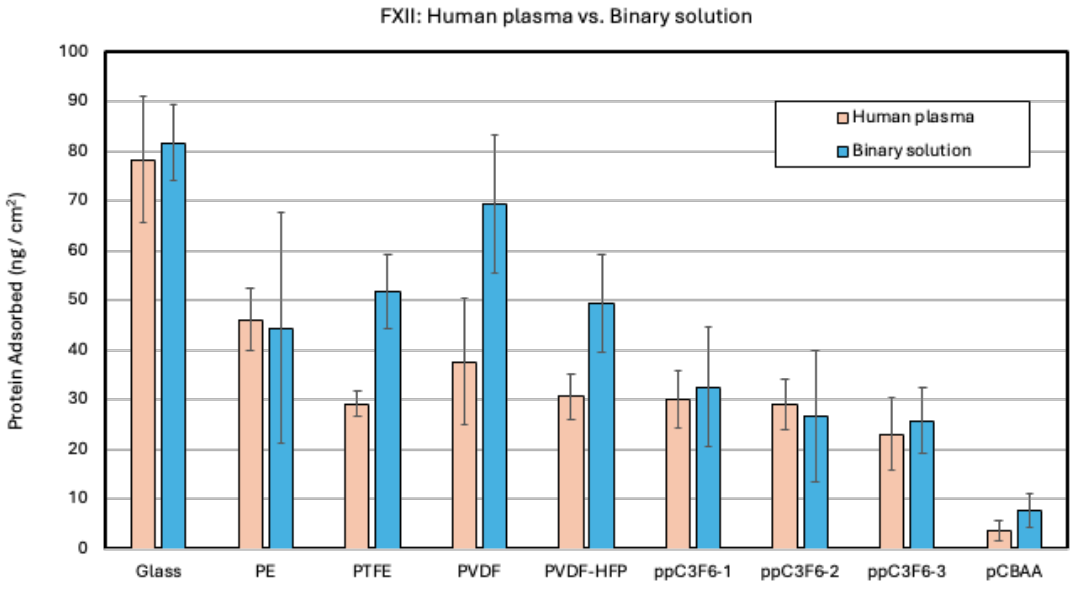

Figure 16. Comparison of FXII Adsorption in Human Plasma vs. Binary Solution

Comparison of FXII adsorption in 1% human plasma (from Figure 8) and FXII/Albumin binary solution (from Figure 12), demonstrating the different impacts of complex plasma proteins and binary competition on FXII binding. FXII adsorption levels were generally lower in plasma, indicating stronger competition for surface binding.

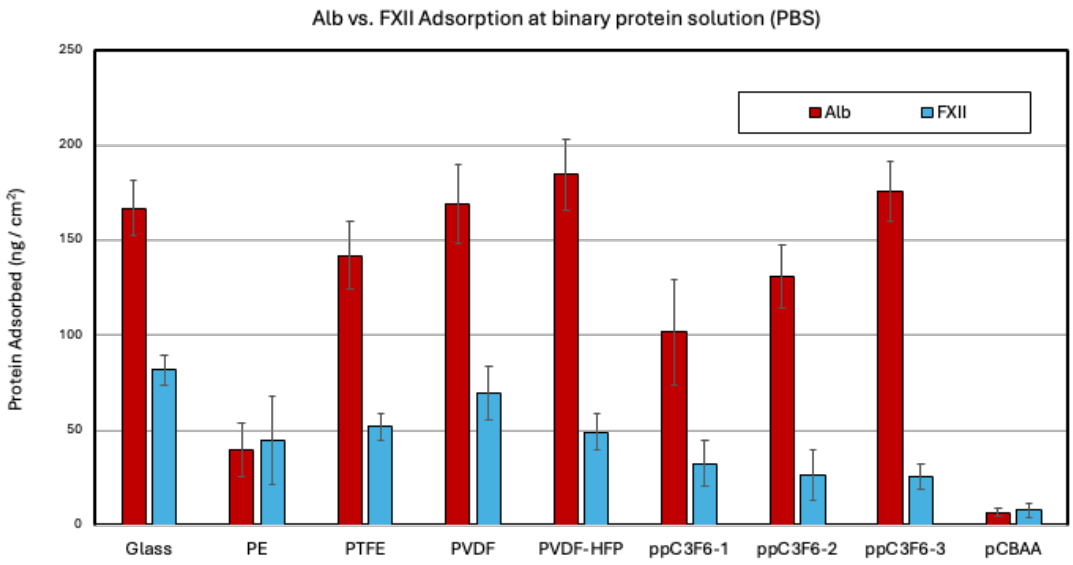

Figure 17. Comparison of Albumin and FXII Adsorption in Binary Solution

Direct comparison of albumin and FXII adsorption in FXII/Albumin binary solution, assessing each surface's selectivity for albumin over FXII. Most surfaces, particularly ppC₃F₆ and pCBAA, showed higher albumin adsorption, suggesting potential for reduced thrombogenicity by forming a protective albumin layer.

Comparison of FXII Adsorption: Single FXII vs. FXII/Albumin Binary Solution

Figure 14 compares FXII adsorption on each biomaterial surface in a single-protein FXII solution versus a binary solution containing both FXII and albumin. This comparison demonstrates the impact of albumin's presence on FXII adsorption levels.

Glass showed the highest FXII adsorption in both conditions, with slightly lower adsorption in the binary solution, indicating moderate competitive binding from albumin. PE and PTFE both exhibited reduced FXII adsorption in the presence of albumin, with levels dropping significantly in the binary solution, suggesting that albumin effectively competes with FXII for surface binding.

PVDF and PVDF-HFP showed a similar result, with reduced FXII adsorption in the binary solution compared to the single-protein solution, indicating that albumin partially displaces FXII on these surfaces. ppC_3F_6 surfaces (ppC_3F_6-1, ppC_3F_6-2, ppC_3F_6-3) also displayed lower FXII adsorption in the binary solution, with ppC_3F_6-3 showing the greatest reduction. This suggests that the ppC_3F_6 surfaces favor albumin adsorption over FXII in competitive conditions. pCBAA exhibited very low FXII adsorption in both conditions, with minimal difference between the single-protein and binary solutions, reflecting its strong anti-fouling properties that resist both proteins.

Comparison of FXII Adsorption: Single FXII vs. Human Plasma

Figure 15 compares FXII adsorption in a single FXII solution versus human plasma, where FXII competes with a range of plasma proteins.

Glass showed the highest FXII adsorption in both conditions, although adsorption decreased significantly in human plasma, suggesting strong competition from other plasma proteins. PE and PTFE both exhibited reduced FXII adsorption in human plasma compared to the single-protein solution, with levels dropping sharply, indicating substantial competition from other proteins in plasma. PVDF and PVDF-HFP also demonstrated reduced FXII adsorption in human plasma, suggesting moderate resistance to FXII binding in a complex protein environment. ppC_3F_6 surfaces showed lower FXII adsorption in human plasma, with ppC_3F_6-3 having the largest reductions. This trend suggests that these surfaces may not favor FXII binding in the presence of diverse plasma proteins. pCBAA again displayed minimal FXII adsorption in both conditions, reflecting its strong resistance to protein attachment even under competitive plasma conditions.

Comparison of FXII Adsorption: Human Plasma vs. Binary Solution

Figure 16 compares FXII adsorption in human plasma versus the binary FXII/Albumin solution, illustrating how adsorption differs between a complex plasma environment and a simpler binary solution.

Glass had the highest FXII adsorption in both conditions, with slightly higher levels in the binary solution than in human plasma. This suggests that FXII adsorption is more competitive in plasma. PE and PTFE showed significantly lower FXII adsorption in human plasma than in the binary solution, indicating that multiple plasma proteins compete more effectively than albumin alone. PVDF and PVDF-HFP demonstrated a similar pattern, with reduced FXII adsorption in human plasma compared to the binary solution, suggesting moderate competitive binding effects. Among ppC_3F_6 surfaces, ppC_3F_6-1 and ppC_3F_6-2 showed the most reduced FXII adsorption in human plasma, suggesting that these surfaces have a preference for albumin over FXII in a competitive plasma environment. pCBAA maintained very low FXII adsorption in both conditions, confirming its high anti-fouling properties.

Comparison of Albumin vs. FXII Adsorption in Binary Solution

Figure 17 compares albumin and FXII adsorption levels in a binary solution containing both proteins, providing insight into each material's selectivity for albumin over FXII.

Glass, PTFE, and PVDF showed high albumin adsorption compared to FXII, indicating a preference for albumin binding in a competitive binary solution. PE exhibited much lower albumin

and FXII adsorption than other surfaces, with albumin levels still higher than FXII, suggesting weaker overall protein binding. PVDF-HFP showed a similar pattern to PVDF, with higher albumin adsorption than FXII, indicating moderate selectivity for albumin in a binary solution. ppC_3F_6 surfaces (ppC_3F_6-1, ppC_3F_6-2, ppC_3F_6-3) showed consistently higher albumin adsorption than FXII, with ppC_3F_6-3 exhibiting the highest albumin adsorption. This indicates that ppC_3F_6 surfaces selectively adsorb albumin, potentially forming a stable, non-thrombogenic layer. pCBAA showed minimal adsorption for both albumin and FXII, confirming its strong anti-fouling properties and resistance to protein binding in a binary environment.

3.4.1.3. Discussion

The comparative analysis across each dataset provides a comprehensive view of FXII and albumin adsorption behaviors on various biomaterial surfaces in both single-protein and competitive conditions. This deeper insight into protein-surface interactions reveals how these materials may perform in blood-contacting applications and highlights key characteristics for reducing thrombogenicity.

FXII Adsorption and Thrombogenic Potential in Single-Protein and Competitive Environments

The single-protein FXII adsorption data (**Figure 8**) shows that **glass** has the highest FXII adsorption, suggesting a strong affinity for FXII due to its surface negative charge, an attractor of the FXII adsorption. This behavior is consistent in competitive environments, as seen in both the FXII/Albumin binary solution (**Figure 14**) and human plasma (**Figure 15**), where glass maintains high FXII adsorption. It indicates a high thrombogenic potential for glass, as its intended employment is to serve as a positive control for the whole intrinsic pathway studies.

PE shows moderate FXII adsorption in both conditions, while PTFE demonstrate relatively higher FXII adsorption in the single-protein solution, but its FXII adsorption drops significantly in the binary and plasma environments (**Figure 14**, **Figure 15**). This suggests that PTFE's hydrophobic surfaces may partially resist FXII adsorption, but not strongly enough to eliminate thrombogenic risk entirely. PVDF and PVDF-HFP showed high FXII adsorption in single-protein conditions, which is further reduced in plasma (**Figure 15**) and the FXII/Albumin binary solution (**Figure 14**). This reduction indicates a moderate resistance to FXII in competitive conditions, suggesting they could have moderate but not very high blood compatibility. The ppC_3F_6 surfaces (ppC_3F_6-1, ppC_3F_6-2, ppC_3F_6-3) show similar trends, with lower FXII adsorption in both competitive environments compared to single-protein conditions. Among the ppC_3F_6 surfaces, ppC_3F_6-3 demonstrated the lowest FXII adsorption in competitive settings, suggesting that the plasma polymerization treatment imparts properties that may favorably impact blood compatibility by reducing FXII binding. pCBAA displayed the lowest FXII adsorption across all conditions, maintaining minimal interaction in both single-protein and competitive environments (**Figure 8**, **Figure 9**, **Figure 14**, **Figure 15**). Its zwitterionic structure likely forms a hydration layer that repels protein adsorption, giving it excellent anti-fouling and anti-thrombogenic properties.

Selective Adsorption of Albumin in Binary Solution (Figure 10, Figure 13, Figure 17)

Albumin is known for its protective, non-thrombogenic role on biomaterial surfaces, as it can block the adsorption of thrombogenic proteins, by forming a passivation layer upon adsorption. The binary FXII/Albumin solution (**Figure 10**) highlights how different surfaces interact with albumin in the presence of FXII, providing insight into their ability to form a stable albumin layer.

Glass, PTFE, and PVDF demonstrated high albumin adsorption in the binary solution, suggesting they may form a protective albumin layer in a dual-protein environment. However, the comparison in **Figure 17** between albumin and FXII adsorption in the binary solution shows that while these materials bind more albumin than FXII, they do not completely prevent FXII adsorption. This indicates that these surfaces could still pose a thrombogenic risk if FXII is not fully blocked by albumin. PE exhibited relatively low adsorption for both albumin and FXII in the binary solution, indicating weak overall protein interactions. This may limit its ability to form a stable albumin layer, thereby diminishing its effectiveness in blood-contacting applications where thrombogenicity needs to be minimized. PVDF-HFP also displayed a relatively high preference for albumin over FXII in the binary solution, suggesting that it may partially support a protective albumin layer. However, this selectivity may not be strong enough for high blood compatibility without further surface modification. Note that, however, PVDF-HFP showed significantly reduced FXII adsorption in the competitive condition, which may improve the blood compatibility second-best to the ppC_3F_6-3 surface. The ppC_3F_6 surfaces, especially ppC_3F_6-3, displayed strong selectivity for albumin over FXII in the binary solution (**Figure 17**), indicating they may preferentially form an albumin passivation layer that could block FXII binding and reduce thrombogenic risk. This selective albumin binding suggests that the RFGD plasma polymerization process enhances the surface's capacity to attract albumin over FXII, thereby improving its potential as a blood-compatible material. Its high albumin tight-binding (high retention) described in **Figure 17**, may attribute to this result. pCBAA showed minimal adsorption for both albumin and FXII in the binary solution, reflecting its strong anti-fouling properties. This material's resistance to protein binding supports its application in scenarios requiring minimal protein interaction and low thrombogenicity.

Impact of Complex Protein Environments: Human Plasma vs. Binary FXII/Albumin Solution (Figure 9, Figure 13, Figure 15, Figure 16)

The human plasma and binary FXII/Albumin solution comparisons reveal how surfaces perform under complex competitive conditions that mimic physiological environments.

In human plasma (**Figure 9**), all surfaces showed reduced FXII adsorption compared to the single-protein solution, reflecting the competitive nature of plasma proteins. Glass continued to show high FXII adsorption in both human plasma and the binary solution (**Figure 16**), suggesting a strong tendency to bind FXII even with competition from other proteins. This persistent FXII binding reinforces the thrombogenic potential of glass, revisiting its role as a positive control in this study. PVDF shows high FXII binding as the competition is lowered, but still exhibits high thrombogenic potential compared to other surfaces in binary solution study, highlighting the need for surface modifications to improve its blood compatibility. PE still showed no significant reductions of FXII adsorption, implying it is not an ideal candidate to be used as a blood compatible surface without further surface modification. PTFE demonstrated further reductions in FXII adsorption in human plasma compared to the binary solution (**Figure 16**), indicating that they are more likely to bind a broader range of plasma proteins rather than FXII alone. While this could moderate its thrombogenicity, the lack of selectivity for non-thrombogenic proteins like albumin may limit its effectiveness in blood-contacting applications. For ppC_3F_6 surfaces, they showed significantly lower FXII adsorption in both plasma and binary solution. This trend suggests that ppC_3F_6 surfaces may preferentially attract albumin over FXII, which could reduce their thrombogenic potential. pCBAA consistently resisted FXII adsorption in both human plasma and the binary solution, indicating that it effectively prevents protein binding even under competitive

conditions. This high anti-fouling capability is beneficial for long-term blood-contacting applications, as it minimizes the risk of thrombosis by preventing unwanted protein interactions.

Overall Implications for Blood-Contacting Applications

The combined data across all conditions highlight the differing blood compatibility potential of each material:

Glass: High FXII adsorption across all conditions indicates a high thrombogenic risk, and it is on the proper context of using glass as a positive control for intrinsic pathway study. Although it adsorbs albumin in competitive environments, it still retains significant FXII, PTFE, PVDF and PVDF-HFP: These surfaces exhibited moderate-to-high thrombogenic potential, suggesting the need for surface modification to enhance their blood compatibility. PE: Moderate FXII adsorption in single-protein solutions and low binding in complex environments indicate reduced thrombogenicity relative to other surfaces. However, its low selectivity for albumin limits its protective capacity. Additional surface treatments may be necessary to improve its albumin-binding potential and reduce FXII activation. ppC_3F_6 Surfaces (ppC_3F_6-1, ppC_3F_6-2, ppC_3F_6-3): These surfaces showed a strong preference for albumin over FXII in binary solutions and reduced FXII adsorption in human plasma. ppC_3F_6-3 performed best overall, demonstrating the highest albumin selectivity and lowest FXII binding in competitive conditions. This selective albumin adsorption and tight-binding phenomena suggests that ppC_3F_6 surfaces, especially ppC_3F_6-3, may effectively form a stable, non-thrombogenic albumin passivation layer that reduces coagulation risks, making them promising for blood-contacting applications. pCBAA: Minimal adsorption of both FXII, albumin, and any other blood proteins in all conditions confirms pCBAA's superior

anti-fouling properties. Its ability to resist protein adsorption altogether makes it ideal for applications requiring minimal thrombogenicity, such as in extracorporeal circuits, vascular grafts, stents, and other long-term blood-contacting devices.

In summary, the combination of single-protein, binary, and plasma conditions reveals critical differences in each material's blood compatibility potential. pCBAA and ppC_3F_6-3 emerge as the most promising surfaces, with pCBAA providing a strong anti-fouling profile and ppC_3F_6-3 showing strong selectivity for albumin and its tight-binding, which may form a protective, non-thrombogenic layer. Conversely, higher FXII fouling across all conditions suggests a higher thrombogenic risk, emphasizing the importance of surface modification to reduce clotting risks in blood-contacting applications. These insights underscore the need for tailored surface engineering to optimize biomaterial's blood compatibility for specific medical applications.

3.4.2. FXIIa activity and bioactivity

The term 'bioactivity' refers to the relative activity of individual protein molecules adsorbed on a surface, offering insights into how protein activity changes with variations in surface chemistry. If the adsorbed FXIIa [23], [72], [73] exhibits limited enzymatic activity due to surface chemistry-protein interactions, high adsorption levels may not necessarily correlate with poor blood compatibility.

3.4.2.1. Methods

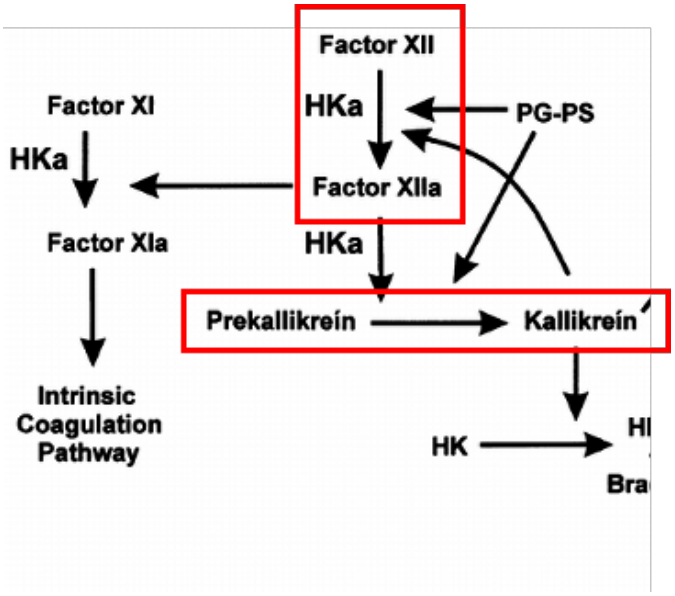

***Scheme 10**. Illustration of the fundamental mechanism of FXIIa activity assay*

FXIIa activity assay

(**Scheme 10**) The experimental design was modified from previous study [18]. 15 mm disc-shaped samples were placed on the bottom of a non-treated 24-well polystyrene culture plate, which covers the whole bottom surface of the plate. Samples were preincubated with PBS, then PBS was removed, and fresh human plasma diluted with Tyrode's buffer was added. The plate was incubated

for 30 minutes at 37 ºC to allow FXII to reach to the sample surface, adsorb, and be activated. During the incubation, the plate was swirled every 10 minutes to distribute the proteins evenly. After 30 minutes of incubation, human plasma was gently removed using a micropipette, and the sample surface was rinsed with PBS to remove unbound protein and other molecules. After 3 times of sequential rinsing, a FXIIa-specific chromogenic substrate (Roche, Boston, MA) with the 5 uM of concentration was introduced. After 30 minutes of incubation with substrate solution, 50 ul of each sample was collected and added to the well with 100 ul of buffer solution in 96 well plates placed on the ice bath to stop further reaction. This transfer results in 3X dilution to measure the FXIIa activity. The optical density (OD) was measured at 405 nm with a plate reader.

FXII bioactivity

The FXII bioactivity is defined as the ratio of FXII activity to FXII adsorption, providing a measure of how active each unit of adsorbed FXII is on a given surface. This approach accounts for both the quantity of FXII adsorbed and the specific activity of the adsorbed protein, addressing the limitations of relying solely on adsorption numbers to evaluate blood compatibility. Using only adsorption levels as an indicator may overlook critical differences in protein behavior; surfaces with similar adsorption levels can exhibit different bioactivities, while surfaces with varying adsorption amounts may display comparable activity levels.

For example, consider two samples: Sample A, with 1000 ng of adsorbed FXII and an activity level of 100, and Sample B, with 100 ng of adsorbed FXII and the same activity level of 100. While both samples achieve identical total activity, the activity per ng of FXII differs markedly; the FXII adsorbed on Sample B is ten times more active per unit than on Sample A. This

comparison highlights the importance of bioactivity as a more comprehensive measure of FXII performance on different surfaces, offering deeper insights into their potential blood compatibility.

3.4.2.2. Results

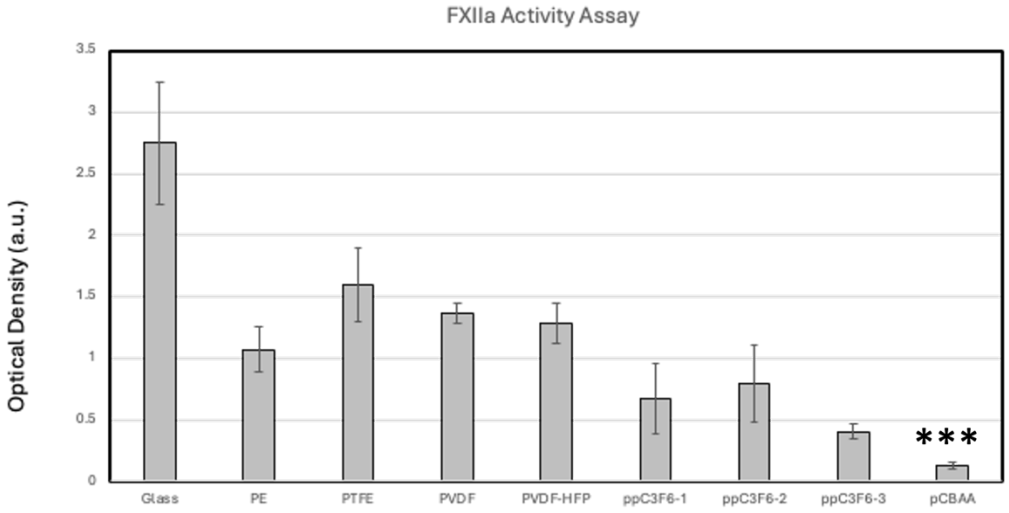

Figure 18. FXIIa Activity on Various Biomaterials in 1% Human Plasma

FXIIa activity measured on each biomaterial surface after incubation in 1% human plasma, reflecting the degree of FXII activation. The Y-axis shows optical density (a.u.), representing FXIIa activity.

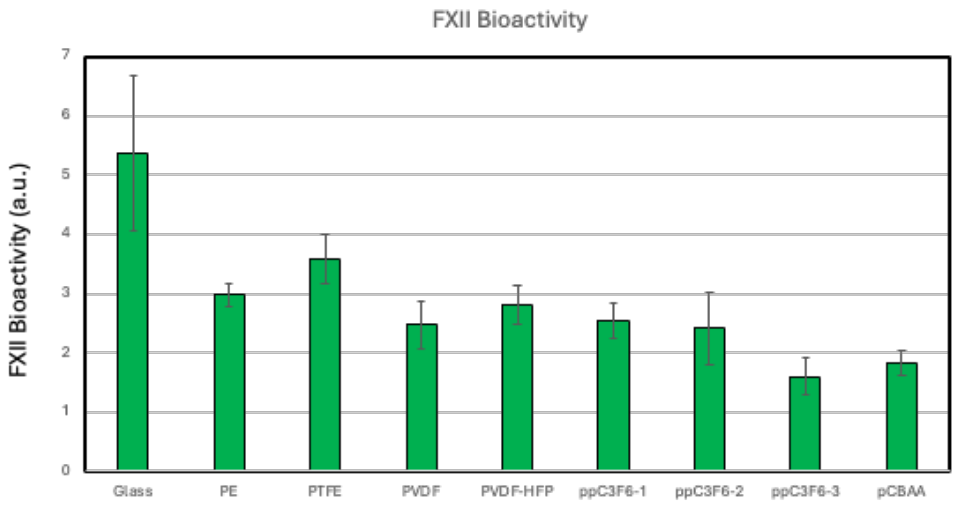

Figure 19. FXII Bioactivity on Biomaterial Surfaces in 1% Human Plasma

FXII bioactivity, defined as the FXIIa activity normalized by the amount of FXII adsorbed (from Figure 8), providing insight into FXII activation efficiency on each surface.

FXIIa Activity in Human Plasma

Figure 18 illustrates the level of FXIIa (activated FXII) on each biomaterial surface after incubation in 1% human plasma. This provides insight into each material's potential to promote FXII activation, which is associated with thrombogenic risk.

Glass displayed the highest FXIIa activity (~2.5 a.u.), indicating strong FXII activation on its surface as intended as the positive control. PE showed moderate FXIIa activity levels, around 1.0 a.u., suggesting a lower FXII activation. PTFE shows relatively high FXIIa activity (~1.5 a.u.), which is still carrying significant FXII activation compared to other surfaces. This suggests that PTFE has a high thrombogenic potential due to its tendency to facilitate FXII activation in plasma. PVDF and PVDF-HFP exhibited high FXIIa activity (~1.3 a.u.), also indicates that these surfaces can be highly thrombogenic. Among the ppC_3F_6 surfaces, ppC_3F_6-3 showed the lowest FXIIa activity (~0.4 a.u.), while ppC_3F_6-1 and ppC_3F_6-2 had slightly higher FXIIa activity levels (~0.7–

0.8 a.u.) than ppC_3F_6-3. The relatively low FXII activation on ppC_3F_6 surfaces suggests that they have a lower tendency to activate FXII, indicating potentially lower thrombogenicity. pCBAA exhibited the lowest FXIIa activity overall (~0.15 a.u.), but regarding the anti-fouling property of zwitterionic polymer, there would be very minimal FXIIa adsorbed and activated on this surface, reflecting high anti-thrombogenic potential.

FXII Bioactivity in Human Plasma

Figure 19 presents the FXII bioactivity on each surface, calculated as the FXIIa activity (**Figure 18**) divided by the amount of FXII adsorbed in human plasma (**Figure 9**). This bioactivity value represents the relative activation potential of the adsorbed FXII on each surface, showing how effectively each unit of FXII is activated.

Glass demonstrated the highest FXII bioactivity value, reinforcing that not only does glass adsorb significant amounts of FXII, but it also strongly promotes its activation. This suggests that FXII adsorbed on glass is highly active, and it aligns with the experimental design for using glass as a positive control. **PTFE** exhibited intermediate FXII bioactivity, suggesting a moderate activation efficiency of FXII on this surface. **PE, PVDF** and **PVDF-HFP** showed lower FXII bioactivity than glass, indicating that while FXII adsorbs to these surfaces, its activation per unit is less efficient than on PTFE. This supports a moderate thrombogenic potential comparative to PTFE.

The ppC_3F_6 surfaces (ppC_3F_6-1, ppC_3F_6-2, and ppC_3F_6-3) showed relatively low FXII bioactivity, particularly ppC_3F_6-3, which had the lowest value among the ppC_3F_6 variants. This implies that while these surfaces adsorb FXII, the activation efficiency of the adsorbed FXII is reduced, supporting the lower thrombogenic potential.

pCBAA demonstrated the low FXII bioactivity, and again, this is presumably because of the protein anti-fouling property, as the adsorption on this surface is the lowest at any condition of radiolabeled protein adsorption assay.

3.4.2.3. Discussion

The comparative FXIIa activity and bioactivity data reveal distinct patterns of FXII activation across the various biomaterial surfaces, with pCBAA and ppC_3F_6 surfaces (particularly ppC_3F_6-3) emerging as particularly promising candidates for reducing thrombogenic risk.

Outstanding Anti-Thrombogenic Performance of pCBAA

pCBAA demonstrated the lowest FXIIa activity and low FXII bioactivity, indicating that both FXII adsorption and activation are minimized on this surface. The zwitterionic properties of pCBAA likely form a highly hydrated layer that effectively resists protein adsorption, thus reducing FXII attachment to an ultralow level. As FXII activity was measured across the entire surface, the minimal activity observed can be attributed to the low amount of adsorbed FXII rather than any strong inactivation effect of the surface itself. This ability to resist both adsorption and activation supports pCBAA's potential as an ideal material for blood-contacting applications where minimizing coagulation and thrombosis is essential. The pCBAA surface's performance aligns with its known anti-fouling properties, making it suitable for applications like vascular grafts and stents where sustained blood compatibility is required.

Reduced FXII Activation on ppC_3F_6 Surfaces

The ppC_3F_6 surfaces—particularly ppC_3F_6-3—also displayed low FXIIa activity and bioactivity, second only to pCBAA. The relatively low FXII activation on these surfaces suggests that the unique properties imparted by RFGD plasma polymerization contribute to reduced FXII bioactivity. Unlike traditional fluoropolymers, the plasma polymerization process likely creates a surface with specific chemical characteristics that inhibit FXII conformational changes necessary for activation. The fluorochemistries and hydrophobic nature of ppC_3F_6 surfaces may facilitate a tight and stable binding of proteins, which could limit the accessibility of FXII's activation sites. Previous research has shown that FXII activation is primarily driven by cleavage at the Arg353-Ile354 bond within its heavy chain [14], [15], [24], a process that could be hindered if the heavy chain region is inaccessible or immobilized upon adsorption.

The precise mechanism by which ppC_3F_6 surfaces reduce FXIIa activity remains uncertain. One possibility is that the plasma polymerization creates surface properties that restrict the conformational mobility of adsorbed FXII, thereby blocking access to critical activation sites. This potential restriction warrants further investigation to assess how plasma polymerization influences FXII structure upon adsorption and to determine whether these conformational effects are unique to ppC_3F_6 or extend to other plasma-polymerized fluoropolymers.

Higher FXII Activation on Conventional Hydrophobic Surfaces

In contrast, PTFE, PVDF, and PVDF-HFP—all hydrophobic surfaces—exhibited relatively higher FXII bioactivity than ppC_3F_6 surfaces, despite sharing similar hydrophobic characteristics. The elevated bioactivity values on these surfaces suggest that they do not impose the same "inactivation" potential that we anticipate from ppC_3F_6. This supports the hypothesis that the RFGD plasma

polymerization of ppC_3F_6 possibly creates distinct properties that influence protein behavior differently than conventional hydrophobic surfaces.

Hydrophobic interactions are known to drive protein adsorption, often leading to conformational changes in proteins that facilitate their activation. However, the higher FXII bioactivity observed on PTFE, PVDF, and PVDF-HFP indicates that FXII retains sufficient flexibility on these surfaces to undergo activation. This suggests that while these materials adsorb FXII efficiently, they may lack the specific surface chemistries or binding constraints necessary to inhibit FXII activation, potentially leading to higher thrombogenic potential in blood-contacting applications.

Implications for Blood-Contacting Applications

These findings highlight the significance of both adsorption resistance and selective inhibition of protein activation in designing blood compatible surface. **pCBAA** stands out as the most effective surface for minimizing thrombogenic risk due to its ultra-low adsorption and minimal FXII activation, making it well-suited for applications where high blood compatibility is critical.

The ppC_3F_6 surfaces also show promising potential, particularly ppC_3F_6-3, which demonstrated a low bioactivity for FXII, suggesting that it might offer a good balance of protein resistance (by preferential binding of albumin over FXII) and possible FXII inactivation. The plasma-polymerized fluorochemistry unique to ppC_3F_6 surfaces appears to impart specific characteristics that limit FXII activation more effectively than standard hydrophobic surfaces like PTFE and PVDF. It indicates that ppC_3F_6 surfaces could also serve as a potential option for blood-contacting applications.

PTFE, PVDF, and PVDF-HFP showed moderate to high FXII bioactivity, reflecting their inability to prevent FXII activation. Their performance highlights the limitations of traditional hydrophobic surfaces in reducing thrombogenicity, as they may still support FXII activation unless modified to mitigate the enzymatic activity, presumably by imposing additional constraints on protein conformation.

To summarize, the combination of FXII adsorption and bioactivity assessments provides a nuanced understanding of each material's thrombogenic risk. pCBAA demonstrates the strongest anti-thrombogenic properties, making it ideal for long-term blood-contact applications. ppC_3F_6 surfaces offer a unique advantage through RFGD plasma polymerization, which appears to suppress FXII activation, though the exact mechanism remains to be studied further. By contrast, traditional hydrophobic materials such as PTFE, PVDF, and PVDF-HFP exhibit limited capacity to restrict FXII activation, suggesting that surface modification or alternative material choices would be necessary to improve their blood compatibility.

3.5. Summary

This chapter systematically evaluated FXII and albumin adsorption, FXII activation, and bioactivity on various biomaterial surfaces to determine their thrombogenic potential and suitability for blood-contacting applications. **Below are key findings of this chapter.**

pCBAA's Superior Anti-Fouling and Anti-Thrombogenic Properties:

The zwitterionic **pCBAA** surface showed the lowest FXII and albumin adsorption, FXII activation, and FXII bioactivity, indicating outstanding anti-thrombogenic properties. The highly hydrated layer on pCBAA effectively repels proteins, making it ideal for applications that require strong resistance to coagulation, such as vascular grafts and stents.

Promising Performance of ppC_3F_6 Surfaces:

ppC_3F_6 surfaces, particularly ppC_3F_6-1, demonstrated low FXII activation and selective albumin binding, likely due to surface characteristics imparted by RFGD plasma polymerization. The plasma-polymerized fluorochemistry may induce a tight protein binding that limits FXII activation, suggesting these surfaces as moderate anti-thrombogenic options. Further study on the mechanism behind this selective binding would enhance their application potential.

Higher Thrombogenicity of Fluoropolymers:

PTFE, PVDF, and **PVDF-HFP**, traditional fluoropolymers, showed higher FXII adsorption and activation, indicating a greater thrombogenic risk. Although they attract proteins, they do not inhibit FXII activation effectively, underscoring the limitations of standard fluoropolymers for blood-contacting applications.

Implications for Biomaterial Selection:

The findings highlight that effective blood compatibility requires not only reducing protein adsorption but also limiting protein activation. pCBAA and ppC_3F_6 surfaces (especially ppC_3F_6-3) demonstrate strong potential as blood compatible biomaterials, while other fluoropolymers need substantial modifications to mitigate thrombogenic risks.

This study underscores the importance of surface engineering to optimize blood compatibility. pCBAA offers the outperformed blood compatibility, while ppC_3F_6 surfaces provide a promising balance of protein selectivity and reduced FXII activation. In contrast, PTFE, PVDF, and PVDF-HFP may require modifications for safe use in blood-contacting applications. These insights inform the development of advanced biomaterials that can minimize thrombosis and improve patient outcomes in clinical use.

Chapter 4. Vroman Effect and Albumin Tight-Binding

Remark of Chapter 4

In our early PhD research phases, we approached blood compatibility without strictly separating intrinsic and extrinsic pathways. These initial studies examined competitive adsorption between albumin and fibrinogen to evaluate albumin's resistance to displacement by fibrinogen, a process driven by the Vroman effect[25], [26], [27], [28], [74], [75]. The proteins studied, arranged by increasing molecular size, included albumin, Factor XII (FXII), and fibrinogen, with fibrinogen being the largest. This size hierarchy suggests fibrinogen's dominance in Vroman effect displacement processes.

Chapter 3 demonstrated that albumin's tight binding on ppC_3F_6 surfaces resisted FXII displacement, establishing albumin's stable interaction within an intrinsic pathway context. Chapter 4 expands beyond this perspective, investigating whether albumin's tight binding on ppC_3F_6 can withstand displacement by fibrinogen, a protein four times larger that typically dominates Vroman displacement processes. Therefore, this chapter serves not as a rigid pathway classification but as a broader exploration of the Vroman effect's impact on blood compatibility, particularly through examination of albumin tight binding against displacement by larger proteins.

4.1. Revisiting Vroman Effect and Albumin Tight-Binding

While we previously discussed the Vroman effect, we return to it here to explore additional aspects of protein adsorption and albumin tight binding on ppC_3F_6 surfaces. Albumin functions as a passivating protein upon surface contact, reducing immunogenic reactions. Its adsorption creates

a stable passivation layer that inhibits nonspecific protein adsorption and prevents the immune system from recognizing the surface as foreign, thereby limiting inflammatory responses. However, in the context of the Vroman effect, larger proteins such as fibrinogen or FXII can displace albumin. The displacement of albumin may vary depending on the surface-albumin binding affinity and tightness. A tighter binding of albumin could resist the Vroman effect and thereby improve blood compatibility.

4.2. Methods

Radiolabeled Albumin and Fibrinogen Competitive Adsorption/Retention Assay

We preincubated all samples with cPBS solution containing 10 mM NaI (cPBSzI) for 1 hour before protein adsorption assays[49], [52], [70], [76], [77]. We conducted protein adsorption studies using competitive binary solutions containing albumin and fibrinogen at 1% plasma concentrations (0.3 mg/ml albumin, 0.03 mg/ml fibrinogen). We created "hot protein" solutions by adding radiolabeled protein to achieve approximately 100 CPM/ng activity. After 2-hour surface exposure, we performed triple cPBSzI rinses to remove unbound proteins. We measured sample radioactivity for 1 minute alongside protein standards using a Perkin-Elmer gamma counter, reporting adsorption data in ng/cm².

For retention studies, we immersed samples in 2% sodium dodecyl sulfate solution for 12 hours, followed by triple cPBSzI rinses. We conducted radioactivity measurements identical to the adsorption study, reporting retention in ng/cm². We calculated retention percentages as (retention/adsorption)*100.

Quartz Crystal Microbalance Dissipation (QCM-D) Study

QCM-D is an *in situ*, real time, and label-free surface analysis technique that bringing up the surface-protein interaction [78], [79], [80]. In collaboration with Sherry Liu, a former PhD student in our group, we conducted QCM-D analyses to further understand the protein-surface interaction at the plasma-polymerized fluoropolymer. The detailed theoretical framework and fundamentals are described in Sherry Liu's 2023 PhD dissertation from University of Washington Bioengineering [81]. We introduced single albumin solution to establish an albumin passivation layer on ppC_3F_6-coated QCM-D sensors, then switched to single fibrinogen solution to evaluate albumin binding stability. This approach allowed us to assess surface resistance to the Vroman effect by measuring the degree of albumin displacement by fibrinogen.

4.3. Results

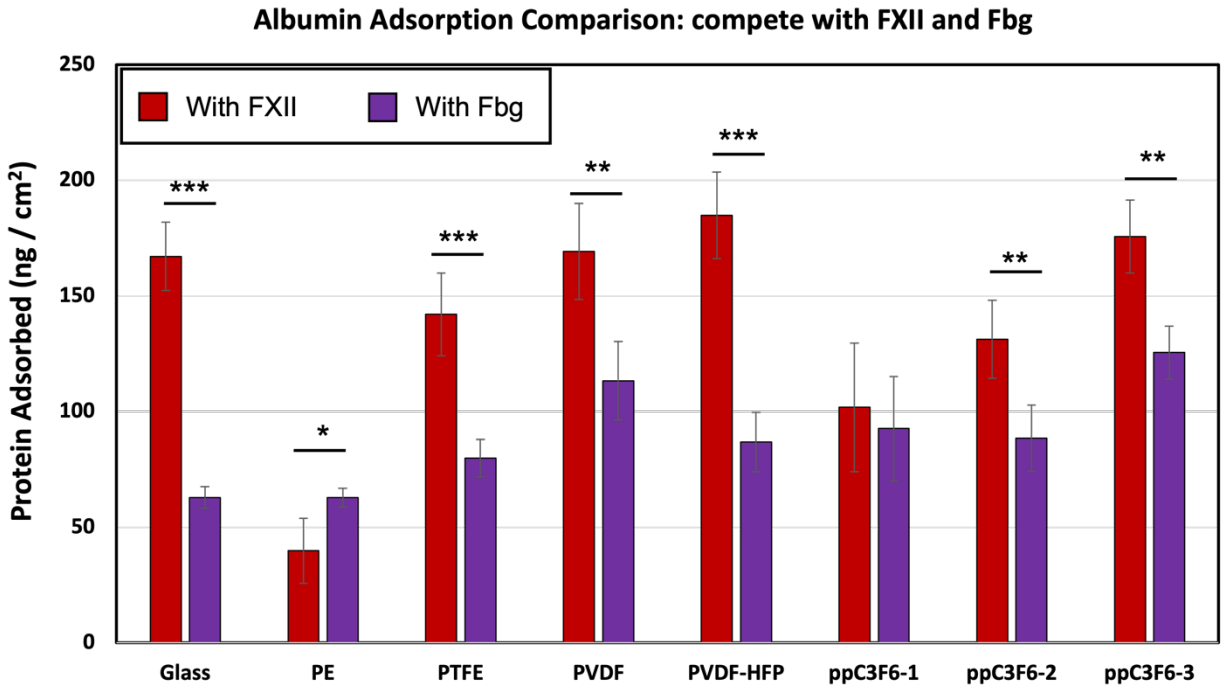

Figure 20. Competitive Albumin Adsorption Comparison*. Red bar indicates albumin adsorption in competition with FXII, while purple indicates competition with fibrinogen.*

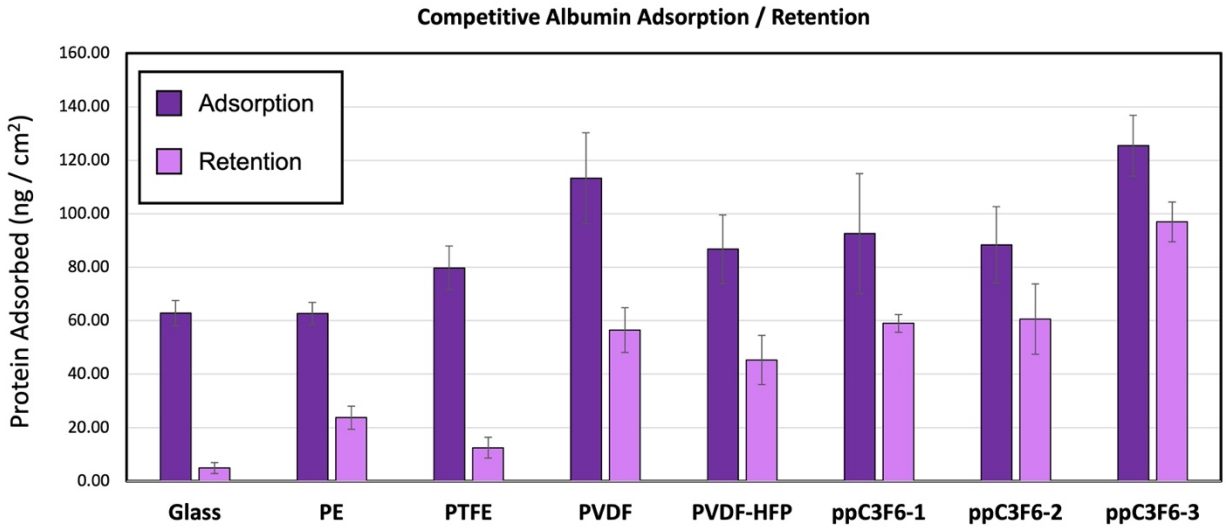

Figure 21. Albumin Adsorption and Retention on Biomaterial Surfaces in Albumin/Fibrinogen Binary Solutions

Initial albumin adsorption (dark purple bars) and retention after rinsing (pink bars) on various biomaterial surfaces after exposure to a binary solution of albumin and fibrinogen. The Y-axis represents adsorbed albumin in ng/cm².

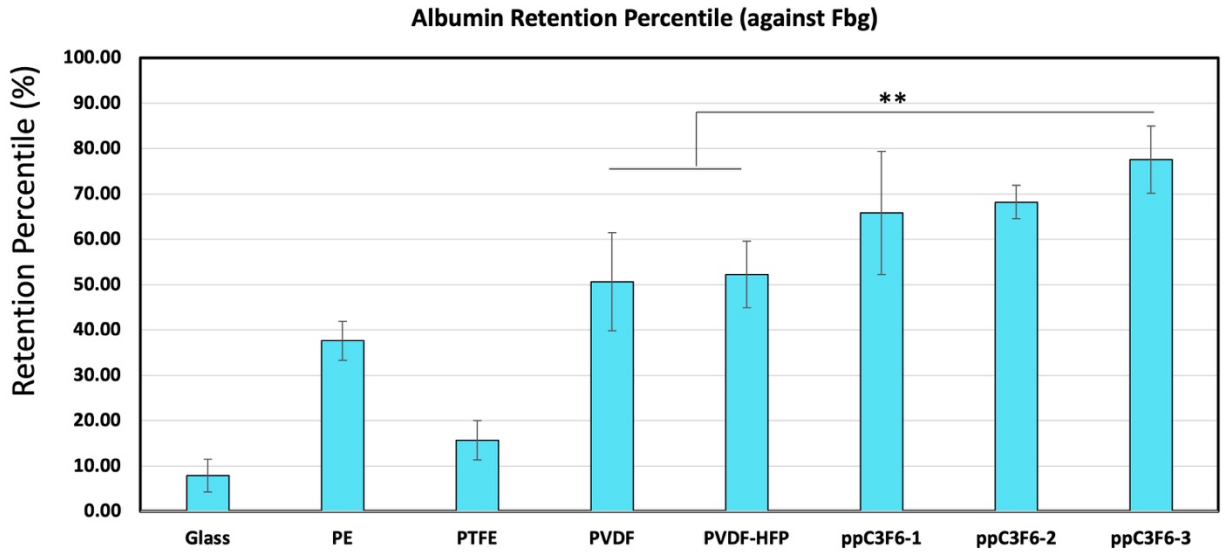

Figure 22. Albumin Retention Precentage on Biomaterial Surfaces. *Percentage of initially adsorbed albumin retained after rinsing, calculated as 100 × [retention]/[adsorption]. The Y-axis represents retention percentage (%).*

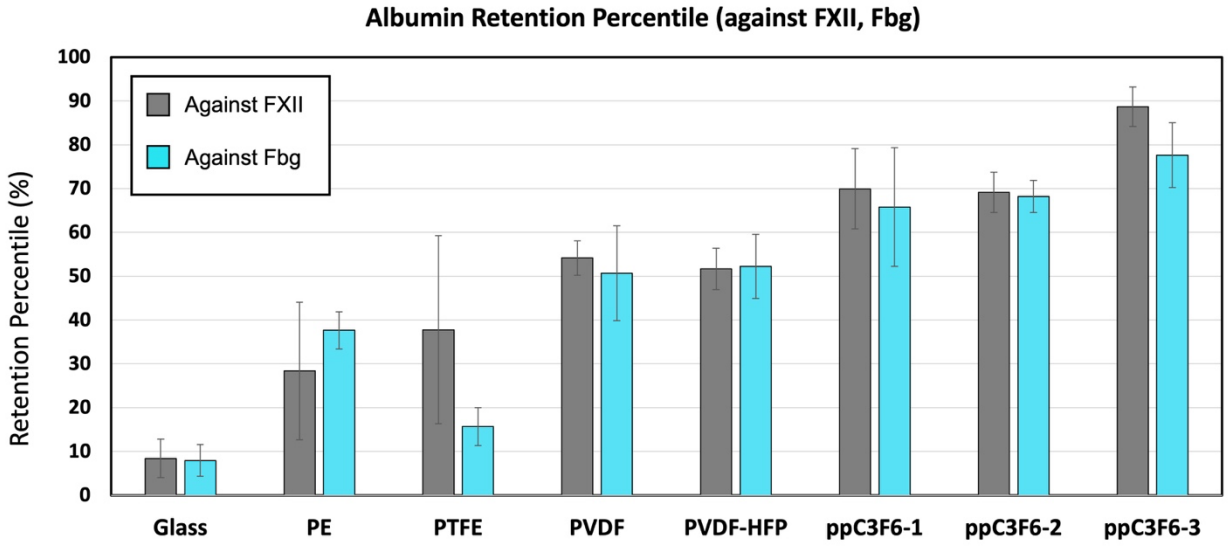

Figure 23. Competitive Albumin Retention Comparison. *Grey bar plot indicates Albumin retention percentage in competition with FXII, and teal bar with Fbg*

Albumin Adsorption and Retention in Binary Solution

Figure 20 illustrates albumin adsorption and retention on biomaterial surfaces exposed to binary solutions of albumin with FXII (red) and albumin with fibrinogen (purple). PVDF demonstrated highest initial albumin adsorption (~120 ng/cm²), followed by PVDF-HFP (~100 ng/cm²), indicating strong albumin affinity in competitive environments. ppC_3F_6 surfaces showed moderate albumin adsorption (~70-80 ng/cm²), suggesting selective binding affinity, though lower than PVDF-based surfaces. PE and PTFE exhibited moderate adsorption (~80-100 ng/cm²), while glass showed minimal adsorption, indicating weak albumin binding in fibrinogen's presence. Post-rinse retention levels revealed that ppC_3F_6 surfaces maintained substantial initially adsorbed albumin (~50-60 ng/cm²), demonstrating stable binding, while glass retained minimal amounts, confirming weak albumin interactions.

Albumin Retention Percentage

Figure 21 presents competitive albumin adsorption and retention data, while **Figure 22** shows the percentage of retained albumin relative to initial adsorption, reflecting surface-specific binding stability. ppC_3F_6 surfaces exhibited highest retention percentages (~80-90%), indicating sustained albumin binding after rinsing and suggesting strong, stable interactions. PVDF and PVDF-HFP showed intermediate retention (~60-70%), demonstrating moderately stable albumin binding compared to ppC_3F_6. Glass, PE, and PTFE showed lowest retention, with glass retaining less than 10% of initial albumin, indicating weak, reversible binding. **Figure 23** compares albumin retention percentiles against FXII (grey) and fibrinogen (teal). Except for PE, most surfaces showed

decreased albumin retention when competing with fibrinogen, consistent with expectations that larger proteins enhance Vroman effect efficiency.

Fibrinogen Adsorption and Retention in Binary Solution

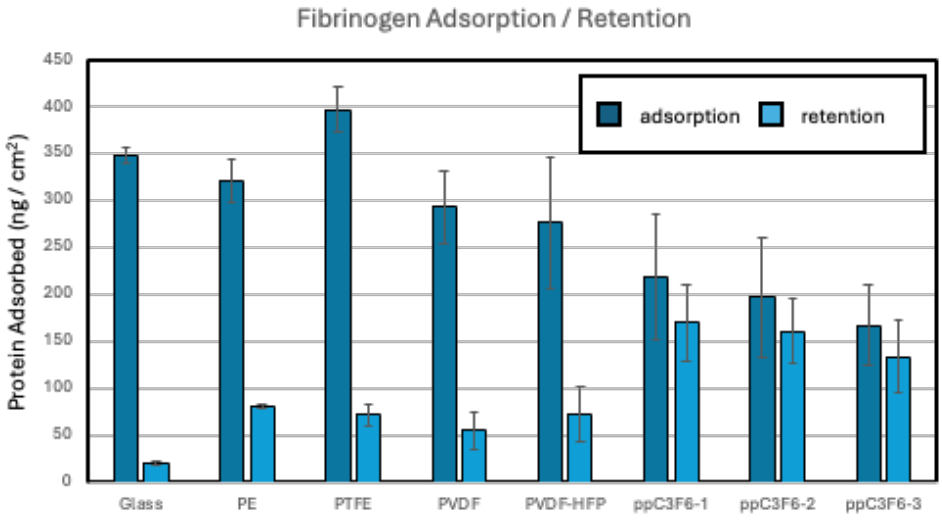

Figure 24. Fibrinogen Adsorption and Retention on Biomaterial Surfaces in Albumin/Fibrinogen Binary Solution

Initial fibrinogen adsorption (dark brown bars) and retention after rinsing (light yellow bars) on various biomaterial surfaces after exposure to a binary solution of albumin and fibrinogen. The Y-axis represents adsorbed fibrinogen in ng/cm².

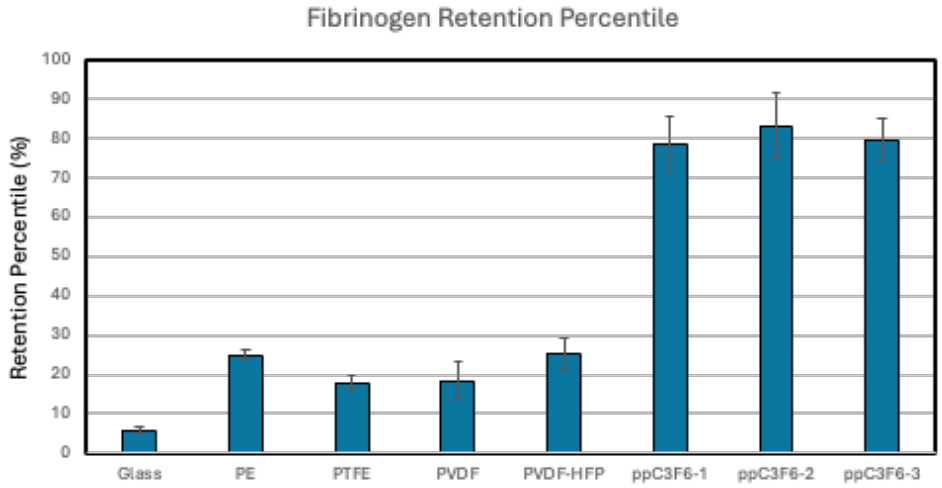

Figure 25. Fibrinogen Retention Percentage on Biomaterial Surfaces

Percentage of initially adsorbed fibrinogen retained after rinsing, calculated as 100 × [retention]/[adsorption]. The Y-axis represents retention percentage (%).

Figure 24 presents fibrinogen adsorption and retention data from albumin/fibrinogen binary solutions. PTFE exhibited highest fibrinogen adsorption (~400 ng/cm²), followed by PE and glass, indicating strong fibrinogen affinity. ppC_3F_6 surfaces showed lower fibrinogen adsorption (~100-200 ng/cm²), demonstrating moderately low initial affinity. After rinsing, ppC_3F_6 surfaces retained significant fibrinogen compared to other surfaces, suggesting strong binding stability, while glass showed minimal retention, indicating weak, reversible fibrinogen binding.

Fibrinogen Retention Percentage

Figure 25 demonstrates fibrinogen retention percentages relative to initial adsorption. ppC_3F_6 surfaces again showed highest retention (~80-90%), indicating stable fibrinogen binding post-rinse. PE, PTFE, PVDF, and PVDF-HFP demonstrated moderate retention (~20-30%), reflecting relatively stable though weaker fibrinogen attachment compared to ppC_3F_6 surfaces. Glass showed lowest retention, maintaining less than 10% fibrinogen, indicating weak and readily reversible binding.

QCM-D Sequential Protein Displacement Study

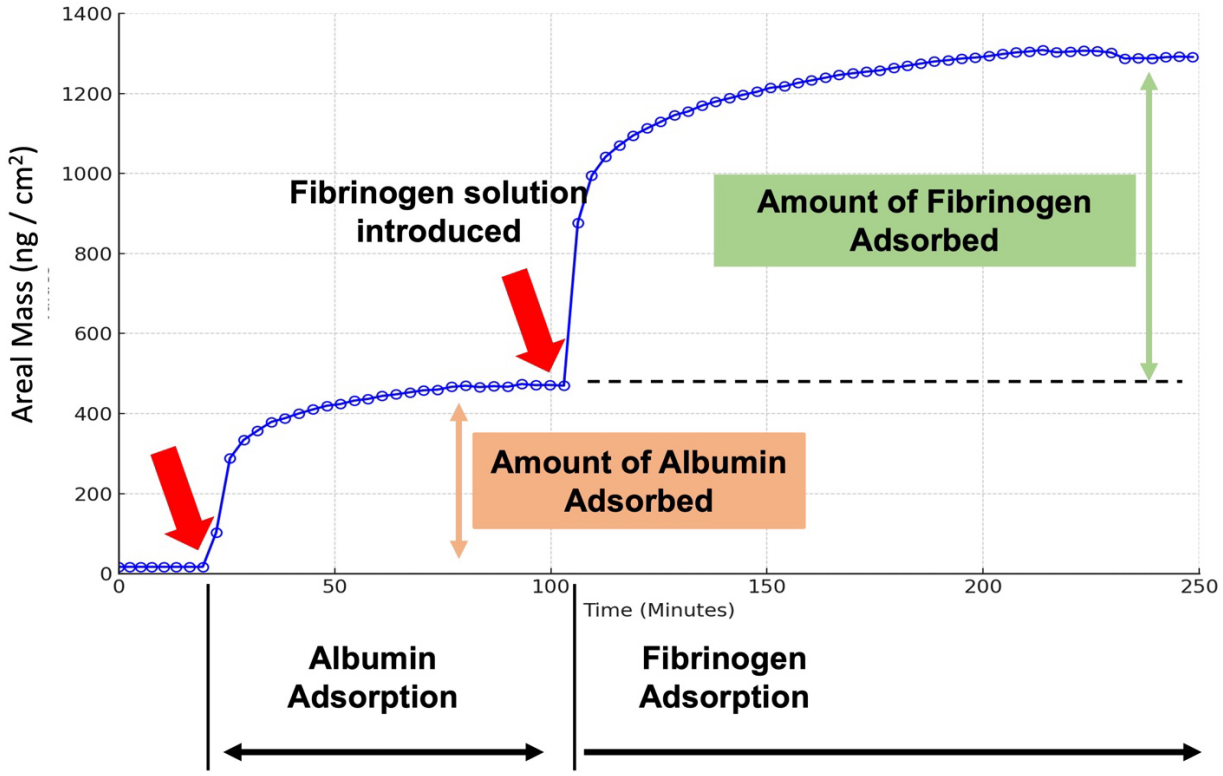

Scheme 11. Interpretation of QCM-D plot in sequential protein displacement study result

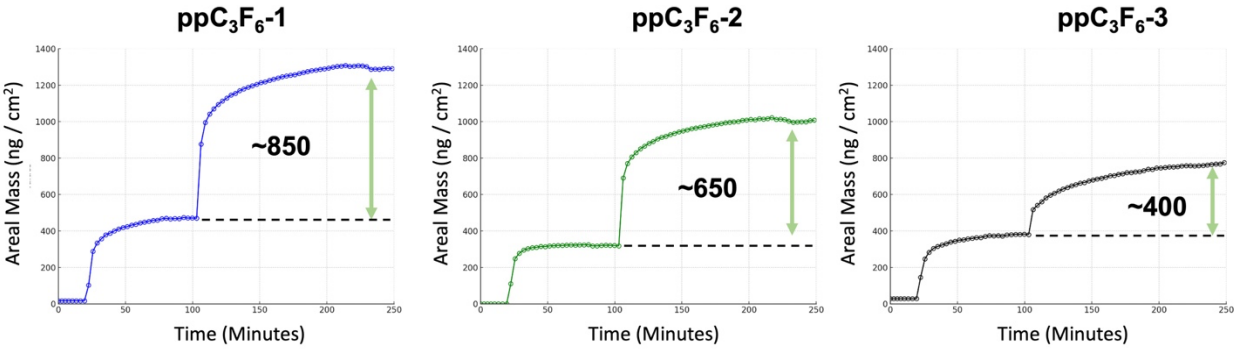

Figure 26. QCM-D sequential protein displacement study result for three ppC₃F₆ surfaces compared

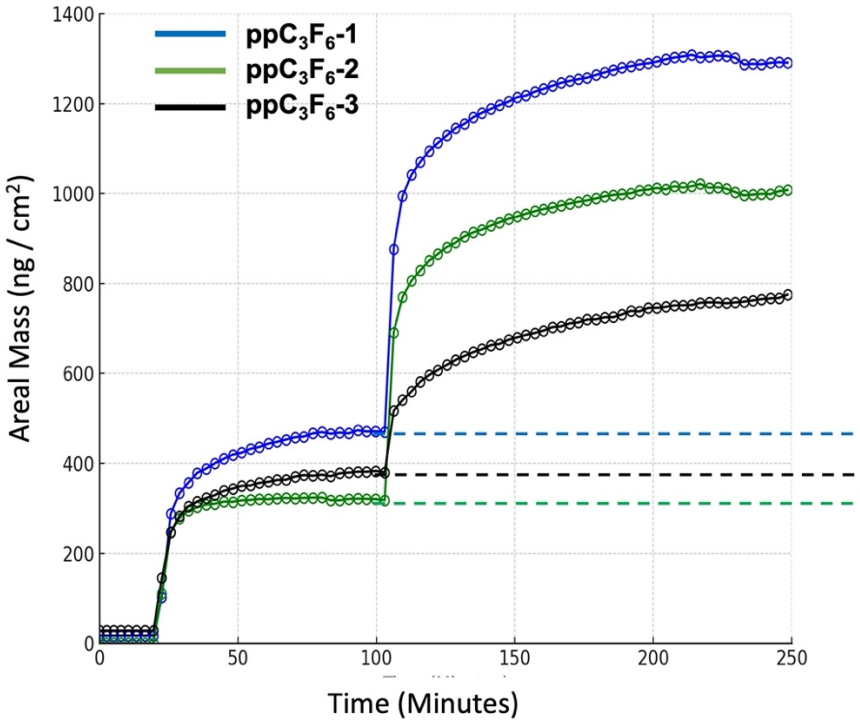

Figure 27. Comparing three QCM-D results. *Three curves compared in one plot for the relative understanding of albumin and fibrinogen behavior at the surface of three ppC_3F_6 groups*

Scheme 11 illustrates interpretation of QCM-D results. Initial flat phases indicate pre-protein exposure, followed by first mass increase around 20 minutes upon albumin introduction. The first plateau indicates stabilized albumin adsorption. Second mass increase occurs upon switching to fibrinogen solution, with the difference between plateaus indicating albumin displacement extent. Lower mass increase suggests higher Vroman effect resistance. **Figure 26** shows distinct responses for each ppC_3F_6 surface: ppC_3F_6-1 showed ~850 ng fibrinogen increase, while ppC_3F_6-2 and ppC_3F_6-3 showed ~650 and ~400 ng increases respectively. This suggests ppC_3F_6-3 exhibits highest Vroman effect resistance through reduced albumin displacement. Though ppC_3F_6-1 showed highest initial albumin adsorption (**Figure 27**), ppC_3F_6-3 demonstrated superior overall albumin binding stability.

4.4. Discussion

The albumin and fibrinogen adsorption and retention results provide crucial insights into each biomaterial's resistance to the Vroman effect. Chapter 3's intrinsic studies demonstrated albumin's ability to resist FXII displacement, forming a protective, stable layer that potentially reduces thrombogenicity. Here, we extend that analysis to fibrinogen, which presents a greater displacement challenge due to its larger size and strong surface affinity[82], [83] . By evaluating albumin's competitive binding against fibrinogen, we better understand each surface's capacity to maintain an anti-thrombogenic albumin layer. Figure 23 reveals greater albumin displacement when competing with fibrinogen compared to FXII, consistent with molecular size effects. Only PE showed increased albumin retention in albumin-fibrinogen binary solutions, a behavior inconsistent with typical Vroman effect patterns. However, the overall trend confirmed fibrinogen's superior ability to displace albumin. Among all surfaces, ppC_3F_6-3 demonstrated superior Vroman effect resistance through enhanced albumin tight binding capacity.

ppC_3F_6 Surfaces: Strong Resistance to the Vroman Effect

The ppC_3F_6 surfaces demonstrated exceptional retention percentages for both albumin and fibrinogen, with albumin retention exceeding 80-90%. This indicates their ability to maintain stable albumin binding even in fibrinogen's presence. The sustained albumin retention suggests effective resistance to the Vroman effect, potentially maintaining a durable, non-thrombogenic albumin layer.

High retention percentages for both proteins indicate that RFGD plasma polymerization creates unique surface properties enabling strong, irreversible protein interactions. This binding stability

proves particularly advantageous in blood-contacting applications, where a firmly bound albumin layer could prevent larger thrombogenic protein adsorption. By resisting displacement, ppC_3F_6 surfaces may reduce long-term thrombotic risks, making them promising candidates for extended blood exposure applications.

Among ppC_3F_6 variants, ppC_3F_6-3 demonstrated superior stability of pre-formed passivating albumin layers through tight binding, evidenced by minimal fibrinogen adsorption in QCM-D studies. While radiolabeled protein and QCM-D results show some discrepancies due to different experimental conditions (binary versus sequential protein exposure), both methods support ppC_3F_6-3's superior albumin binding stability.

Moderate Displacement Resistance on PVDF and PVDF-HFP

PVDF and PVDF-HFP surfaces showed moderate albumin retention percentages (~60-70%), indicating partial resistance to fibrinogen displacement. These surfaces maintained significant adsorbed albumin after rinsing, suggesting formation of a moderately stable layer, though not as robust as ppC_3F_6 surfaces. Their retention of both albumin and fibrinogen indicates partial Vroman effect resistance, though they may experience protein exchange during extended plasma exposure.

The moderate albumin stability on these surfaces could benefit short-term blood-contacting applications by forming protective albumin layers that prevent immediate fibrinogen adsorption. However, their lower retention compared to ppC_3F_6 surfaces suggests reduced effectiveness for long-term applications where sustained Vroman effect resistance is essential.

Low Displacement Resistance on PE, and PTFE

PE, and **PTFE** demonstrated the lowest retention percentages for both albumin and fibrinogen, with albumin retention values under 30%. These low retention rates suggest weak and easily

reversible protein binding, making these surfaces highly susceptible to the Vroman effect. The data imply that albumin bound to these surfaces can be readily displaced by larger proteins like fibrinogen, which would lead to a higher thrombogenic risk over time.

In blood-contacting applications, surfaces that do not resist displacement are likely to experience dynamic protein exchange, allowing thrombogenic proteins such as fibrinogen to dominate the surface. This characteristic makes PE and PTFE less suitable for use in long-term blood-contact devices without significant surface modification to enhance protein retention. Their high susceptibility to displacement underscores the need for coatings or treatments that improve albumin's binding stability.

To summarize, this study reinforces protein retention and Vroman effect resistance as crucial factors in developing blood-compatible biomaterials. ppC_3F_6 surfaces show strong potential for blood-contacting applications through robust resistance to albumin displacement by fibrinogen. ppC_3F_6-3 particularly demonstrated superior Vroman effect resistance. Conversely, PVDF, PVDF-HFP, and especially PE and PTFE showed limitations in protein exchange resistance, suggesting unsuitability for long-term blood exposure without modification. These findings emphasize the importance of surface engineering for optimized protein retention and stability in clinical applications.

4.5. Summary

ppC_3F_6 surfaces demonstrated strong tight-binding characteristics for both albumin and fibrinogen, exhibiting robust resistance to the Vroman effect's size-dependent protein displacement. Building on Chapter 3's findings of improved blood compatibility, we anticipate enhanced performance in

not only the intrinsic pathway, but also could be extended to the extrinsic pathway, particularly regarding fibrinogen-driven thrombus formation through platelet recruitment. Further platelet and fibrinogen bioactivity studies may illuminate how RFGD plasma-polymerization affects surface properties, potentially revealing fibrinogen inactivation upon adsorption. These combined properties—albumin tight binding and thrombogenic protein inactivation - may significantly benefit blood-contacting medical devices.

Chapter 5. Summary and Concluding Remarks

5.1. Summary

Despite intensive investment in blood compatibility research, we still lack perfect blood-compatible biomaterials, a challenge that has persisted for decades. This dissertation contributes to improving our understanding of blood compatibility assessment and advances insights toward developing superior blood-compatible surfaces. We have demonstrated two parallel strategies for enhancing blood compatibility: zwitterionic polymers that repel protein fouling, and ppC_3F_6 that promotes tight albumin binding while reducing FXII activity. The concept of 'bioactivity' provides a key solution to inevitable protein fouling on hydrophobic surface coatings. Unlike zwitterionic surfaces, hydrophobic surfaces cannot avoid protein adsorption entirely. Accepting this limitation, we propose 'inactivating' surface-adsorbed thrombogenic proteins as an alternative strategy. The unique properties of ppC_3F_6 demonstrated in this dissertation may serve as a cornerstone for mitigating thrombus formation. Further investigation into why RFGD plasma deposition confers protein tight-binding properties will help optimize blood-contacting surface engineering. The superior performance of zwitterionic polymer in our blood compatibility assays supports the interim conclusion that pCBAA significantly improves blood compatibility.

Our radiolabeled protein adsorption studies examined simultaneous protein competition rather than sequential Vroman effect displacement. Time-course studies of protein adsorption and displacement, or sequential protein exposure through techniques like QCM-D or SPR, may provide additional insights into these dynamics.

From an assessment perspective, defining blood compatibility through single assays remains premature. Rather than pursuing a single gold standard methodology for anti-thrombogenicity evaluation, we need systematic contributions to understand molecular-level events and protein dynamics at blood-surface interfaces. Building a collaborative scientific understanding remains essential for achieving perfect blood-compatible biomaterials.

Note for ppC_3F_6 surfaces: Dave Castner's group at the University of Washington's NEXAFS synchrotron study revealed different polymeric chain alignments in ppC_3F_6 surfaces[84]. Notably, downstream-deposited surfaces (ppC_3F_6-3) showed high chain alignment. Further analysis of plasma-polymerized surface chain structures, particularly ppC_3F_6, may illuminate how atomic-level structural differences influence surface-blood interactions.

Functional Groups / Atoms	Electronegativity
F	3.98
CF_3	3.5-3.6
CF_2	3.2-3.4
CF	3.0-3.2
CHx	~3.0
C	2.55

Table 3. Table for the functional groups/atoms and their corresponding electronegativity

Regarding fluorocarbon functional groups (**Figure 7**), fluoropolymer superiority over commercial organic medical polymers likely stems from fluorinated carbon groups' high electronegativity on surfaces (**Table 3**). While high electronegativity of fluorocarbon groups may influence blood-surface interactions, a single fluorocarbon group's density unlikely governs overall behavior. Typically, higher electronegativity increases surface hydrophilicity, yet fluoropolymers remain hydrophobic due to fluorine atoms' low surface energy and non-polar structure. Beyond

fluoropolymers' inherent surface properties, plasma-polymerized fluorocarbon may introduce additional protein-surface interaction characteristics, possibly through specific fluorocarbon group ratios affecting protein behavior at the interface. This observation remains phenomenological, limiting our understanding of blood compatibility on plasma-polymerized fluoropolymer surfaces and highlighting the need for further ppC_3F_6 surface investigations.

Grand Review of Dissertation Study

1. A single assay cannot fully represent molecular-level events at blood-surface interfaces that promote or mitigate intrinsic pathway activation.
2. The superior performance of zwitterionic CBAA surfaces validates previous studies on zwitterionic materials for biocompatibility and blood compatibility.
3. While improved performance of ppC_3F_6 surfaces may depend on surface fluorocarbon group ratios, the underlying mechanisms remain unclear and cannot be generalized to non-RFGD polymers.
4. Enhanced ppC_3F_6 performance aligns with our group's previous findings, supporting continued development of RFGD surface coatings for medical applications.
5. Blood compatibility's complexity prevents establishing a single standard regarding hydrophilic versus hydrophobic surfaces, as each offers unique benefits for blood compatibility.

5.2. Future Works and Perspectives

Despite its low physiological concentration compared to albumin or fibrinogen, FXII effectively competes with other blood proteins for surface binding[85], [86], [87], [88]. While FXII cofactors [85], [89] partially explain this phenomenon, other bloodstream components may influence FXII behavior. Understanding FXII's superior adsorption mechanism would provide valuable insights for engineering blood-compatible surfaces. This investigation continues through collaborations described in Chapter 6.

Our blood compatibility assays primarily employed protein solutions or human plasma. The radiolabeled protein assays used 1% plasma concentration or diluted human plasma, which incompletely represents physiological conditions. While these modifications provide foundational understanding of blood compatibility assessment, they cannot fully replicate realistic conditions. Future work should utilize whole blood for all assays except radiolabeled studies, where high isotope concentrations required for 100% plasma would exceed safety limits. Development of radio-free or reduced-radioactivity methods would benefit future studies. Additionally, using freshly drawn plasma rather than fresh frozen plasma might improve experimental accuracy.

Beyond whole blood studies, clinical application remains the ultimate goal of blood compatibility research. In vivo and ex vivo studies therefore become crucial. While our group currently conducts animal studies, these investigations fall outside this dissertation's scope.

Earlier dissertation phases emphasized material characterization, though incomplete data prevented inclusion. The molecularly smooth nature of ppC_3F_6 surfaces compared to other fluoropolymers warrants further investigation. Additional surface analyses examining water

contact angle, film thickness, and roughness could enhance our understanding of blood-surface interactions.

Future time-course protein-surface interaction studies using radiolabeled protein adsorption assays could provide improved understanding of adsorption kinetics across various surface chemistries, while time-course retention studies would illuminate protein binding dynamics.

5.3. Concluding Remarks

Catastrophe Revisits: Blood Compatible Biomaterials

As discussed in Chapter 1, the biomaterials field continues to face significant challenges in achieving perfect blood compatibility. Despite decades of research, there remains no consensus on the ideal characteristics of biomaterials, no perfect blood-compatible surfaces, and no universally accepted, standardized methods to assess blood compatibility comprehensively. The studies presented in this dissertation represent a step forward in addressing these issues by offering new insights and methodologies. However, it is clear that resolving the "blood compatibility catastrophe" will require sustained and collaborative efforts across the biomaterials and medical communities [90].

Blood compatibility is a critical issue that directly impacts the performance and safety of implantable medical devices. It is intrinsically linked to clinical outcomes and remains one of the most important unresolved challenges in the field. However, despite its importance, the community has yet to reach a consensus on whether hydrophobic or hydrophilic surfaces are more effective. Neutral wettability surfaces, such as PET (polyethylene terephthalate), have been consistently shown to exhibit poor blood compatibility. In contrast, specific hydrophobic and hydrophilic

surfaces, such as fluoropolymers and zwitterionic polymers, respectively, have demonstrated improved performance in various studies, including the research presented here.

The contributions of this dissertation are intended not as definitive answers but as part of a larger, ongoing dialogue in the field. By exploring the interplay between material properties, protein interactions, and coagulation pathways, this work aims to provide a foundation for future innovations. To this end, the following key insights and directions are offered:

1. Zwitterionic pCBAA surfaces (poly(carboxybetaine acrylamide)) may enhance blood compatibility by mitigating intrinsic coagulation pathways under low-shear hemodynamic flow. This improvement is largely attributed to their protein non-fouling properties, which reduce undesirable protein interactions on the surface.

2. ppC_3F_6 surfaces demonstrate a strong preferential binding to albumin with high retention due to their "tight-binding" mechanism. This characteristic may reduce the likelihood of thrombogenic protein displacement (e.g., the Vroman effect), though complete suppression of protein adsorption remains a significant challenge, even with advanced zwitterionic materials.

3. Albumin plays a crucial role in passivating surfaces by resisting the displacement caused by thrombogenic proteins such as FXII and fibrinogen. Maintaining a tightly bound layer of albumin could provide a protective barrier that minimizes clot formation.

4. A higher albumin adsorption ratio is desirable for promoting blood compatibility. Designing materials that selectively attract and retain albumin while repelling other proteins could represent a promising avenue for future biomaterial design.

5. Although albumin pre-coating may offer short-term benefits, its degradation over time limits its long-term efficacy. Developing non-immunogenic, non-biodegradable forms of albumin—or functional analogs—could address this limitation and offer a potential solution.

6. Adjusting the CF_2:CF_3 ratio in ppC_3F_6 surfaces appears to improve blood compatibility, suggesting that fine-tuning surface chemistry at the molecular level can significantly influence performance.

7. Protein adsorption is not inherently thrombogenic. If adsorbed proteins remain inactive and cannot trigger coagulation cascades, their presence on a surface does not necessarily result in thrombosis. For example, ppC_3F_6 surfaces may mitigate the serine protease activity of adsorbed FXII, potentially reducing its thrombogenicity. However, completely eliminating FXIIa activity remains beyond the current capabilities of material science.

8. The dynamics of thrombin generation vary significantly over time and across different surfaces. This variability highlights the importance of conducting time-dependent analyses to capture the full scope of blood compatibility rather than relying solely on single-time-point measurements.

Taken together, these findings provide a clearer understanding of the complex interplay between material properties, protein interactions, and hemodynamic conditions. While the studies conducted in this dissertation offer valuable insights, they also underline the limitations of current approaches and the need for interdisciplinary collaboration to achieve a breakthrough.

In conclusion, the development of truly blood-compatible materials will require not only novel surface chemistries but also a deeper understanding of the biological systems involved. The

integration of advanced biomaterial design, high-throughput testing methods, and computational modeling could accelerate progress in this field. By building on the insights presented here, future research can aim to close the gap between material design and clinical application, ultimately contributing to safer and more effective blood-contacting medical devices.

Chapter 6. Extra Works

6.1. Platelet adhesion assay for fibrinogen bioactivity study, and early PhD studies

As part of a collaborative effort to advance blood compatibility research, extensive studies were conducted in partnership with Sherry Liu (SL, former PhD student). A key focus of this collaboration was the evaluation of fibrinogen bioactivity on a subset of fluoropolymer surfaces (ppC_3F_6-1, PVDF, PVDF-HFP). This was achieved through platelet adhesion assays and platelet ELISA analyses targeting PF4 and PAC-1 biomarkers, both of which are indicative of platelet activation [91], [92], [93], [94], [95], [96].

To assess platelet activation, platelet adhesion assays were performed, yielding a comprehensive dataset of SEM images. Platelet morphology was categorized into five distinct activation states, which were manually classified and counted. However, the manual counting process introduced human variability and was labor-intensive, thereby complicating the analysis. To address these challenges, a prospective enhancement to this workflow involves the application of supervised machine learning-based computer vision techniques. [NO_PRINTED_FORM]These techniques aim to automate image analysis and enable accurate quantification of platelet morphology. This development is currently being pursued in collaboration with Mr. Woohyun Eum at the University of Florida. Successful implementation of this automated system is expected to elucidate the role of fibrinogen on ppC_3F_6 surfaces and provide deeper insights into fibrinogen activity and its interaction with biomaterials.

As detailed in Chapter 4, the preliminary phase of this doctoral research extended these investigations into the extrinsic coagulation pathway, employing platelet adhesion assays comparable to those used in the fibrinogen bioactivity studies. While the collaboration with SL focused on three fluoropolymer groups, earlier stages of this research encompassed a broader range of fluoropolymers, including PTFE, FEP, and additional ppC_3F_6 variants. The establishment of an automated platelet counting system is anticipated to facilitate the analysis of these unprocessed datasets, providing valuable insights into platelet-surface interactions across a diverse spectrum of fluoropolymer materials.

6.2. Heparin immobilization on the plasma-polymerized allylamine surface and its blood compatibility assays

Heparin immobilization [97], [98], [99], [100] is a widely utilized strategy for suppressing intrinsic pathway activation on blood-contacting surfaces. In this study, low molecular weight heparin (LMWH) was immobilized onto plasma-polymerized allylamine surfaces via EDC-NHS chemistry. These modified surfaces were evaluated for blood compatibility using thrombin generation assays and fibrin clot formation time assays. The results of these analyses provide a deeper understanding of how heparin-modified surfaces interact with the coagulation cascade, offering potential pathways for further optimization.

6.3. I-125 Radiolabeled protein adsorption to compare with QCM-D study

To enhance the understanding of protein adsorption, displacement, and retention mechanisms, collaborative studies with SL were conducted using PVDF, PVDF-HFP, and ppC_3F_6-1 surfaces. SL employed quartz crystal microbalance with dissipation monitoring (QCM-D) for real-time, in situ analysis, while radiolabeled protein adsorption studies were conducted by KHK.

QCM-D is a label-free technique that measures the overall mass change on a surface but does not differentiate between specific proteins in a binary or ternary protein solution. In contrast, radiolabeled protein adsorption studies provide specificity by directly labeling target proteins with isotopes. Comparing these two methods allows for a comprehensive cross-verification of data, enhancing the reliability and depth of insights into protein-surface interactions. This integrative approach sheds light on the dynamic behavior of proteins on fluoropolymer surfaces, advancing the design of biomaterials with improved blood compatibility.

6.4. Factor XII mechanism study

This project, conducted in collaboration with Dr. Junghyun Lee (UW Medicine Dermatology), seeks to deepen the understanding of Factor XII (FXII) activation mechanisms. Despite its significantly lower plasma concentration compared to albumin and fibrinogen, FXII plays a critical role in initiating the coagulation cascade upon surface contact.

From previous studies[101], [102], [103], [104], [105], our preliminary findings indicate that DNA concentration influences FXII adsorption and activation. Subtraction studies were performed on

human plasma treated with DNase, RNase, and TPEN (a zinc chelator), followed by assessments of FXIIa activity. Notably, DNase-treated plasma showed reduced FXIIa activity, suggesting that DNA may facilitate FXII surface interactions. To further investigate this phenomenon, experiments involving I-125 radiolabeled FXII adsorption are planned, incorporating varying concentrations of DNase-treated plasma and DNA-enriched samples. These studies aim to clarify the molecular mechanisms underlying FXII activation and its interaction with biomaterial surfaces, potentially guiding the design of next-generation blood-compatible materials.

References

[1] J. R. Mcloughlin and A. V Tobolsky, “THE VISCOELASTIC BEHAVIOR OF POLYMETHYL METHACRYLATE,” *J Colloid Sci*, 1952.

[2] S. H. Armstrong *et al.*, “Separation of Polysaccharides, Peptides and Proteins from Human Plasma Immunological assay for human serum albumin was carried out with horse serum containing an antibody to Electrophoretic and ultracentrifugal analyses were per-formed by M,” 1953.

[3] B. E. S Duthie, “The Action of Fibrinogen on certain Pathogenic Cocci,” 1955.

[4] S. R. Hanson, L. A. Harker, B. D. Ratner, and A. S. HOFFMAN Seattle Wash, “In vivo evaluation of artificial surfaces with a nonhuman primate model of arterial thrombosis,” 1980.

[5] A. M. Garfinkle, A. S. Hoffman, B. D. Ratner, L. O. Reynolds, and S. R. Hanson, “Effects of a tetrafluoroethylene glow discharge on patency of small diameter dacron vascular grafts,” *Trans Am Soc Artif Intern Organs*, 1984.

[6] B. Ratner, “Forty-nine years in Biomaterials Science: An interview with Buddy Ratner,” 2017, *Future Medicine Ltd.* doi: 10.4155/fsoa-2016-0078.

[7] B. D. Ratner, “Editorial The blood compatibility catastrophe.”

[8] B. D. Ratner, “The catastrophe revisited: Blood compatibility in the 21st Century,” *Biomaterials*, vol. 28, no. 34, pp. 5144–5147, Dec. 2007, doi: 10.1016/j.biomaterials.2007.07.035.

[9] B. D. Ratner, “Blood compatibility-a perspective,” 2000.

[10] M. Schenone, B. C. Furie, and B. Furie, “The blood coagulation cascade,” 2004. [Online]. Available: http://journals.lww.com/co-hematology

[11] M. Gorbet, C. Sperling, M. F. Maitz, C. A. Siedlecki, C. Werner, and M. V. Sefton, “The blood compatibility challenge. Part 3: Material associated activation of blood cascades and cells,” Aug. 01, 2019, *Acta Materialia Inc*. doi: 10.1016/j.actbio.2019.06.020.

[12] D. Gailani and T. Renné, “Intrinsic pathway of coagulation and arterial thrombosis,” Dec. 2007. doi: 10.1161/ATVBAHA.107.155952.

[13] S. P. Grover and N. Mackman, “Intrinsic pathway of coagulation and thrombosis: Insights from animal models,” *Arterioscler Thromb Vasc Biol*, vol. 39, no. 3, pp. 331–338, Mar. 2019, doi: 10.1161/ATVBAHA.118.312130.

[14] A. Shamanaev, M. Litvak, and D. Gailani, “Recent advances in factor XII structure and function,” Sep. 01, 2022, *Lippincott Williams and Wilkins*. doi: 10.1097/MOH.0000000000000727.

[15] I. Ivanov *et al.*, “Proteolytic properties of single-chain factor XII: a mechanism for triggering contact activation,” 2017, doi: 10.1182/blood-2016-10.

[16] R. Zhuo, C. A. Siedlecki, and E. A. Vogler, “Autoactivation of blood factor XII at hydrophilic and hydrophobic surfaces,” *Biomaterials*, vol. 27, no. 24, pp. 4325–4332, Aug. 2006, doi: 10.1016/j.biomaterials.2006.04.001.

[17] R. Zhuo, C. A. Siedlecki, and E. A. Vogler, “Competitive-protein adsorption in contact activation of blood factor XII,” *Biomaterials*, vol. 28, no. 30, pp. 4355–4369, Oct. 2007, doi: 10.1016/j.biomaterials.2007.06.019.

[18] W. Dick, W. Cullmann, and K. Adler, “Factor XII Assay with the Chromogenic Substrate Chromozym PK® *),” *J. Gin. Chem. Gin. Biochem*, vol. 19, pp. 357–361, 1981.

[19] N. Mackman, R. E. Tilley, and N. S. Key, “Role of the extrinsic pathway of blood coagulation in hemostasis and thrombosis,” Aug. 2007. doi: 10.1161/ATVBAHA.107.141911.

[20] E. W. Davie and J. D. Kulman, “An overview of the structure and function of thrombin,” Apr. 2006. doi: 10.1055/s-2006-939550.

[21] B. F. Edward Plow, R. P. McEver, B. S. Coller, V. L. Woods, J. A. Gerard Marguerie, and M. H. Ginsberg, “Related Binding Mechanisms for Fibrinogen, Fibronectin, von Willebrand Factor, and Thrombospondin on Thrombin-Stimulated Human Platelets,” 1985. [Online]. Available: www.bloodjournal.org

[22] C. Naudin, E. Burillo, S. Blankenberg, L. Butler, and T. Renné, “Factor XII Contact Activation,” Nov. 01, 2017, *Thieme Medical Publishers, Inc.* doi: 10.1055/s-0036-1598003.

[23] Q. Cheng *et al.*, “A role for factor XIIa-mediated factor XI activation in thrombus formation in vivo,” *Blood*, vol. 116, no. 19, pp. 3981–3989, Nov. 2010, doi: 10.1182/blood-2010-02-270918.

[24] A. Shamanaev *et al.*, “Model for surface-dependent factor XII activation: the roles of factor XII heavy chain domains,” *Blood Adv*, vol. 6, no. 10, pp. 3142–3154, May 2022, doi: 10.1182/bloodadvances.2021005976.

[25] L. Vroman and A. L. Adams, “Identification of Rapid Changes at Plasma-Solid Interfaces,” 1969.

[26] L. Vroman and A. L. Adams, “FINDINGS WITH THE RECORDING ELLIPSOMETER SUGGESTING RAPID EXCHANGE OF SPECIFIC PLASMA PROTEINS AT LIQUID~SOLID INTERFACES *,” North-Holland Publishing Co, 1969.

[27] L. Vroman and E. F. Leonard, “The effect of flow on displacement of proteins at interfaces in plasma,” *Biofouling*, vol. 4, no. 1–3, pp. 81–87, Aug. 1991, doi: 10.1080/08927019109378197.

[28] L. Vroman, A. L. Adams, G. C. Fischer, and P. C. Munoz, “Interaction of High Molecular Weight Kininogen, Factor XII, and Fibrinogen in Plasma at Interfaces,” 1980. [Online]. Available: http://ashpublications.org/blood/article-pdf/55/1/156/1713989/156.pdf

[29] H. Ai-Khaffaf and D. Charlesworth, “Albumin-coated vascular prostheses: A five-year follow-up,” 1996.

[30] Y. Marois *et al.*, “An albumin-coated polyester arterial graft: in tivo assessment of biocompatibility and healing characteristics,” 1996.

[31] D. Kiaei, A. S. Hoffman, and T. A. Horbett, “Tight binding of albumin to glow discharge treated polymers,” *J Biomater Sci Polym Ed*, vol. 4, no. 1, pp. 35–44, Jan. 1993, doi: 10.1163/156856292x00286.

[32] C. D. Tidwell *et al.*, “Static time-of-flight secondary ion mass spectrometry and x-ray photoelectron spectroscopy characterization of adsorbed albumin and fibronectin films,” *Surface and Interface Analysis*, vol. 31, no. 8, pp. 724–733, Aug. 2001, doi: 10.1002/sia.1101.

[33] K. Kottke-Mar&ant, J. M. Anderson, Y. Umemura, and R. E. Marchant, “Effect of albumin coating on the in vitro blood compatibility of Dacron@ arterial prostheses,” 1989.

[34] R. C. Eberhart, J. R. Munro, M. Frautschi, F. J. Clubb, and V. W. I. Sevastianov~, “Influence of Endogenous Albumin Binding on Blood-Material Interactions,” *Annals New York Academy of Sciences*, 1987.

[35] M. L. Godek, R. Michel, L. M. Chamberlain, D. G. Castner, and D. W. Grainger, “Adsorbed serum albumin is permissive to macrophage attachment to perfluorocarbon polymer surfaces in culture,” *J Biomed Mater Res A*, vol. 88, no. 2, pp. 503–519, Feb. 2009, doi: 10.1002/jbm.a.31886.

[36] E. Brynda, M. Houska, M. Jiroušková, and J. E. Dyr, “Albumin and heparin multilayer coatings for blood-contacting medical devices,” *J Biomed Mater Res*, vol. 51, no. 2, pp. 249–257, 2000, doi: 10.1002/(SICI)1097-4636(200008)51:2<249::AID-JBM14>3.0.CO;2-X.

[37] S. Lin *et al.*, “An albumin biopassive polyallylamine film with improved blood compatibility for metal devices,” *Polymers (Basel)*, vol. 11, no. 4, Apr. 2019, doi: 10.3390/polym11040734.

[38] I. H. Jaffer and J. I. Weitz, “The blood compatibility challenge. Part 1: Blood-contacting medical devices: The scope of the problem,” Aug. 01, 2019, *Acta Materialia Inc*. doi: 10.1016/j.actbio.2019.06.021.

[39] M. F. Maitz *et al.*, “The blood compatibility challenge. Part 4: Surface modification for hemocompatible materials: Passive and active approaches to guide blood-material interactions,” Aug. 01, 2019, *Acta Materialia Inc*. doi: 10.1016/j.actbio.2019.06.019.

[40] J. L. Brash, T. A. Horbett, R. A. Latour, and P. Tengvall, “The blood compatibility challenge. Part 2: Protein adsorption phenomena governing blood reactivity,” Aug. 01, 2019, *Acta Materialia Inc*. doi: 10.1016/j.actbio.2019.06.022.

[41] S. Van Nguyen, K. Albaugh, P. T. A. Brooks, D. W. Hess, M. J. Rand, and J. F. Roberts, “The Preparation and Properties of Thin Film Silicon-Nitrogen Compounds Produced by a Radio Frequency Glow Discharge Reaction,” *J Electrochem Soc*, 1967.

[42] J. K. Stille *et al.*, “Reaction of Halobenzenes in a Radiofrequency Glow Discharge The Reaction of Halobenzenes in a Radiofrequency Glow Discharge,” *J Org Chem*, vol. 54, no. 2, p. 65, 1966, [Online]. Available: https://pubs.acs.org/sharingguidelines

[43] S. P. Mukherjee and P. E. Evans, “THE DEPOSITION OF THIN FILMS BY THE DECOMPOSITION OF TETRA-ETHOXY SILANE IN A RADIO FREQUENCY GLOW DISCHARGE,” *Thin Solid Films*, 1972.

[44] K. C. Brown, “POLYMERIZATION IN RADIO FREQUENCY GLOW DISCHARGES-I,” Pergamon Press, 1972.

[45] G. Turban, Y. Catherine, and B. Grolleau, “REACTION MECHANISMS OF THE RADIO FREQUENCY GLOW DISCHARGE DEPOSITION PROCESS IN SILANE-HELIUM,” *Thin Solid Films*, vol. 60, pp. 147–155, 1979.

[46] J. Mokry, J. Karbanova, J. Lukas, V. Paleckova, and B. Dvorankova, “Biocompatibility of HEMA copolymers designed for treatment of CNS diseases with polymer-encapsulated cells,” *Biotechnol Prog*, vol. 16, no. 5, pp. 897–904, Sep. 2000, doi: 10.1021/bp000113m.

[47] A. Galperin, K. Smith, N. S. Geisler, J. D. Bryers, and B. D. Ratner, “Precision-Porous PolyHEMA-Based Scaffold as an Antibiotic-Releasing Insert for a Scleral Bandage,” *ACS Biomater Sci Eng*, vol. 1, no. 7, pp. 593–600, Dec. 2015, doi: 10.1021/acsbiomaterials.5b00133.

[48] N. E. RICHARDSON, D. J. G. DAVIES, B. J. MEAKIN, and D. A. NORTON, “The interaction of preservatives with polyhydroxyethylmethacrylate (polyHEMA),” *Journal of*

Pharmacy and Pharmacology, vol. 30, no. 1, pp. 469–475, 1978, doi: 10.1111/j.2042-7158.1978.tb13295.x.

[49] D. Kiaei, A. S. Hoffman, T. A. Horbett, and K. R. Lew, "Platelet and monoclonal antibody binding to fibrinogen adsorbed on glow-discharge-deposited polymers," 1995.

[50] D. Kiaei, A. S. Hoffman, T. A. Horbett, and K. R. Lew, "Platelet and monoclonal antibody binding to fibrinogen adsorbed on glow-discharge-deposited polymers."

[51] W.-B. Tsai, Q. Shi, J. M. Grunkemeier, C. Mcfarland, and T. A. Horbett, "Platelet adhesion to radiofrequency glow-discharge-deposited fluorocarbon polymers preadsorbed with selectively depleted plasmas show the primary role of fibrinogen," 2004. [Online]. Available: www.vsppub.com

[52] D. Kiaei, A. S. Hoffman, and T. A. Horbett, "Platelet Adhesion to Fibrinogen Adsorbed on Glow Discharge-Deposited Polymers," 2018. [Online]. Available: https://pubs.acs.org/sharingguidelines

[53] M. D. Garrison, R. L. Èhl, R. Â. M. Overney, and B. D. Ratner, "Glow discharge plasma deposited hexa¯uoropropylene ®lms: surface chemistry and interfacial materials properties." [Online]. Available: www.elsevier.nl/locate/tsf

[54] L. Cao, S. Sukavaneshvar, B. D. Ratner, and T. A. Horbett, "Glow discharge plasma treatment of polyethylene tubing with tetraglyme results in ultralow fibrinogen adsorption and greatly reduced platelet adhesion," *J Biomed Mater Res A*, vol. 79, no. 4, pp. 788–803, Dec. 2006, doi: 10.1002/jbm.a.30908.

[55] L. Cao, S. Sukavaneshvar, B. D. Ratner, and T. A. Horbett, "Glow discharge plasma treatment of polyethylene tubing with tetraglyme results in ultralow fibrinogen adsorption and greatly reduced platelet adhesion," *J Biomed Mater Res A*, vol. 79, no. 4, pp. 788–803, Dec. 2006, doi: 10.1002/jbm.a.30908.

[56] L. Cao *et al.*, "Plasma-deposited tetraglyme surfaces greatly reduce total blood protein adsorption, contact activation, platelet adhesion, platelet procoagulant activity, and in vitro thrombus deposition," *J Biomed Mater Res A*, vol. 81, no. 4, pp. 827–837, Jun. 2007, doi: 10.1002/jbm.a.31091.

[57] L. M. Szott, M. J. Stein, B. D. Ratner, and T. A. Horbett, "Complement activation on poly(ethylene oxide)-like radiofrequency glow discharge-deposited surfaces," *J Biomed Mater Res A*, vol. 96 A, no. 1, pp. 150–161, Jan. 2011, doi: 10.1002/jbm.a.32954.

[58] S. H. Song, P. Koelsch, T. Weidner, M. S. Wagner, and D. G. Castner, "Sodium dodecyl sulfate adsorption onto positively charged surfaces: Monolayer formation with opposing headgroup orientations," *Langmuir*, vol. 29, no. 41, pp. 12710–12719, Oct. 2013, doi: 10.1021/la401119p.

[59] X. Lin *et al.*, "Ultralow Fouling and Functionalizable Surface Chemistry Based on Zwitterionic Carboxybetaine Random Copolymers," *Langmuir*, vol. 35, no. 5, pp. 1544–1551, Feb. 2019, doi: 10.1021/acs.langmuir.8b02540.

[60] X. Lin *et al.*, "Photoreactive Carboxybetaine Copolymers Impart Biocompatibility and Inhibit Plasticizer Leaching on Polyvinyl Chloride," *ACS Appl Mater Interfaces*, vol. 12, no. 37, pp. 41026–41037, Sep. 2020, doi: 10.1021/acsami.0c09457.

[61] R. Ukita *et al.*, "Zwitterionic poly-carboxybetaine coating reduces artificial lung thrombosis in sheep and rabbits," *Acta Biomater*, vol. 92, pp. 71–81, Jul. 2019, doi: 10.1016/j.actbio.2019.05.019.

[62] Q. Shao, Y. He, A. D. White, and S. Jiang, "Difference in hydration between carboxybetaine and sulfobetaine," *Journal of Physical Chemistry B*, vol. 114, no. 49, pp. 16625–16631, Dec. 2010, doi: 10.1021/jp107272n.

[63] R. Ukita *et al.*, "Zwitterionic poly-carboxybetaine coating reduces artificial lung thrombosis in sheep and rabbits," *Acta Biomater*, vol. 92, pp. 71–81, Jul. 2019, doi: 10.1016/j.actbio.2019.05.019.

[64] W. Van Oeveren, J. Haan, †p Lagerman, and †p Schoen, "Comparison of Coagulation Activity Tests In Vitro for Selected Biomaterials," 2002.

[65] S. L. J. Blok, G. E. Engels, and W. van Oeveren, " In vitro hemocompatibility testing: The importance of fresh blood ," *Biointerphases*, vol. 11, no. 2, Jun. 2016, doi: 10.1116/1.4941850.

[66] H. T. Spijker, R. Bos, H. J. Busscher, T. G. Van Kooten, and W. Van Oeveren, "Platelet adhesion and activation on a shielded plasma gradient prepared on polyethylene," 2002.

[67] A. Tripodi, "Thrombin generation assay and its application in the clinical laboratory," May 01, 2016, *American Association for Clinical Chemistry Inc.* doi: 10.1373/clinchem.2015.248625.

[68] T. Baglin, "The measurement and application of thrombin generation," Sep. 2005. doi: 10.1111/j.1365-2141.2005.05612.x.

[69] S. Alibeik, S. Zhu, J. W. Yau, J. I. Weitz, and J. L. Brash, "Surface modification with polyethylene glycol-corn trypsin inhibitor conjugate to inhibit the contact factor pathway on blood-contacting surfaces," *Acta Biomater*, vol. 7, no. 12, pp. 4177–4186, 2011, doi: 10.1016/j.actbio.2011.07.022.

[70] J. L. Bohnert, B. C. Fowler, T. A. Horbett, and A. S. Hoffman, "Plasma gas discharge deposited fluorocarbon polymers exhibit reduced elutability of adsorbed albumin and fibrinogen," *J Biomater Sci Polym Ed*, vol. 1, no. 4, pp. 279–297, 1989, doi: 10.1163/156856289X00154.

[71] S. I. Ertel, B. D. Ratner,*'f And, and T. A. Horbett*'t ', "The Adsorption and Elutability of Albumin, IgG, and Fibronectin on Radiofrequency Plasma Deposited Polystyrene," 1991.

[72] K. Chatterjee, J. L. Thornton, J. W. Bauer, E. A. Vogler, and C. A. Siedlecki, "Moderation of prekallkrein-factor XII interactions in surface activation of coagulation by protein-adsorption competition," *Biomaterials*, vol. 30, no. 28, pp. 4915–4920, Oct. 2009, doi: 10.1016/j.biomaterials.2009.05.076.

[73] A. Golas, P. Parhi, Z. O. Dimachkie, C. A. Siedlecki, and E. A. Vogler, "Surface-energy dependent contact activation of blood factor XII," *Biomaterials*, vol. 31, no. 6, pp. 1068–1079, Feb. 2010, doi: 10.1016/j.biomaterials.2009.10.039.

[74] H. Noh and E. A. Vogler, "Volumetric interpretation of protein adsorption: Competition from mixtures and the Vroman effect," *Biomaterials*, vol. 28, no. 3, pp. 405–422, Jan. 2007, doi: 10.1016/j.biomaterials.2006.09.006.

[75] S. L. Hirsh, D. R. McKenzie, N. J. Nosworthy, J. A. Denman, O. U. Sezerman, and M. M. M. Bilek, "The Vroman effect: Competitive protein exchange with dynamic multilayer protein aggregates," *Colloids Surf B Biointerfaces*, vol. 103, pp. 395–404, Mar. 2013, doi: 10.1016/j.colsurfb.2012.10.039.

[76] W.-B. Tsai, J. M. Grunkemeier, and T. A. Horbett, "Human plasma fibrinogen adsorption and platelet adhesion to polystyrene," 1999.

[77] M. Mecwan, "Tending towards Non-fouling: A study of the interaction between proteins and surfaces prepared by radio frequency glow-discharge plasma," University of Washington, 2019.

[78] A. D. Easley, T. Ma, C. I. Eneh, J. Yun, R. M. Thakur, and J. L. Lutkenhaus, "A practical guide to quartz crystal microbalance with dissipation monitoring of thin polymer films," Apr. 01, 2022, *John Wiley and Sons Inc*. doi: 10.1002/pol.20210324.

[79] C. Tonda-Turo, I. Carmagnola, and G. Ciardelli, "Quartz crystal microbalance with dissipation monitoring: A powerful method to predict the in vivo behavior of bioengineered surfaces," Oct. 30, 2018, *Frontiers Media S.A.* doi: 10.3389/fbioe.2018.00158.

[80] R. J. Mosley, M. V. Talarico, and M. E. Byrne, "Recent applications of QCM-D for the design, synthesis, and characterization of bioactive materials," *J Bioact Compat Polym*, vol. 36, no. 4, pp. 261–275, Jul. 2021, doi: 10.1177/08839115211014216.

[81] S. Liu, "Characterizing blood protein surface interactions for the development of thromboresistant fluoropolymer coatings," University of Washington, 2023.

[82] W. Norde, T. A. Horbett, and J. L. Brash, *Proteins at Interfaces III: Introductory Overview*, ACS Symposium Series. Washington DC: American Chemical Society, 2012. [Online]. Available: https://pubs.acs.org/sharingguidelines

[83] T. A. Horbett and J. L. Brash, *Proteins at Interfaces II Fundamentals and Applications*, ACS Symposium Series. Washington DC: American Chemical Society, 1987. [Online]. Available: https://pubs.acs.org/sharingguidelines

[84] D. G. Castner, J. Kenneth, B. Lewis, D. A. Fischer, B. D. Ratner, and J. L. Gland1, "Determination of Surface Structure and Orientation of Polymerized Tetrafluoroethylene Films by Near-Edge X-ray Absorption Fine Structure, X-ray Photoelectron Spectroscopy, and Static Secondary Ion Mass Spectrometry," 1993.

[85] J. H. Griffin and C. G. Cochrane, "Mechanisms for the involvement of high molecular weight kininogen in surface-dependent reactions of Hageman factor (blood coagulation/factor XII/prekallikrein/factor XI/fibrinolysis)," 1976.

[86] N. Naito *et al.*, "Combination of polycarboxybetaine coating and factor XII inhibitor reduces clot formation while preserving normal tissue coagulation during extracorporeal life support," *Biomaterials*, vol. 272, May 2021, doi: 10.1016/j.biomaterials.2021.120778.

[87] T. H. Fischer, H. S. Thatte, T. C. Nichols, D. E. Bender-Neal, D. A. Bellinger, and J. N. Vournakis, "Synergistic platelet integrin signaling and factor XII activation in poly-N-acetyl glucosamine fiber-mediated hemostasis," *Biomaterials*, vol. 26, no. 27, pp. 5433–5443, 2005, doi: 10.1016/j.biomaterials.2005.01.023.

[88] A. Golas, C. H. Joshua Yeh, C. A. Siedlecki, and E. A. Vogler, "Amidolytic, procoagulant, and activation-suppressing proteins produced by contact activation of blood factor XII in buffer solution," *Biomaterials*, vol. 32, no. 36, pp. 9747–9757, Dec. 2011, doi: 10.1016/j.biomaterials.2011.09.020.

[89] R. C. Wiggins, B. N. Bouma, C. G. Cochrane, and J. H. Griffin, "Role of high-molecular-weight kininogen in surface-binding and activation of coagulation Factor XI and prekallikrein," 1977.

[90] B. D. Ratner, "The catastrophe revisited: Blood compatibility in the 21st Century," *Biomaterials*, vol. 28, no. 34, pp. 5144–5147, Dec. 2007, doi: 10.1016/j.biomaterials.2007.07.035.

[91] S. L. Goodman, "Sheep, pig, and human platelet-material interactions with model cardiovascular biomaterials," 1999.

[92] F. Jung, S. Braune, and A. Lendlein, "Haemocompatibility testing of biomaterials using human platelets," *Clin Hemorheol Microcirc*, vol. 53, no. 1–2, pp. 97–115, 2013, doi: 10.3233/CH-2012-1579.

[93] A. S. Hoffman, D. Kiaei, A. Safranj, T. A. H. Bioengineering, C. E. Departments, and S. R. Hanson, "Binding of Proteins and Platelets to Gas Discharge-Deposited Polymers," 1991.

[94] E. F. Plow, M. D. Pierschbacher, E. Ruoslahti, G. Marguerie, and M. H. Ginsberg, "Arginyl-Glycyl-Aspartic Acid Sequences and Fibrinogen Binding to Platelets," 1987. [Online]. Available: www.bloodjournal.org

[95] R. Khalifehzadeh and B. D. Ratner, "Trifluoromethyl-functionalized poly(lactic acid): A fluoropolyester designed for blood contact applications," *Biomater Sci*, vol. 7, no. 9, pp. 3764–3778, Sep. 2019, doi: 10.1039/c9bm00353c.

[96] R. Khalifehzadeh, W. Ciridon, and B. D. Ratner, "Surface fluorination of polylactide as a path to improve platelet associated hemocompatibility," *Acta Biomater*, vol. 78, pp. 23–35, Sep. 2018, doi: 10.1016/j.actbio.2018.07.042.

[97] R. Biran and D. Pond, "Heparin coatings for improving blood compatibility of medical devices," Mar. 01, 2017, *Elsevier B.V.* doi: 10.1016/j.addr.2016.12.002.

[98] J. Buturovic´,Buturovic´, R. Ponikvar, A. Kandus, M. Boh, J. Klinkmann, and P. Ivanovich, "Filling Hemodialysis Catheters in the Interdialytic Period: Heparin Versus Citrate Versus Polygeline: A Prospective Randomized Study," 1998.

[99] J. M. M. Heyligers *et al.*, "Heparin immobilization reduces thrombogenicity of small-caliber expanded polytetrafluoroethylene grafts," *J Vasc Surg*, vol. 43, no. 3, pp. 587–591, Mar. 2006, doi: 10.1016/j.jvs.2005.10.038.

[100] J. Lei *et al.*, "Heparin with Different Molecular Weight on Hemocompatibility and Adsorption of Activated Carbon," *Coatings*, vol. 13, no. 7, Jul. 2023, doi: 10.3390/coatings13071248.

[101] S. A. Chaudhry *et al.*, "Cationic zinc is required for factor XII recruitment and activation by stimulated platelets and for thrombus formation in vivo," *Journal of Thrombosis and Haemostasis*, vol. 18, no. 9, pp. 2318–2328, Sep. 2020, doi: 10.1111/jth.14964.

[102] M. M. Bernardo, D. E. Day, S. T. Olson, and J. D. Shore, "Surface-independent acceleration of factor XII activation by zinc ions: I. Kinetic characterization of the metal ion rate enhancement," *Journal of Biological Chemistry*, vol. 268, no. 17, pp. 12468–12476, Jun. 1993, doi: 10.1016/s0021-9258(18)31412-1.

[103] A. Matafonov, I. S. Ivanov, M. Sun, and D. Gailani, "Coagulation Factor XI and Factor XII in DNA-Induced Thrombin Generation," *Blood*, vol. 124, no. 21, pp. 581–581, Dec. 2014, doi: 10.1182/blood.v124.21.581.581.

[104] J. I. Weitz, "Factor XI and factor XII as targets for new anticoagulants," 2016.

[105] T. Shi *et al.*, “2-Glycoprotein I binds factor XI and inhibits its activation by thrombin and factor XIIa: Loss of inhibition by clipped 2-glycoprotein I,” 2004. [Online]. Available: www.pnas.orgcgidoi10.1073pnas.0400281101

Supplementary Data

pSBMA vs. pCBAA

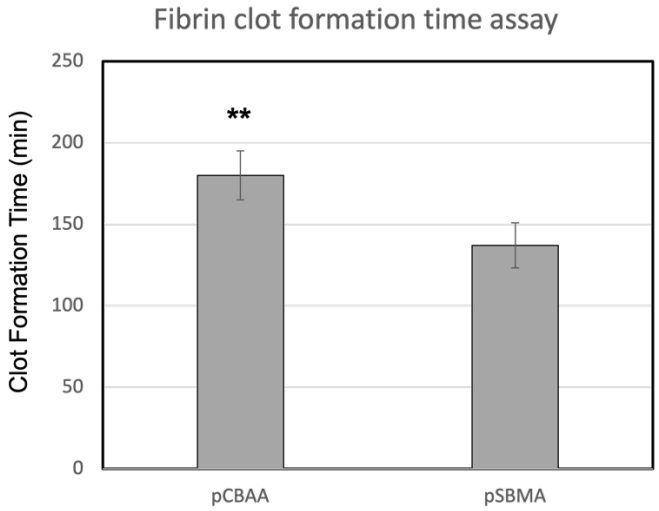

Figure S 1. Clot formation time assay comparison between pCBAA and pSBMA

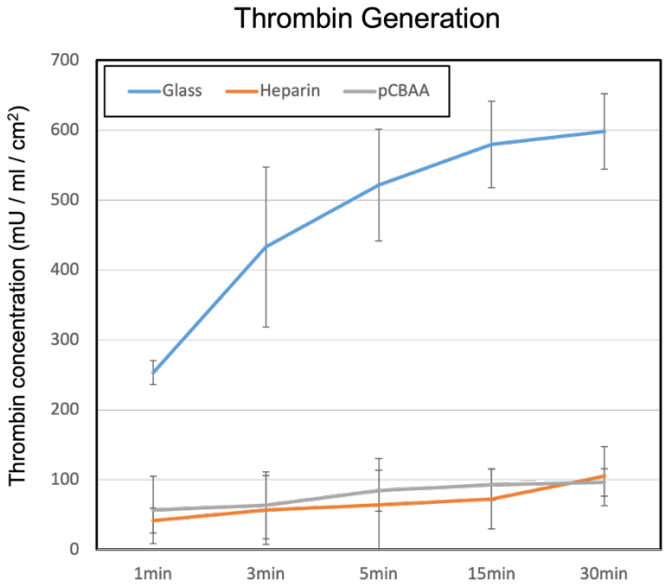

Figure S 2. Thrombin generation assay results of Glass, Heparin-immobilized surface, and pCBAA

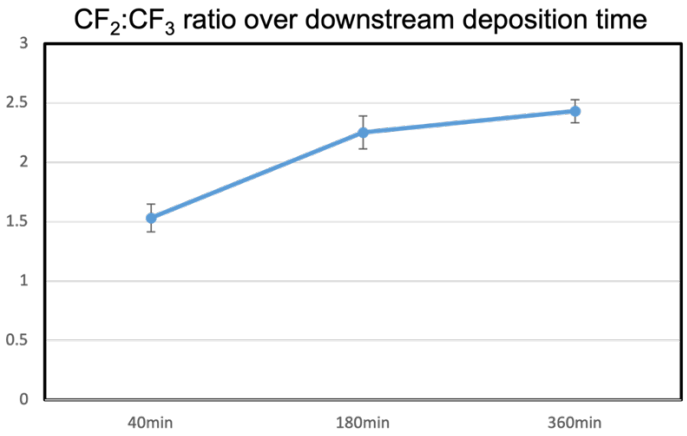

Figure S 3. CF_2:CF_3 ratio change over downstream deposition time

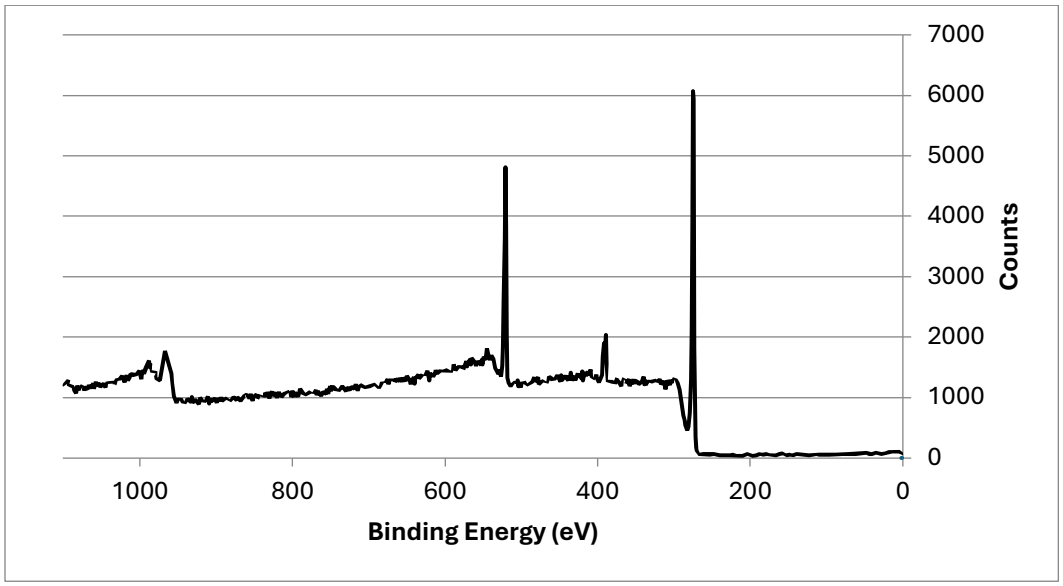

Figure S 4. Survey scan spectra of pCBAA copolymer

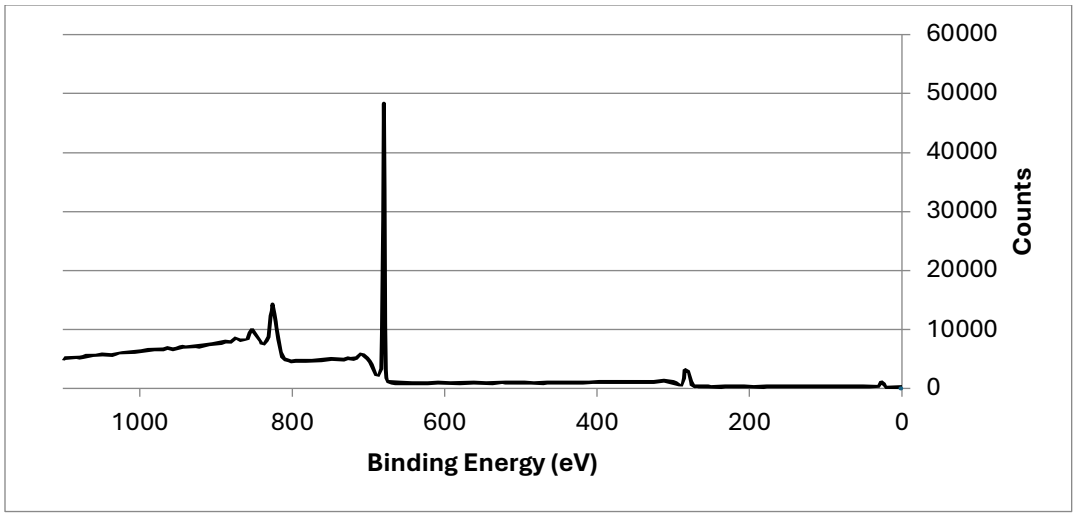

Figure S 5. ***Survey scan spectra of ppC₃F₆-1***

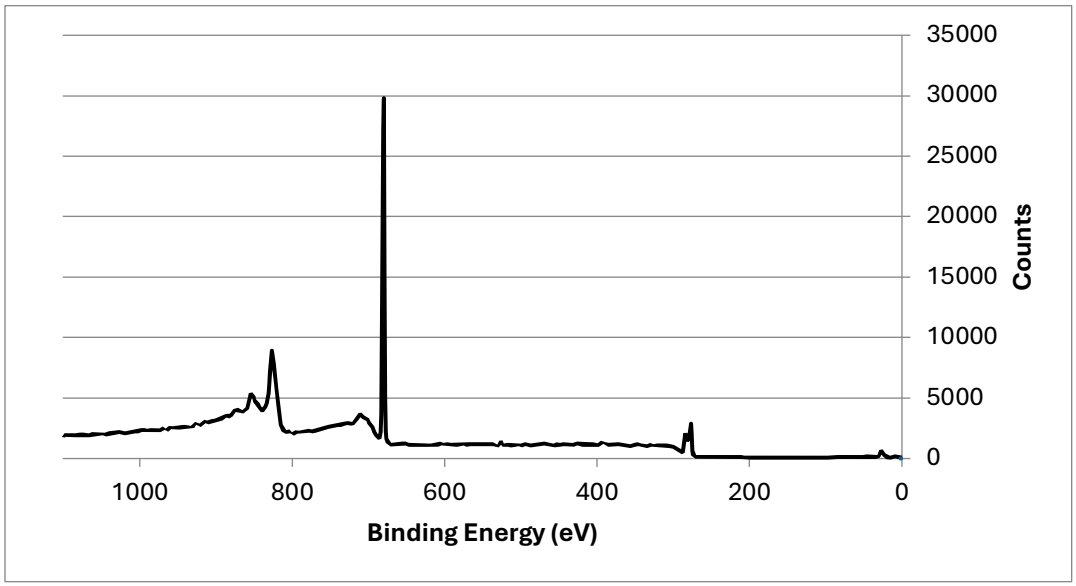

Figure S 6. Survey scan spectra of ppC₃F₆-2

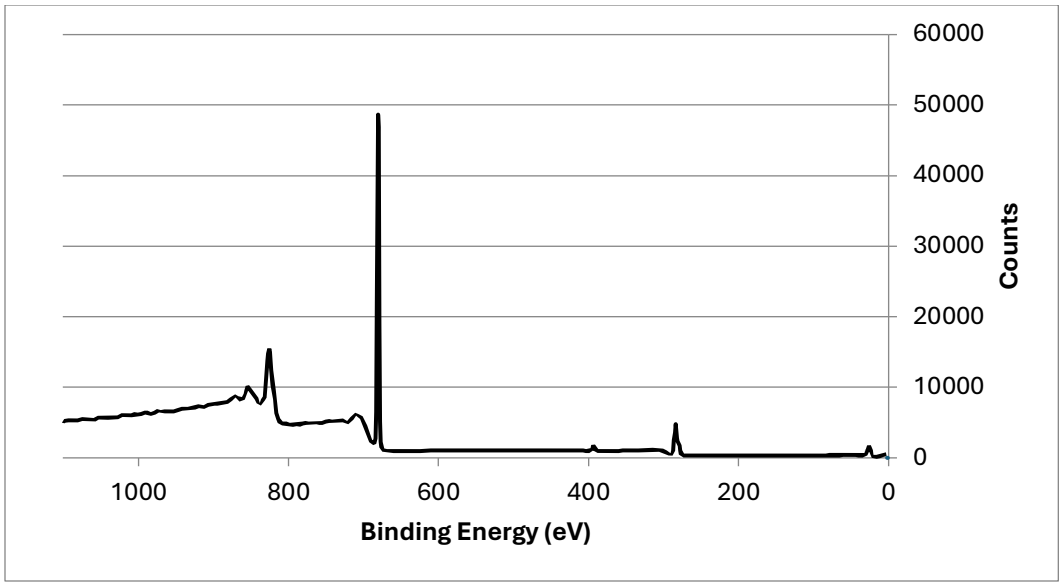

Figure S 7. Survey scan spectra of ppC₃F₆-3

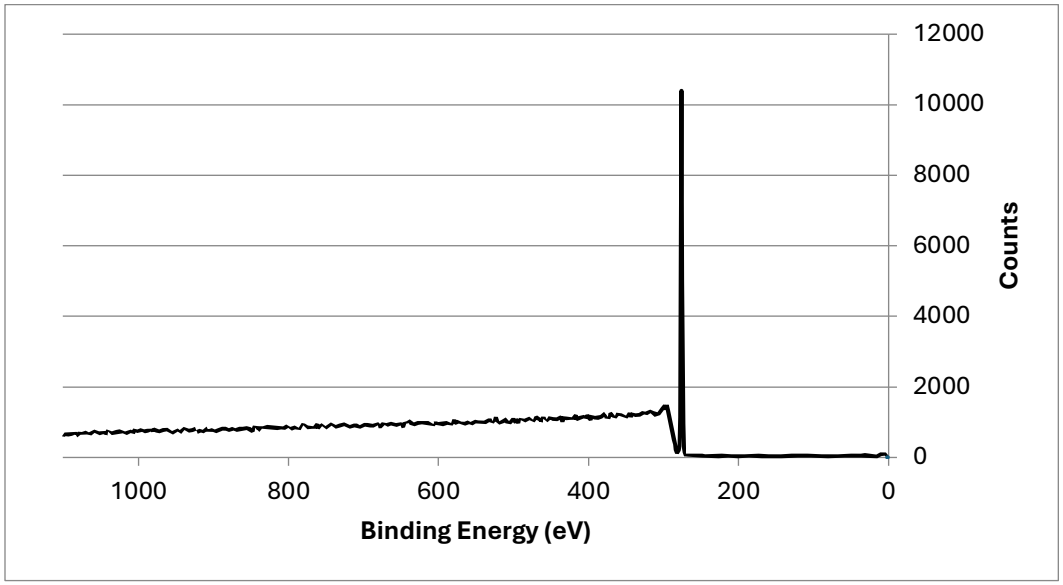

Figure S 8. Survey scan spectra of PE

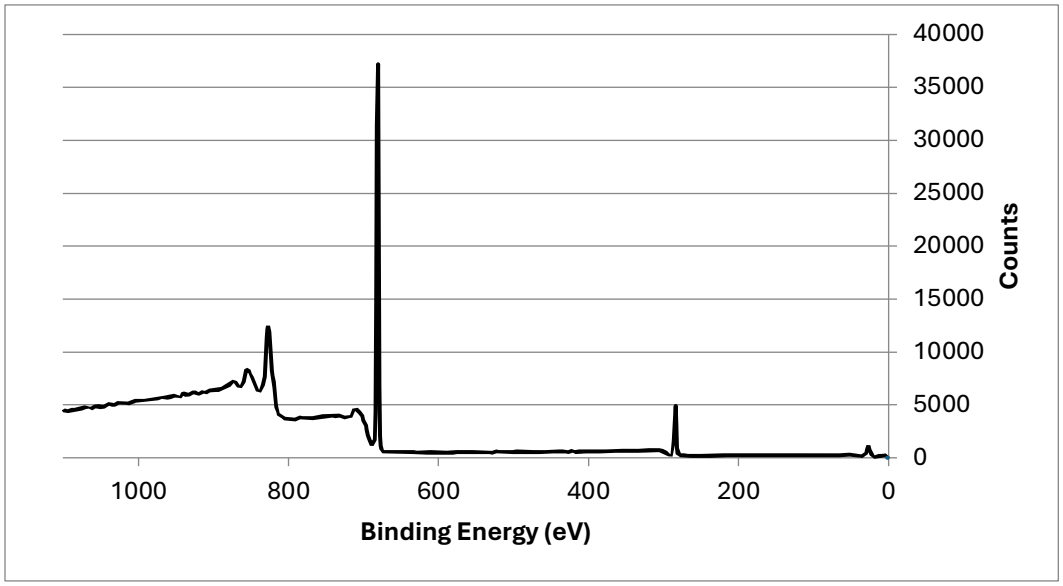

Figure S 9. Survey scan spectra of PTFE

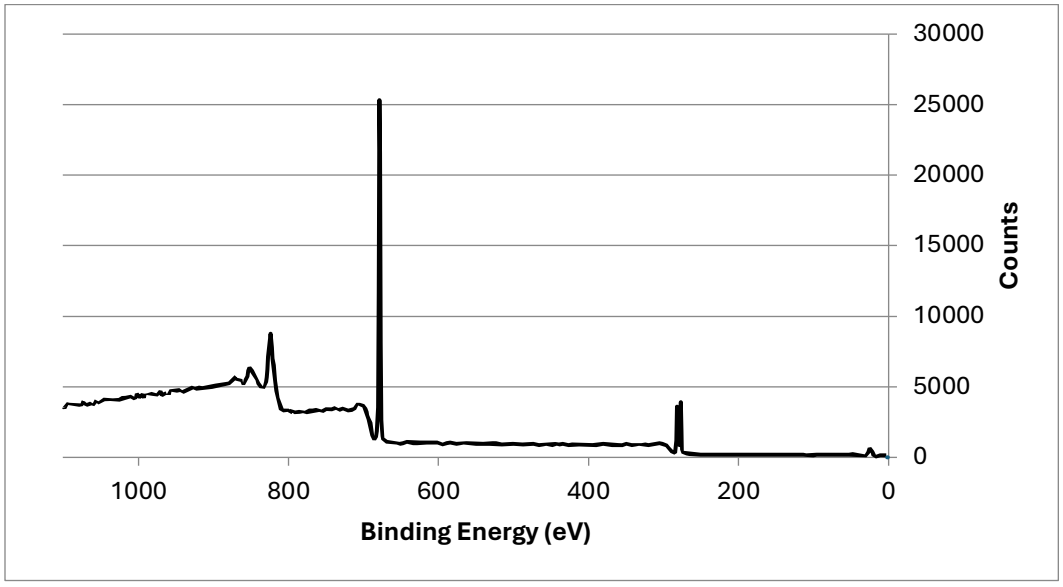

Figure S 10. Survey scan spectra of of PVDF

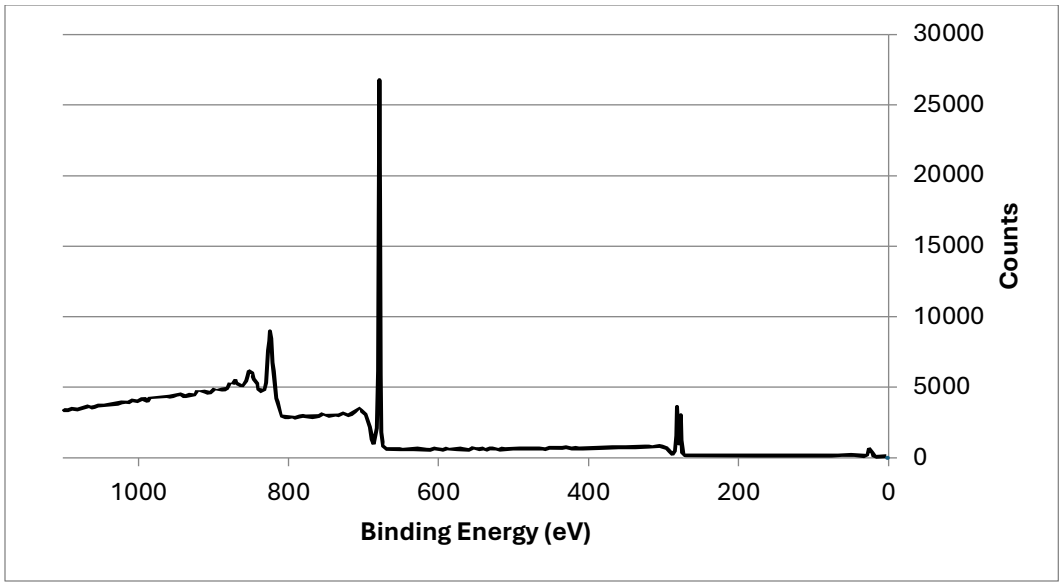

Figure S 11. Survey scan spectra of PVDF-HFP

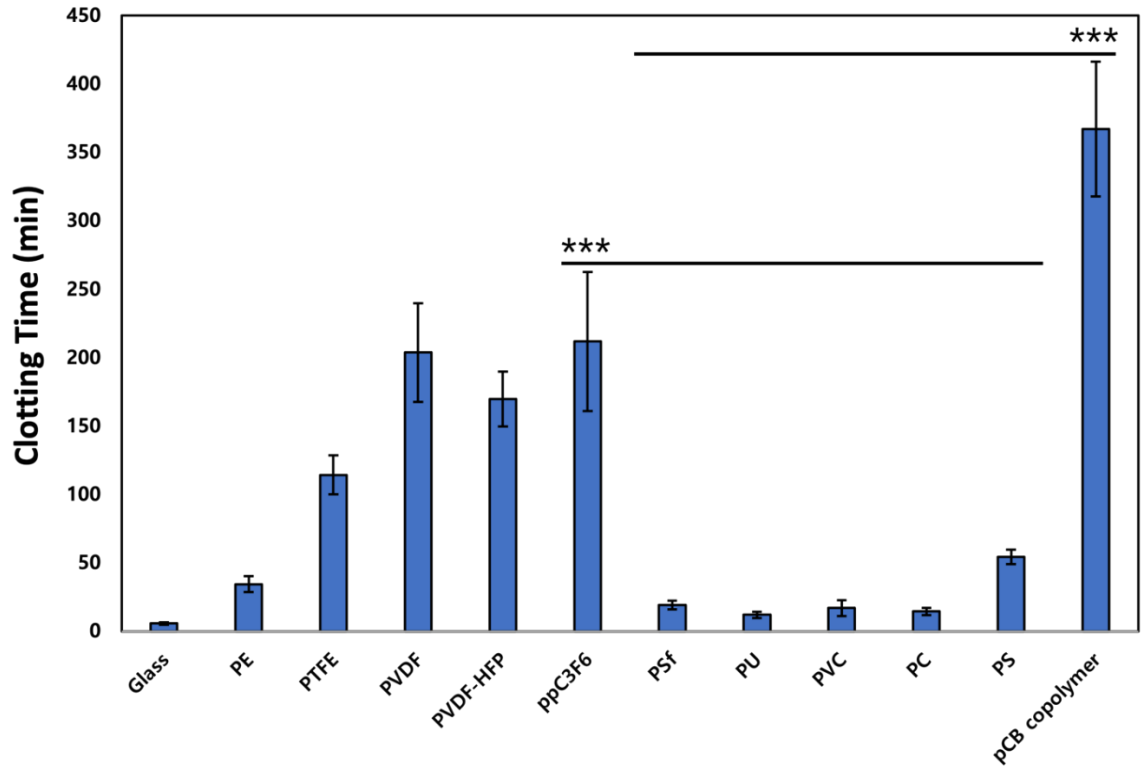

Figure S 12. Clot formation time additional graph, included all the organic medical polymers

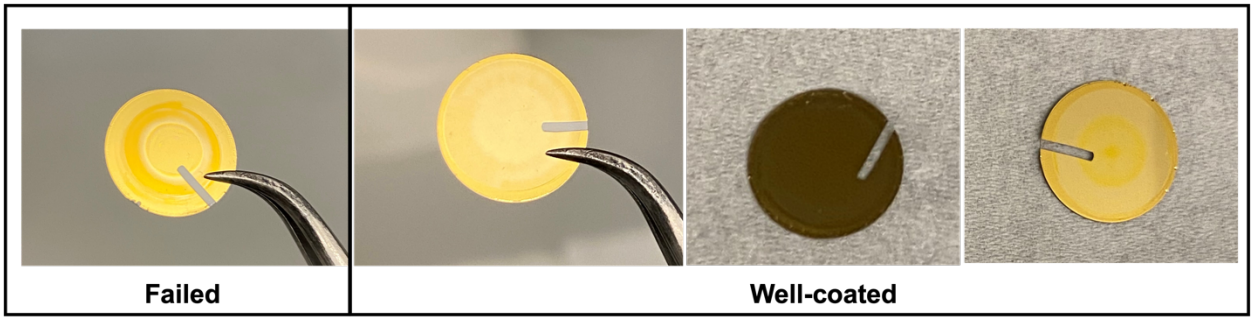

Figure S 13. Images of organic medical polymer spin casting results

Appendix

Appendix 1. I-125 radiolabeled protein adsorption procedures (revised)

Radiolabeled protein adsorption assay SOP

full sequence & action wise sheet

Prepared by Kyung-Hoon Kim

Purpose

The purpose of this SOP is to describe the procedure of preparing the essential buffers and materials for the assay of radiolabeled competitive protein adsorption, and the stepwise procedure for the entire radiolabeling assay for competitive protein adsorption and retention.

Reservation

Log in to the Ratner Lab Hot Room calendar and make a reservation.

Materials

1. Order I-125 a week in advance. Ask Sharon (or corresponding lab manager) about this procedure. Generally, all the radioactive supplies are able to be found on the Perkin-Elmer website. I-125 has particular product number and volume. **(product information update required: Perkin-Elmer I-125, catalog #: NEZ033A005MC (or NEZ033A003MC. The later three digits means activity you want to order), sodium iodide, ~17Ci/mg, 100mCi/ml, 10x-5M NaOH (pH 8-11))**
2. The materials should be prepared in prior to assay date. The maximum dimension of the sample should be limited up to diameter of 8 mm. Generally, the shape of 8mm disk is recommended due

to the size of gamma tube. (*the thickness should be considered as an active surface area in the final S/A calculation)

3. cPBSz and cPBSzl buffer should be prepared the day before. Preparing 10X cPBSz buffer is recommended for the future assay, but to make sure you better to prepare 1L of 1X cPBSz and 1X cPBSzI solution a day before. It's going to be much more accurate in dealing with pH, since the iodination efficiency is depending on the pH of solution.
    a. The stock solution of cPBSz could be stored in the North fridge of the Ratner group main laboratory. On the contrary, cPBSzl should be prepared freshly every time of the experiment. 4~5L of 1X cPBSzl should be made in prior to the day of experiment.
4. Adjust pH after making both of solution in the concentration of 1X. After pHing and dilution, both cPBSz and cPBSzl should be degassed for 2 hours or overnight. Use overflow container and the vacuum port installed on the individual lab bench.
5. Borate buffer, NaCl solution could be prepared in prior to the day before.
6. Check with the Iodine Monochloride solution. Do not use if the solution is older than 6 months. You could prepare fresh solution referring to the Razieh's protocol.
    a. Usually using the one wrapped with the aluminium foil is okay (confirmed with Marvin on April 2019)

Product information

Sodium Chloride (NaCl)

Sodium Azide (Nazl)

Sodium Iodide (NaI)

Citric Acid, monohydrate

Sodium Phosphate, monobasic

Boric Acid (H_3BO_3)

I-125

Perkin-Elmer I-125, catalog #: NEZ033A005MC (or NEZ033A003MC. The later three digits means activity you want to order), sodium iodide, ~17Ci/mg, 100mCi/ml, 10x-5M NaOH (pH 8-11)

BUFFER RECIPES

cPBSzI

4 liters of 10x		**1 liters of 10x**	
Chemical	**Amt. in grams**	**Chemical**	**Amt. in grams**
NaCl	257.18	NaCl	64.30
NaI	59.96	NaI	14.99
citric acid, monohydrate	84.06	citric acid, monohydrate	21.02
Na phosphate, monobasic	55.20	Na phosphate, monobasic	13.80
- pH to 6.93 using approx. 63 g solid NaOH - Add azide to solution after pHing.		- pH to 6.93 using approx. 15.75 g solid NaOH - Add azide to solution after pHing.	
Na azide	8.00	Na azide	2.00
- A 1:10 dilution yields 1X CPBSzI at pH=7.4		- A 1:10 dilution yields 1X CPBSzI at pH=7.4	
4 liters of 1x		**1 liters of 1x**	
Chemical	**Amt. in grams**	**Chemical**	**Amt. in grams**

NaCl	25.72	NaCl	6.43
NaI	6.00	NaI	1.50
citric acid, monohydrate	8.41	citric acid, monohydrate	2.10
Na phosphate, monobasic	5.52	Na phosphate, monobasic	1.38
- pH to 7.4 using approx. 6.3 g solid NaOH - Add azide to solution after pHing.		- pH to 7.4 using approx. 1.57 g solid NaOH - Add azide to solution after pHing.	
Na azide	0.80	Na azide	0.20

cPBSz

4 liters of 10x		**1 liters of 10x**	
Chemical	**Amt. in grams**	**Chemical**	**Amt. in grams**
NaCl	280.30	NaCl	70.08
citric acid, monohydrate	84.07	citric acid, monohydrate	21.02
Na phosphate, monobasic	55.20	Na phosphate, monobasic	13.80
- pH to 6.93 using approx. 63 g solid NaOH - Add azide to solution after pHing.		- pH to 6.93 using approx. 15.75 g solid NaOH - Add azide to solution after pHing.	
Na azide	8.00	Na azide	2.00
- A 1:10 dilution yields 1X CPBSz at pH=7.4		**- A 1:10 dilution yields 1X CPBSz at pH=7.4**	
4 liters of 1x		**1 liters of 1x**	
Chemical	**Amt. in grams**	**Chemical**	**Amt. in grams**
NaCl	28.03	NaCl	7.01
citric acid, monohydrate	8.41	citric acid, monohydrate	2.10
Na phosphate, monobasic	5.52	Na phosphate, monobasic	1.38
		NO NaI for cPBSz!!!!!!!!!	

- pH to 7.4 using approx. 5 g solid NaOH - Add azide to solution after pHing. ** 5g => start w/ 8 pellets, crushed		- pH to 7.4 using approx. 1.57 g solid NaOH - Add azide to solution after pHing. **1.57g = ~ 3 pellets maybe?	
Na azide	0.80	Na azide	0.20

2M NaCl

100 mL		**50 mL**	
Chemical	**Amt. in grams**	**Chemical**	**Amt. in grams**
NaCl	11.70	NaCl	5.85

2X Borate

100 mL		**50 mL**	
Chemical	**Amt. in grams**	**Chemical**	**Amt. in grams**
NaCl H_3BO_3 - pH to 7.75	1.87 2.47	NaCl H_3BO_3 - pH to 7.75	0.94 1.24

1X Borate

100 mL		**50 mL**	
Chemical	**Amt. in grams**	**Chemical**	**Amt. in grams**
NaCl H_3BO_3 - pH to 8.0	0.94 1.24	NaCl H_3BO_3 - pH to 8.0	0.47 0.62

THE DAY OF IODINATION

1. Move all the materials, solutions, and buffers to the hot room
2. Fill up the rinse system with the rest of 1X cPBSzl. Install the tubing accordingly to make it reach to the iodination hood. Check if the rinse system works properly.
3. Get the ice from the Main Lab and fill the Styrofoam box in the iodination ventilation acryl box. Use the green bucket to transfer the ice from main lab to the hot room
4. Aliquot (?)
5. Set up the PS cups to the rotating table in the iodination hood.
6. Prepare the 1st chromatography column and take cap off, bottom break, pour off the excess buffer into the sink, and put on stand in hood, fill w/degassed cPBSz buffer to rinse.
    a. Do it twice at least. One single rinse takes 15~20 minutes
7. Make 5 ml of 10 mg/ml Alb solution w/ 1X Borate (1X borate for Alb tag, 1X cPBSz for Fbg tag)
    a. Store in 15ml conical tube
    b. Do sonication to dissolve the Alb
    c. For Fbg, it's fine to have just 1 ml of 10 mg / ml solution
8. Make ICL/NaCl mixture in a 15ml conical tube: 5mL of 2M NaCl + **112.5 ul** 0.02M stock ICl (3:1 ratio)
    a. 3:1 for Albumin / 2:1 for Fibrinogen -> this is the calculation based on molecular weight. See attachment below:

Samely, start with Fbg Mw=340 kDa, Ending up with 5ml of NaCl + 75 ul of ICl for Fbg

another: Do not forget to add the 1g / 1000mg conversion factor, which is not included in the above calculation sheet.

9. Prepare 3 gamma counter tube below, and place them on the ice. Label outside the Hood
    a. Tube 1: 0.5 ml of 2X Borate
    b. Tube 2: 0.5 ml of ICl/NaCl mixture
    c. Tube 3: 0.5 ml of 10mg/ml Alb in 1X Borate / 0.5 ml of 10mg / ml Fbg in cPBSz
10. decay factor = exp(-0.01153 x _____ days) = _____

    1mCi = 10 µL/decay factor = _____ µL ^{125}I to add. (usually ~10 to 15 ul)
11. Add calculated amount of I-125 to 0.5 ml 2X borate (TUBE 1). Usually this is around 10 ul.
12. Add ICL/NACL mix (TUBE2) to TUBE 1
13. Add 0.5 ml of 10mg / ml Alb (TUBE3) to TUBE 1. Be careful not to create any bubbles
14. Keep on ice for 20 minutes to allow protein labeling reaction.
15. (DURING 20 min)
    a. While reaction proceeds, prepare 40 cups into the ROTATING TABLE, and add 2 EXTRA cups IN FRONT (these are gonna be the testing cups for getting DROPS properly)
        i. MOVE chromatography column to align over cups
    b. Set up 40 gamma tubes for activity standards
16. Add 1.5 ml labeled protein to column along the sidewall: be careful to avoid creating bubbles.
    a. 0.5 ml for each cup (~10 drops)
17. Once drop stop, add 0.5 ml CPBSZ, and then START COLLECTION. Collect 0.5 ml in cup, rotate table, and repeat for 40 cups

a. KEEP the buffer level in column HIGH

18. **DRAIN and rinse 2nd column to save the time**, and set it up on the second arm of the stand in the hood

19. Using NEW GAMMA COUNTER (added on Dec 12, 2019)

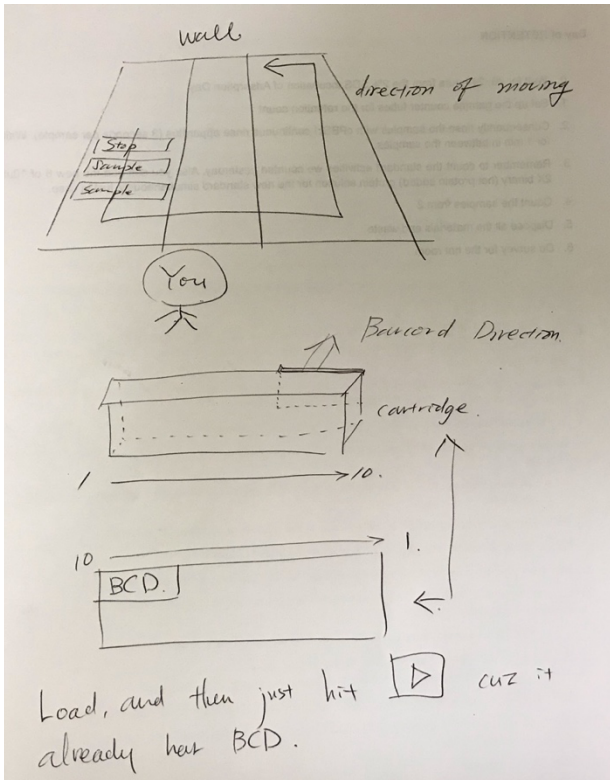

a. As described above, the moving direction of cartridge is counter-clockwise. Usually you should set up ‘protocol-indicating cartridge’ at the closest position to your body, and ‘stop cartridge’ at the farthest position from your body. In case if you have many samples, you can use bare cartridge (cartridge without barcode (BCD)) additionally, placing between ‘protocol indicating one’ and ‘stop one’

b. BKG is background barcode and it usually takes 10 minutes of reading. Not sure so it needs to be clarified further

c. Barcode should be facing toward the wall when you’re loading

d. Compare Stop-Stop vs. Empty-Stop. Stop-Stop immediately makes run stopped, while

Empty-Stop indicates ‘measure-and-then-stop’.

e. Just hit the run button (looks like ‘play’) at the right bottom. You don’t have to specify the protocol because barcode will let machine know what protocol should be used

f. **TROUBLESHOOT:** In case if the software does not respond, just terminate the software and rerun it. You don’t need to reboot the whole system. Just do as below: (sometimes it freezes)

    i. Press ‘windows’ key on the keyboard

    ii. Type ‘taskmgr’ and then enter. The task manager will show up

    iii. Go to ‘process’ tab, then find “WIZUI”.

    iv. Highlight WIZUI and then terminate the process

    v. Once it’s terminated, then find ‘wizard ~~~’ icon on the desktop, then proceed it.

    vi. It will take ~5 to 10 minutes to warm up and to be ready

g. Run ‘background’ first in order to make sure the units (white cone) are not contaminated

h. You’ll get the result from printer

20. After 40 collections are done, then take 5ul of each cup for the iodination count w/ gamma counter. Put them to the gamma tubes

    a. 0.1 min count (actually number/counting time doesn’t matter because what you’re doing at this moment is just purifying, so don’t be afraid of the details of count protocol)

    b. Aim for 3~4 million cpm for 2nd run (purifying run)

    c. Anything <2 million is not enough activity.

d. If there's still a free I125 peak, repeat the STEP 20

21. Pool samples from protein peak in first run (3~4 cups with highest cpm), and run through the second column. Repeating collection and peak purification

22. Collect purified labeled protein (~3 cups) and run six 5ul activity standards for 0.1 min.

    a. Use these numbers to prep calculations for adsorption, but repeat count/activity calculation the day-of to have accurate numbers

    b. Activity = Average # counts for 0.1 min / 5 X 10e-3 ml = XXX cpm / ml

23. Aliquot if necessary. Place in lead pig, freeze in -80C. If there's no freezer, use dry ice.

24. Dispose of all radioactive waste in LSA box or liquid waste bucket

THE DAY OF ADSORPTION

Brought 1X CPBSzI to the hot lab and fill the rinse system

Degas 250ml of 1X cPBSzI O/N or 2 hours

1. Presoak the samples for 2 hours in 0.75ml of degassed 1X cPBSzI in cups in a cupholder on the benchtop

    a. **Waiting 1 min in between** samples when adding the buffer. Cover samples with aluminum foil

2. Thaw iodinated protein in hood, find its activity

3. Check the rinse system if it works properly

4. Prepare 2X incubation protein solution with degassed 1X cPBSzI in 250ml PBS bottle.
    a. A 1X binary incubation protein solution will have 0.3mg/ml albumin and 0.03mg/ml of Fibrinogen. So double those concentration (0.6mg/ml Alb, 0.06mg/ml Fbg). Shake gently to mix (sonication?)
    b. #of samples X (0.75ml/sample) X 1.1 = ml of 2X incubation protein solution, round up to convenient number
        i. # of samples X **0.825 ml** =
        ii. EX) FEP, PTFE, PE, PVDF, PVDF-HFP, HFP = 6X4 = 24,
        iii. **0.825 X** 24 = 19.8 -> ~20 ml of 2X binary protein solution
            1. 20 ml of cPBSzI + 12 mg Alb + 1.2 mg Fbg
            2. For Razieh's Fbg Stock: **91 ul add for 1.2 mg Fbg**
        iv. 0.825 X 28 = ~ 24 ml, / 24 ml of cPBSzI + 14.4 mg Alb + 1.44 mg Fbg
            1. For Razieh's Fbg Stock: **109 ul add for 1.44 mg Fbg**
        v. 0.825 X 32 = ~ 27 ml, / 27 ml of cPBSzI + 16.2 mg Alb + 1.62 mg Fbg
            1. For Razieh's Fbg Stock: **123 ul add for 1.62 mg Fbg**
    c. Check the Razieh's fbg stock number: it contains 13.18 mg of Fbg per 1 ml. Calculate accordingly
    d. 13.18 mg / ml Fbg stock = 0.6 mg / x ml? -> 0.6 / 13.18 = 0.046 ml = 46 ul
5. Calculate minimum protein to signal ratio:
    a. [Nanogram (ng) protein/cm^2 to measure] X (area/samples) = 100 cpm. Solve for 1ng protein = x cpm.

i. Note that the double-sided area of 8 mm disc: 0.4 cm X 0.4 cm X phi = 0.50265

ii. Double-sided: multiply 2, which results in 1.01 cm^2

iii. So you can neglect the area/samples factor in your calculation when aiming 1ng = 100 CPM

b. CALCULATION

i. Volume of binary 2X protein solution (ml) X Concentration of target protein (x mg / ml) X conversion factor (10^6 ng / mg) = Mass of target protein in ng

ii. As we aim 100cpm / 1 ng, multiply 100 to the (i)

iii. Calculate the average standard activity of hot Alb (or Fbg) solution that you counted with 6EA of 5 ul (Step # 21 of IODINATION), and then calculate the standard signal per ul (generally you can get this value via divide your avg value by 5 ul)

iv. Divide the **(ii) (total CPM required)** by **(iii) (standard CPM per ul)** will give you the volume you should add to the 2X binary protein solution

v. Example of calculation:

1. 20 ml of 2X binary protein solution (12 mg Alb, 1.2 mg Fbg in cPBSzI)

2. Avg. 3,370,000 CPM for 5ul of standard activity (Measured from **Step # 21 of Iodination**)

3. 20 ml X $\frac{0.06\ mg\ Fbg}{1\ ml}$ X $\frac{10^6\ ng}{1\ mg}$ = 1.2 X 10^6 ng, Total CPM = 1.2 X 10^8 CPM (as we aim 100 CPM / ng)

4. Average hot Fbg Standard Activity = 3.37 X 10^6 CPM / 5 ul = 6.74 X 10^5

CPM / ul

5. Therefore, (1.2 X 10^8 CPM / 6.74 X 10^5 CPM/ul) = 178 ul of hot Fbg solution to add

6. **Check the activity standards with 2X protein solution** (with hot protein added) , take 6 of 10ul standards, and **DO NOT TOSS the standards after counting**. 1 minute of count is enough **(use protocol 16)**
7. Add the hot 2X protein solution (0.75 ml per each) to the samples, and have the 1 minute of time interval between each samples. This is the **ADSORPTION procedure**
8. Cover samples with the aluminum foil, and move to the 37C incubator
9. While waiting, prepare 2 wt% SDS solution. Weigh 2g of SDS powder, and add them into the 100ml of DI water
    a. **Make a volume of 2% SDS equal to 1.5mLs*# samples. Allow SDS to dissolve, avoiding bubbles**.
10. While waiting, prepare gamma tube accordingly to the number of samples for 'adsorption' counting
11. Set up the rinse system properly, and check again if it works properly
12. Start rinse (2-step, 5 seconds / 3 seconds) and put the samples into a new gamma tube individually
13. Count for 1 minute. Remember do sample count with the activity standards (although you've done with the activity standards)
    a. KEEP the order of your each samples, even if they're same groups.
        i. EX: FEP1, FEP2, FEP3, FEP4 should be in a same order so that you can read the 'retention value' tomorrow accordingly. You should keep the order.

14. While counting, prepare 1.5 ml SDS solution per each new cup, place them on the rack
15. After counting, move the samples to the SDS-loaded cup (please watch out for the ORDER of the samples in the same group)
16. Cover with aluminum foil
17. You're gonna do the 'retention' after 20~24 hours from now on. Record the time accordingly.

Day of RETENTION

0. Wait for 20~24 hours from the 2% SDS incubation of Adsorption Day
1. Set up the gamma counter tubes for the retention count
2. Rinse the samples consequently with cPBSzI continuous rinse apparatus (3 seconds per sample). Wait for 1 min in between the samples.
3. Remember to count the standard activities we counted yesterday. Also, you can add the new 6 of 10ul 2X binary (hot protein added) protein solution for the new standard simultaneously, just in case.
4. Count the samples from 2
5. Dispose all the materials and waste
6. Do survey for the hot room

Experimental Option A: QCM-D Matching Run

Has four modules with n=4 for each group

Note that the total number of sample needed are 32 of each group. Make sure if you have enough number of samples before you start

a. Need 4 of each group / Single albumin solution: 120 min of Alb only, Alb hot

b. Need 4 of each group / Single fibrinogen solution: 120 min of Fbg only, Fbg hot

c. Need 8 of each group / Binary protein solution: 120 min of Alb+Fbg

    i. *Alb + cold Fbg (Alb hot)

    ii. *Fbg + cold Alb (Fbg hot)

d. Need 16 of each group / Sequential run: 120 min of mixed.

    i. Sequence: 20 min presoak in PBS, 60 min Alb, 20 min PBS, 60 min Fbg

        1. 60 min Alb* + 60 min Fbg

2. 60 min Alb + 60 min Fbg*
3. Reversal: 60 min Fbg* + 60 min Alb
4. Reversal: 60 min Fbg + 60 min Alb*

Radioactivity count is performed by every 20 min or 30 min. Do 30 min as a practice run, then do 20 min for better information

8 assay sets in total: Protein volume calculation

Recommend run the assay in two separated session (Alb vs. Fbg)

1. Alb only: need 2ml per sample, therefore 4n X 3group = 12 samples X 2 ml = 24 ml required. Prepare 26ml hot Alb solution (0.3 mg / ml) for safety: total 4,4,4 = 12 samples required.
2. Binary Alb hot: need 2ml per sample, 26ml hot Alb + cold Fbg solution (0.3 mg / ml Alb* + 0.03 mg / ml Fbg): total 4,4,4 = 12 samples required
3. 60 min Alb* then Fbg (samely, 26ml hot Alb only & another 26ml cold Fbg)
4. 60 min Fbg then Alb* (samely, 26ml hot Alb only & another 26ml cold Fbg)

Totally, ~100 ml of Alb* is required

Prepare 26 ml of Binary hot Alb

Prepare 78 ml of hot Alb only solution

Another set:

1. Fbg only: need 2ml per sample, therefore 4n X 3group = 12 samples X 2 ml = 24 ml required. Prepare 26ml hot fBG solution (0.3 mg / ml) for safety.
2. Binary Fbg hot: need 2ml per sample, 26ml hot Alb + cold Fbg solution (0.3 mg / ml AlB + 0.03 mg / ml Fbg*)
3. 60 min Alb then Fbg* (samely, 26ml COLD Alb only & another 26ml HOT Fbg)
4. 60 min Fbg* then Alb (samely, 26ml COLD Alb only & another 26ml HOT Fbg)

Totally, ~100 ml of Fbg* is required

Prepare 26 ml of Binary hot Fbg

Prepare 78 ml of hot Fbg only solution

Note

Each run should perform radioactivity count by every 20 min, and that means the total time of experiment will take longer than 120 min.

Usually, from the beginning to the end, one single set run takes ~4 hours. Plan accordingly.

Procedure

Calculate the volume of protein solution you need accordingly.

Appendix 2. RFGD plasma deposition of ppC_3F_6 procedures (revised)

Standard Operating Procedure for Hexafluoropropylene (ppC_3F_6) RFGD Plasma Treatment

Note: Clean cold trap with methanol and make sure it is dry before using it. After use, the cold trap should be removed at the end of the week or when people are done using it, and should be kept in liquid nitrogen in the meantime to prevent collected vapors from rising. The terms "vacuum pump valve/bottom vacuum valve" are interchangeable, as are the terms "glass reactor valve/top vacuum valve."

MFC = Mass Flow Controller

RF = Radio Frequency Plasma Generater = RF Power

PG = Pressure Gauge

Vent valve = air intake valve (black)

A. Install cold trap (see SOP for cold trap installation/removal).

B. Set Up Reactor

1. Turn on three power switches: MFC (2), RF (AC on, NOT RF on).
2. Make sure top and bottom vacuum valves are closed, with cold trap installed (see cold trap SOP).

3. Close main chamber loosely with large Viton o-ring in place between two (2) halves of the glass chamber. Make sure vent valve is closed.
4. Turn on the vacuum pump for at least 30 minutes before proceeding.
5. Get liquid nitrogen (LN2) from Chemistry store (3.4 L) using a 4 L dewar flask.
6. Fill cold trap with LN2 through funnel. Use cryogenic gloves.
7. Open lower vacuum valve slowly, avoiding the gurgling sounds of excess air intake.
8. Open top vacuum valve slowly again and adjust main chamber and large Viton o-ring if good seal isn't in place.
9. Clean all lines, one gas at a time ONLY. On the MFC unit, turn all upper switches up – green lights and lower switches down. Open argon line first, then CH4 (if using), then C3F6. DO NOT open gas tank valves, which are on each tank, or those valves closest to the tanks themselves.
10. Wait for pressure to stabilize – should be low, below 15 mT.

C. Air Plasma Reactor Etching: ~500 mT, 30-40 W (watts), 30 minutes

1. When base pressure (0 mT) is reached, close all gas lines.
2. Open vent valve until PG reads ~500 mT.
3. Turn RF power ON. Set forward (FWD) power to 5W by switching the AVG RF POWER to FWD. Switch the AVG RF POWER to reverse (REV). Turn the knob (INC/DEC) in the Tegal matching network above the glass chamber counterclockwise until the needle in the AVG RF POWER goes down to its minimum.

4. Flip the AVG RF POWER switch back to FWD and increase the FWD power to 10-20 W increments. Toggle sequence in step 3 again (between FWD and REV) until desired power is reached. Visually confirm presence of plasma.
5. Immediately start stopwatch.
6. Wait for 30 minutes and monitor reflected power for several minutes. It is advised to leave the room when plasma is on, but check that plasma is still on and pressure is still correct halfway through etching.
7. Turn RF power OFF.
8. Close vent valve.
9. Wait until pressure returns to base pressure (0 mT).
10. Close all lines (MFC and gas valves).

D. Load substrate, at least 30 minutes before commencing monomer deposition.
    1. Let Argon (Ar) gas in: switch Argon MFC to ON and FLOW and open Argon valve.
    2. Close top vacuum valve.
    3. Open vent valve until chamber is no longer under vacuum. Close argon valve.
    4. Loosen the ultratorr in the deposition chamber end cap.
    5. Unsecure the two halves of the deposition chamber (metal twist/o-ring).
    6. Lay down the end cap and large o-ring sideways on a clean large kimwipe.
    7. Put substrate on glass plate, slide glass plate into deposition chamber between the rings or electrodes, ensuring level placement. Ensure that samples are placed as close to center of plate/symmetrically as possible. Use a ruler if you need to.

8. Draw a picture of sample placement (it's a good idea to have a small piece of clean Si wafer substrate on the glass plate for later XPS analysis). Try to minimize air exposure time in this step, as that increases hydrocarbon contamination on samples.
9. Secure the two halves of the deposition chamber.
10. Tighten the ultratorr to the deposition chamber end cap.
11. Close vent valve.
12. Slowly open top vacuum valve. Be extremely slow and cautious, checking to make sure your samples have not moved around on the plate. Pulling vacuum too quickly will make them fly off. If samples have moved, go back to step 1.
13. Ensure the two halves of the deposition chamber are pulled together without a leak (see part F for testing leak).
14. Let it pump down for at least 30 min.

E. Record the base pressure (should be 0 mT).

F. Record the leak rate
    1. Close all MFC (2) and gas (C3F6 and Argon) valves.
    2. Wait for pressure to stabilize (0 mT).
    3. Close top valve.
    4. Wait 1 minute and record the difference between starting and ending pressure. More than 10 mT increase means there is a leak. If you wish to identify the source of a leak, spray methanol at joints/potential leakage areas and see if pressure rises on PG.

5. Refill LN2 for the cold trap.

G. Sample argon etching: 40 W, ~200 mT, 62.1 sccm, 5 minutes

1. Ensure all lines but argon lines are closed.
2. Open the argon line (2 switches up, 3 valves, tank).
3. Ensure the Calibration Factor is set to 1.45 at the back of the argon MFC. If not, unlock and adjust, then lock again.
4. Set the argon flow rate to 62.1 sccm by turning the Set Point knob on the MFC.
5. Wait until pressure stabilizes to around ~210 mT. Stay at that pressure for a few minutes.
6. Turn RF power ON. Set forward (FWD) power to 5 W, adjust reflected power to minimum (using REV and matching network as described in part C) and check FWD again. Start timer. After 5 minutes, turn RF power OFF.
7. Close Argon MFC.
8. Pump down to base pressure (0 mT).
9. Close argon valve.

H. C3F6 deposition: 1 minute @ 60 W, 150 mT, 10 sccm then 20 min @ 20 W, 150 mT, 10 sccm

1. If using a new tank, fill the initial portion of line with C3F6 by opening the C3F6 valves (one on tank and the next valve down the line). Then close both. Pump down to base pressure and perform a leak test (see part F). If using an old tank, just open C3F6 valves (including tank valve).

2. Press ZERO (0.014 mT) on the AdapTorr (Model AC-2) by TylanGeneral.
3. Set Calibration Factor to 0.14 at the back of Power Supply Readout Type 246 using the back knob: Unlock dial, turn counterclockwise to get number display to zero, set to 72, then lock. Turn both switches on C3F6 MFC up to begin flow.
4. Set C3F6 flow rate to 10.0 sccm by turning the Set Point knob.
5. Set pressure to 150 mT by pressing AUTO on AdapTorr. If need be, adjust using UP/DOWN set buttons.
6. Wait until pressure stabilizes to 150 mT. Record number needed on AdapTorr to get 150 mT on PG for future reference.
7. Turn on RF power
    a. Set forward (FWD) power to 5 W, adjust reflected power to minimum (using REV and matching network as described in part C) and switch to FWD again. Ramp up in 20 W increments, minimizing reflected power in each step, until you reach desired power. Start timer.
        i. Adhesion layer = 60 W, 150 mT, 1 minute
        ii. Coating layer = 20 W, 150 mT, 20 minute
        iii. Adjust reflected power to 0 if possible, visually confirm plasma, leave room during treatment to avoid high power exposure, checking in halfway that pressure is still correct and plasma is on.
8. Turn RF power OFF.

I. Quench sample with monomer flow only: 0 W, 150 mT, 5 minutes

1. After 5 minutes, set AdapTorr to OPEN.
2. Pump down to base pressure (0 mT).
3. Close all gas lines.
4. Wait for 30 minutes. This step as well as the time duration is optional, it helps decrease smells released in the next step. See part J for alternative.

J. Remove substrate (similar to loading substrates, see part D)

1. Open argon line (2 switches, 3 valves, tank).
2. Set argon flow rate by switching the argon MFC to flow (up) and adjusting the flow rate to 72 sccm using the Set Point knob on the front.
3. Wait for 3 minutes.
4. Close the argon line.
5. Wait to pump down to base pressure. If you skipped step 4 of quenching, you may repeat steps 1-5 here two more times to flush the system a total of 3 times with argon.
6. Flow argon gas again.
7. Close top valve.
8. Slowly open vent valve when pressure reads 5 mT.
9. Unsecure the two halves of the deposition chamber (metal twist/o-ring) when the pressure reaches atmosphere. Place cap with o-ring face-up on clean kim wipe.
10. Put substrate on a petri dish using tweezers, fill gently with nitrogen from the tank by the hood (test pressure on wrist first so you don't blow your sample around), label (name, date, substrate, monomer, treatment parameters), and paraffin seal. Sample can temporarily be stored in large hood, but must be put in a secondary container if

transferring outside of the large hood (sealed bag, larger petri dish: fill secondary container with nitrogen and seal).

K. Repeat part C, air plasma reactor etching.

L. Close all lines, close vacuum valves, open vent valve, remove cold trap
    1. Cover ends of flex hoses and cold trap with aluminum foil.
    2. Place the cold trap in a beaker/box inside the fume hood.
    3. Please check SOP for removing/installing cold trap.

M. Shut RF AC power OFF.

N. Shut vacuum pump OFF
    1. Turn vacuum pump switch OFF.
    2. Loosen clamp tube by the pump and let air in slowly by tilting the tube (helps create barrier for oil reflux).
    3. Tighten tube clamp again.

Appendix 3. RFGD plasma deposition of Allylamine procedures (revised)

Preparation of Amine-treated surface using RFGD plasma deposition

By Kyung-Hoon Kim / B.Ratner Lab

Extracted and modified from Dr. Marvin Mecwan's Thesis

Allylamine from Sigma Aldrich

Cat. 145831 (98%)

Cat. 241075 (99%)

Note:

- Should use plasma reactor in Foege hall N323B
- Do not use the HEMA inlet that is closer to the wall. You will use the inlet very close to the electrode, which is lower than the HEMA one in terms of altitude.
- Should have full of LN2 (~ 4 liters) for cold trap and monomer degassing
- Should detach the cold trap and clean it with methanol after you are done

- **BE EXTRA CAREFUL WHEN LOADING/DELOADING THE SAMPLES AND OPENING/CLOSING THE REACTOR. The opened reactor can be rotated, which might cause 'breaking' the middle inlet (made from glass) to get down to the ground toughly.**

1. Glass coverslips should be cleaned with formal cleaning protocol
2. Etching with Argon: 40W, 250 mTorr, 10 min
3. Adhesion layer (w. AAmine): 80W, 250 mTorr, 1 min
4. Coating layer (w. AAmine): 10W, 150 mTorr, 10 min
5. Quenching 5 min

From Dr. Sang-hun Song's paper (*Langmuir* **2013**, 29, 12710-12719)

- 13.56-MHz RF power source
- Evacuating to the base pressure of 10 mTorr with rotary vacuum pump
- Oxygen etching, 350 mTorr, 80W for 30 min
- Argon activation, 350 mTorr, 30W for 30 sec
- AAm adhesion, 350 mTorr, 80W for 30 sec
- AAm deposition, 350 mTorr, 10W for 5 min / thickness of 130 nm / refractive index was 1.581
- HApp adhesion, 250 mTorr, 80W for 1 min

- HApp adhesion, 250 mTorr, 10W for 1 min / thickness of 220 nm / rms roughness was 0.5 nm by AFM

Appendix 4. RFGD plasma deposition of pHEMA procedures (revised)

SOP: Operation of pHEMA RFGD plasma machine (Foege lab)

Written by Kyung-Hoon Kim / Buddy Ratner Lab / Revised 7/1/2020

1. Preparation:
    a. Cleaned reactor (use methanol to remove the material residue polymerized inside the reactor)
    b. Cleaned sample
    c. Check the HEMA monomer solution (could be found at the lab fridge)
        i. Polyscience, 2-Hydroxyethyl Methacrylate, Ophthalmic Grade (04675-500, 500g)
    d. Get LN2 from the chemistry store (stockroom at the Bagley hall)
2. Install the cold trap and fill the LN2
3. Open the black valve (one close to the door) to break the vacuum in reactor. Tight the gasket at another end of the reactor.

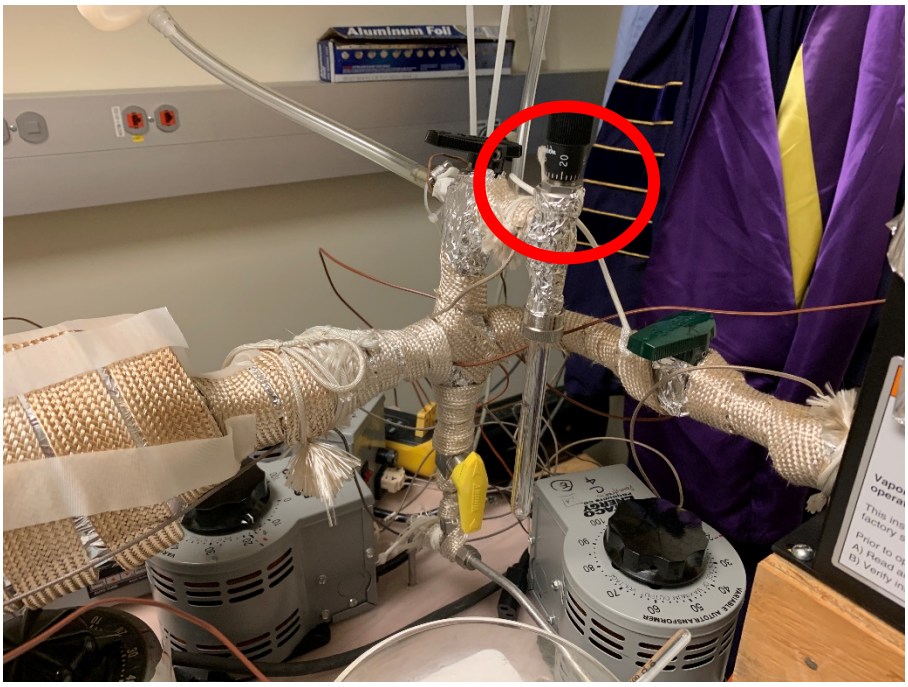

4. After cleaning the reactor, close the reactor, and pump it down i.e. reach the vaccum.
5. *Close the rightmost air supply valve (black valve) and close the reactor. Open the gasket to get the vacuum*
6. Insert the monomer flask in the outlet
    a. Get 5~10 ml of HEMA monomer from the lab. Use round-bottom flask
    b. Degas the monomer using the freeze thaw method, do atleast 3 cycles.
7. Open the reactor and put the samples into the reactor accordingly
    a. *If you did not clean the inside of the reactor, then do it at this point. Load the sample later.*
8. Close the reactor and pump it down.
9. Perform Argon etch. Open the Argon tank valve. Turn 3-way valve under the left MFC to the ‘Ar’, and open the yellow valve to let the Argon gas get into the reactor

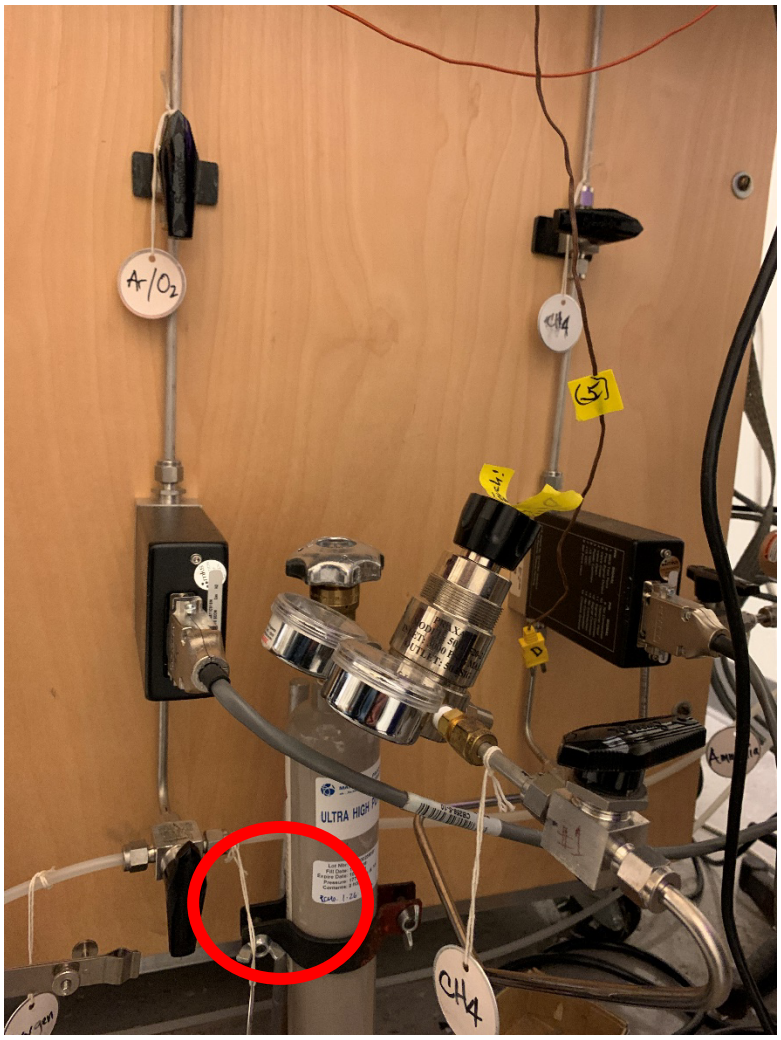

10. [Ar etching] Open the MFC valve, then press “OPEN” at the pressure gauge machine (black one located under the table, right to the white RF machine), press 1 and wait for the pressure to be reached to 250 mTorr
    a. 5 minutes of Ar etch at 40 W
    b. SCCM 4
11. Turn off the plasma

12. Close the 3 way valve. Set the flow meter to open and pump down the reactor to vacuum. Close the valves on flowmeter, the opne on the left side.
13. CH4 adhesion required: Turn the 3-way valve (one connected to the right MFC) to the CH4, open the MFC valve, then turn on the MFC controller (right one) to clean up the line, waiting the gauge get the base pressure
14. Open the CH4 cylinder valve so that CH4 gas could be supplied to the reactor
15. Let the pressure stabilize and then open the control valve on the flow meter and set the pressure to 150 mTorr.
16. Perform CH4 adhesion
    a. 5 minutes of CH4 adhesion layer deposition at 80W, 150 mTorr
    b. SCCM 1.4
17. Turn off the plasma
18. Close the CH4 tank valve,Turn off the 3 way valve nect to the tank and press OPEN on the flow meter, wait till the pressure reaches to the base pressure, then close the MFC valve, then turn off the MFC machine. In this way, the leftover gas in the line could be removed

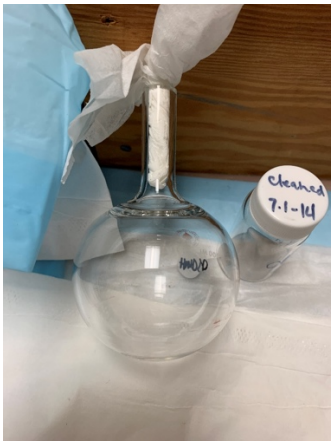

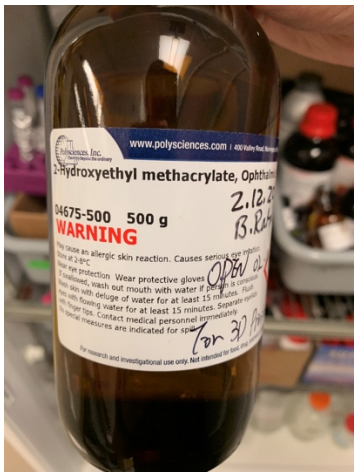

19. Turn on the heat plate to preheat, as we should use it for the HEMA monomer supply—we should boil the HEMA solution to let them evaporate, and get into the chamber for the deposition

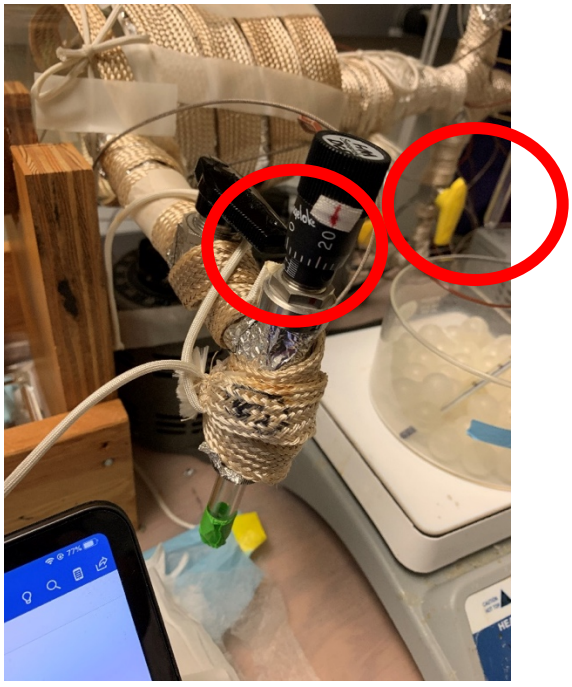

20. HEMA degassing should be performed by repetitive freezing-and-melting (3 cycles)
    a. Install the HEMA-loaded round bottom flask to the middle inlet of the reactor

b. Place PYREX glass bath underneath the round bottom flask

c. Gently pour LN2 so that HEMA solution could be frozen

d. Once it's completely frozen (or near-completely frozen), then thaw it. The gas trapped in the HEMA solution will go away as the solid HEMA melts

e. Repeat 3-4 times

21. HEMA deposition should be performed. Make sure there is no other gas supply to the reactor—check all the valves around, including yellow one and MFC valves. Don't know if the green one should be closed as well.

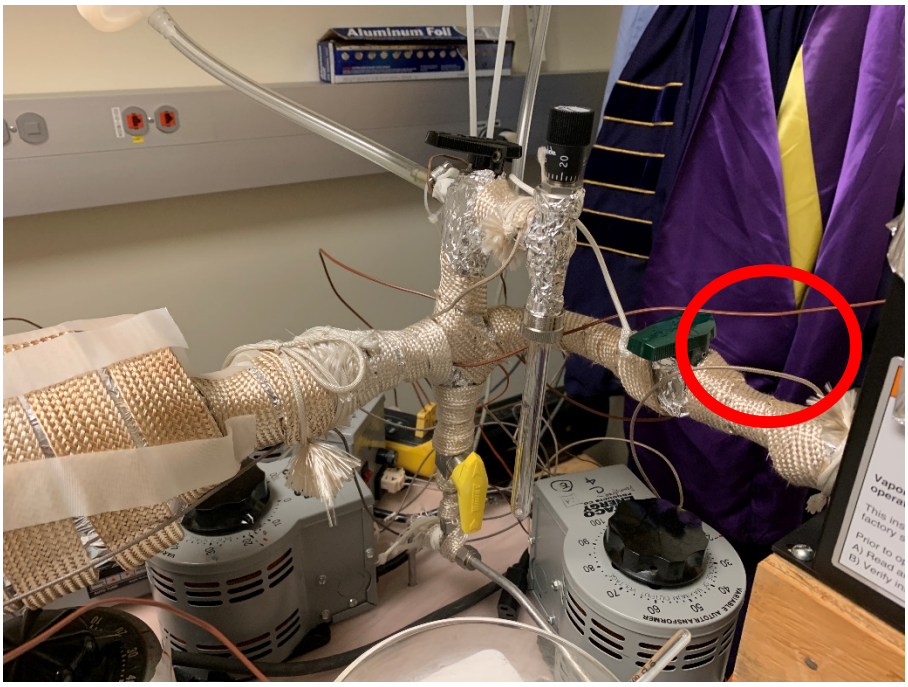

22. HEMA deposition: 145°C heating pad usually get 65°C:

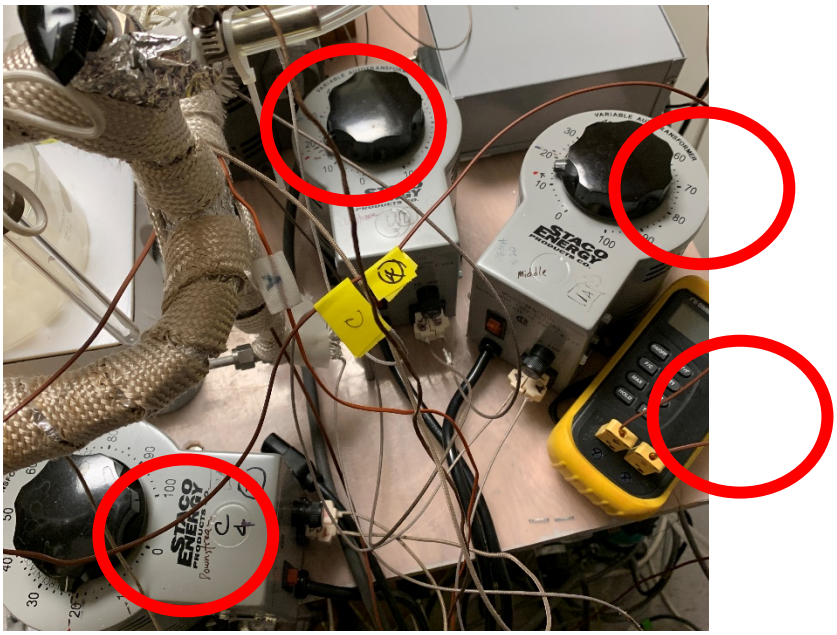

a. 1 minute of HEMA at 100W, 250 mTorr: as long as it's stable enough, then go start adhesion run
b. 20 minutes of HEMA at 6~7W, 250 mTorr (Maybe the same preset with 17-a (above))
c. 5 minutes of quenching, and do Argon flashing 3 cycles
    i. Ar – open – Ar – open

23. Perform Argon etch (same condition), then turn off the RFGD power.
24. Oxygen etch: 60W, 250mTorr, 30~45 min
25. Check all the 3-way valves are neutral, then close the valve.
26. After done, turn off the MFC and 'open'. Wait for the base pressure
27. Close the yellow valve. Turn off all the MFC. Open the middle valve (HEMA supply inlet).
28. Turn thermo off -> then close middle inlet of HEMA. Do Argon flashing on MFC. 1-> enter
29. Close the gasket (one far from the door) of reactor and open the valve slowly (one close to the door)

Appendix 5. Platelet Adhesion Assay / SEM SOP

Protocol for Platelet Adhesion Assay & SEM Analysis

Kyung-Hoon Kim, Revised 06/24/2022

A. Solution Preparation (made at room temperature, i.e. RT, unless otherwise noted)

a. 5X Tyrodes Buffer (100 mL stock)

Make stock in advance, mix on orbital shaker until dissolved:

16g NaCl	2g dextrose
400mg KCl	23.3mL 30% BSA
110mg NaH2PO4xH2O	5mL 1M HEPES
2g NaHCO3	71.7mL ddH_2O

The BSA is liquid and located in the door of North Fridge (N323C). All dry chemicals are in a box on a shelf above Sharon's bench.

HEPES is located in Irini's shelf

Stir until dissolved, aliquot 10mL in 15mL Falcon tubes.

Freeze and store 5X stock at -20°C in TC freezer.

b. 0.25M $CaCl_2$, dihydrate (100X)

Make in advance:

1g $CaCl_2x2H_2O$

28mL ddH_2O

Stir until dissolved, aliquot 1mL in 1.5mL Eppendorf tubes, freeze and store at -20°C.

c. 0.1M $MgCl_2$ (100X)

Make in advance:

238mg $MgCl_2$

25mL ddH_2O

Stir until dissolved, aliquot 1mL in 1.5mL Eppendorf tubes, freeze and store at -20°C.

d. 1X Tyrodes Buffer (TyB) – volume set for 18 samples + some extra

Day before: Make 300mL, equilibrate 1hr in 5% CO_2 incubator, pH to 7.2-7.4, then store in 4°C fridge overnight. Equilibrate at least 1hr before use next day.

240mL ddH_2O

60mL 5X Tyrodes buffer, thawed in TC water bath.

Measure 240mL of ddH_2O into clean glass bottle.

Pipet 60mL of 5X Tyrodes Buffer to water, triturate to mix.

Loosen cap and equilibrate in 5% CO_2, 37°C, for at least 1hr.

Check pH = 7.2-7.4 using TC pH meter and fresh titrating 1M HCl/NaOH.

Always return solution to 5% CO_2 incubator with loosened cap during centrifuge runs/times not in use.

Day-of : Aliquot 40 mL in a conical tube for blocking preincubated samples.

Day-of: Aliquot another 40 mL for the preincubation solution, which couLd be:

- 1% human plasma: add 400 µL pooled human plasma (in -80°C fridge bottom shelf with the apyrase)
- Human serum albumin (HSA): 0.3 mg/mL, i.e. 12 mg
- HSA + Human Fibrinogen (Fbg): HSA + 0.03 mg/mL, i.e. 1.2 mg Fbg
- Invert and mix on orbital shaker, minimize foam formation.

e. 1X DuLbecco's PBS (Phosphate-Buffered Saline, Lonza catalog # 17-513), for rinsing nonadherent platelets. Volume needed will be 2mL/sample* 8 rinses*# samples.

   Sterile filter dilution from 10X purchased stock in advance, can keep at RT.

f. 0.2M Sorenson's Buffer (Electron Microscopy Sciences, # 11600-05, pH=7.2)

g. Karnovsky's Solution, for fixing platelets. Can be made in advance during platelet incubation period or fresh before use.

i. Add the following in A 50mL conical tube. Mix by inverting. You can use the same pipette tip if keeping order.

5.0mL ddH_2O

5.0mL 0.2M Sorenson's Buffer

15.0mL 0.2M sodium cacodylate

6.0mL Karnovsky's solution stock made from original recipe

h. CaCo Rinse, for fixing platelets. Make on day 2 of fixing if left fixing overnight, or fresh.

i. Add the following in a 100mL media bottle:

25.0mL dH20

25.0mL 0.2M Sorenson's Buffer

50.0mL 0.2M sodium cacodylate

i. Osmium tetroxide stain, for lipids/membranes. Make during fixing immediately before use. Take care to break glass capsule gently with kim wipes as a safety barrier.

i. Add the following in a 50 mL conical tube:

2.0mL ddH_2O

2.0mL 0.2M Sorenson's Buffer

8.0mL 0.2M sodium cacodylate

4.0mL 4% OsO_4

j. Ethanol/ddH_2O solutions of 50%, 70%, 80%, 80%, 100% (keep stocks).

B. Platelet Adhesion Assay & Fixing

a. Add 1 mL of PRP/Tyrodes buffer to each sample.

b. Place in 37°C and 5% CO_2 BSL-2 incubator (top right) for 120 minutes. Platelets will settle via gravity and attach to surface, so stir plate gently at 30 minutes.

c. Rinse 6X with 1X phosphate buffered saline to remove non-adherent platelets.

d. Fix samples. Note: All the following steps are done in a fume hood over an absorbent pad, collect all rinses in suction flask and dispose of as labeled hazardous waste.

   i. Fix samples 2 hrs at RT or overnight at 4°C in 2 mL Karnovsky's solution per well. Parafilm plate and place in dated/labeled secondary container. If leaving overnight, allow the plate and contents to warm up to room temperature before continuing with next ethanol dehydration steps.

   ii. Rinse using 2.0 mL CaCo rinse per well, 3 x 10 min RT

   iii. Stain using 1.5 mL OsO_4 stain per well, 30 min RT

   iv. Rinse using 2.0 mL CaCo rinse per well, 3 x 10 min RT

   v. Rinse in 50% ethanol, 2 x 5min

   vi. The 1st and 2nd 50% ethanol rinse is collected as hazardous waste. Empty the waste flask, rinse 2X with 10mLs 50% ethanol and collect that rinse as hazardous waste before collecting the 70% ethanol rinse. Beginning with the 70% ethanol rinse you will collect the washes as ethanol only waste ([final]=85%).

vii. Rinse in 70% ethanol, 1 x 15 min (stop here if you're done for the day, leave at 4°C overnight). This is the recommended stopping point to minimize duration of the next day's prep. If you have too many samples for one CPD run, consider leaving one plate in 70% ethanol overnight and doing CPD the next day.

viii. Rinse in 80% ethanol, 1 x 15 min

ix. Rinse in 90% ethanol, 1 x 15 min

x. Rinse in 100% ethanol, 1 x 15 min

xi. Change 100% ethanol rinse, parafilm the plate underneath its cover, and transport to MolES for CPD in a secondary container. Take care that the samples remain under 100% ethanol during transport and when transferred to ethanol-filled CPD chamber. YOU WILL NEED A SECOND PAIR OF HANDS FOR THIS. Allow 3-3.5hrs total for CPD and sputter coating, and after sputter coating, store the samples in a sealed container with a dessicator packet.

Appendix 6. Thrombin Generation Assay SOP

Thrombin Generation Assay SOP

Kyung-Hoon Kim

B. Ratner Lab / Center for Dialysis Innovation

Last updated: May 29, 2023

- Please refer to the insert in Haemoscan TGA kit for the detail. This SOP is a revised version modified from the original SOP of Haemoscan TGA kit

NOTE

- **<u>We'll use 400 ul of diluted plasma for each of sample:</u>**
    - it barely covers the entire 15mm biomaterial sample and do not have much contact with polystyrene well surface of 24 well plate

- **Modified TGA plasma:** fibrinogen and ATIII depleted plasma
- **Reagent A: calcium**
- **Reagent B: phospholipids (phosphatidyl serine and phosphatidyl choline)**
- **Lyophilized TGA plasma:**

- Reconstitute one vial of plasma with 750 ul of demineralized (DI) water. Let it stand for 10 min at room T, mix a few times by end-over-end tumbling and it is ready for use.
- This could be stored at -20C or in the fridge. The lower the longer period of storage time.

Principles (surmising)

1. Plasma contained in the kit is made from a pool of healthy donors, intended to be "normal". Biomaterial is the activating source.
2. Incubation time for the thrombin generation measurement is limited 6 minutes, in order to discriminate between strong and mild activators. The tube without biomaterial is generating thrombin very slowly and does not reach high values in 6 minutes. We use a calculation sheet (attached) which results in units per surface area per time.
3. For an ideal case, we can hypothesize that there will be nearly 'NO' thrombin generated if the biomaterial is fully blood compatible. But currently we don't have any materials like that, which means there will be always some thrombin formed from biomaterials. However, the super inert material will show no detectable amount above the negative background (empty tube). We might be able to get negative results when factors of the clotting cascade are being adsorbed or degraded by the tested biomaterial surface.

Sample (solution, reagent……) preparation

****note: start with thrombin calibrator prep, as it is the most stable one**

1. **Take ice** from the ice machine. The size of box should be more than 20 cm X 20 cm for the convenience.

2. **TGA Plasma Dilution**
    a. Note that every single kit contains 5 vials of TGA plasma
    b. 1 vial has 750ul of undiluted TGA plasma in it
    c. Add 750 ul of Saline to the 750ul of undiluted TGA plasma, so that 1.5 ml of diluted TGA plasma would be ready to use
        i. Note that TGA plasma need to be diluted 2X. Use Saline:Plasma = 1:1 as volumetric ratio.
    d. **Add 750 ul of Saline to the one single vial of TGA plasma, while it is thawing**. Mix gently and **do not shake**. After reconstitution, **diluted TGA plasma should be stored on ice.** TGA plasma should be used within 30 minutes from the time of reconstitution. Calculate the volume of diluted TGA plasma accordingly to the area of biomaterials.
    e. Original ratio should be 60 ul / 0.1 cm^2, but by the experience, it is enough to use **400 ul for 15mm circular sample. It covers all the surface, and barely touch the well wall.**

- Note that now Haemoscan sells the lyophilized TGA plasma. Add 750 ul of DI water (demineralized water) to it, resuspend it gently, then leave it in the room temperature for 5 minutes. Then add 750 ul of saline to dilute.

3. Substrate solution preparation
    a. **Add 2.4 ml of Buffer B** to one single vial of **substrate solution**. Prepare this freshly before use. This is approximately 3 ml and sufficient for 48 wells of a 96-well plate.
    b. Cover it with aluminum foil before use.
    c. Calculate according to your sample numbers and the volume of TGA plasma you are going to use. It is recommended that 7:1 ratio for TGA plasma : substrate solution added at the 96 well plate
    d. No need to be stored at the ice

4. Thrombin Calibrators: **(1) Dilute 20 ul of Thrombin unit stock with 1980 ul of Buffer A**. Be careful not to run out of Buffer A. This vial only contains 11 ml, which is only good for one single run. Not sure if the calibrators could be reused. Prepare calibrators accordingly to the below
    a. Make sure you diluted 20ul of Thrombin unit stock into the 1980 ul of buffer A, as mentioned above
    b. Blank: **only buffer A (usually 1000 ul)**, aliquot 400 ul ////// 0 mU/ml
    c. CAL1: **25 ul** of **dil. Thrombin** + **975 ul** of Buffer A ////// 25 mU/mL

d. CAL2: **50 / 950** ////// 50 mU/ml

e. CAL3: **100 / 900** ////// 100 mU/ml

f. CAL4: **150 / 850** ////// 150 mU/ml

g. CAL5: **200 / 800** ////// 200

h. CAL6: **300 / 700** ////// 300

i. CAL7: **400 / 600** ////// 400

5. Place calibrators on ice until further use
6. **IMPORTANT**
    a. See the General Procedure-4a&b. Since you may not have enough time to do it during the procedure, in case if you have large number of samples, you SHOULD prepare 490 ul of buffers B in every vial before you start. **In short, do 4-b first of all.**

General Procedure

//Prepare the target biomaterial-deposited 24 well plate. Make sure the well is clean and not damaged. : **This is going to be a future assay method once we finalize 2~3 candidate materials. Never mind at the initial run of optimization and screening materials.**

1. Put biomaterials in the 24 well plate. You should make sure they are cleaned. Also preincubate the samples with PBS in order to equilibrate.

2. Before adding TGA plasma to the well, calculate how much **Reagent A+Reagent B** mixture you would need, according to the number of samples. Note that **220 ul per each sample** is required. The ratio of mixture should be **9:1 for A:B**. Make it before step 3, and then incubate it at 37 ºC for 15 min.

3. Add 500 ul of diluted TGA plasma to each well, and then incubate at 37 ºC for 15 min.
    a. The diluted TGA plasma is probably has no platelets in its composition.

4. Prepare 4 vials for one group of material. (SPL1~4 for each)
    a. For example, if you are testing 1) control, 2) reference A, 3) reference B, 4) test material A, 5) test material B, then it means you have 5 groups. In this case you should prepare 5 groups X 4 vials = 20 vials.
    b. **Add 490 ul of Buffer B to every vial**, and then **place them on the ice** immediately.
5. **<u>At t=15 of incubation, add 150 ul of step 2 (450 ul rgt. A + 50 ul rgt. B mixture)</u>** to the well (or vial) of biomaterial immersed in TGA plasma. Mix gently by swirling

6. At t=16,
    a. Mix gently the reaction medium in well (w/ biomaterials) (by pipetting?)

b. **Collect a sample of 10 ul out of the reaction mixture** into the vial labeled SPL1 (with 490 ul of buffer B), vortex and store in ice (t'=1 min). Repeat every 1 minute for the residual SPL2, 3, 4 for each biomaterial.

7. Take **150 ul of calibrators and SPL1,2,3,4 (diluted samples)** for each biomaterials to the 96-well plate. Having same term in between each pipetting is recommended (~10 seconds)
    a. Prepare plate map to assure which well contains what solution

8. **Add 100 ul of diluted substrate solution to each well** to **let thrombin react to the chromopore** (for OD enhance respective to the amount of thrombin generated)

9. Incubate 20 min at 37 ºC

10. **Add 50 ul of stop solution** to each well with same order as did in step 6.

11. Incubate 2 min at 37 ºC

12. Read OD at 405 nm and 540 nm. Measurement height would be 7.5 mm from the bottom. OD measurement should be done within 20 minutes from the time when stop solution was added.
    a. You can use EnSight machine in the Bryers Lab. Contact Elizabeth Leber.

13. Plot the calibration curve from the readout of calibrators, and read the thrombin generated from biomaterials according to the calibration curve.

Kyung-Hoon (Harold/Harry) Kim

Kyunghoon was born in Daejeon, South Korea. He received his BS in Chemical and Biological Engineering with a focus on bioengineering, at Korea University, Seoul. His undergraduate research was system bioengineering, the metabolic pathway engineering study of *Saccharomyces cerevisiae.* Then he entered the Korea Advanced Institute of Science and Technology (KAIST) in Daejeon, for his master's study, in Chemical and Biomolecular Engineering. His master's thesis and project was about the development of integrative microfluidic device for the direct intracellular delivery of biomolecules using zinc-oxide nanowires and disulfide conjugation chemistry, by computer-controlled pneumatic pump system. After graduation, he joined Nanobio Application Team at the Korean National Nanofabrication Center as a senior research scientist, worked for 2 years where he developed a hierarchical nanostructure for pathogen capture and rapid diagnostics. In 2017, he joined UW Bioengineering for his doctoral study, and in 2018 he joined the Buddy Ratner's Biomaterial Group as well as the Center for Dialysis Innovation (CDI), where he initiated the studies of blood compatible biomaterials, including blood-surface interaction in 1) blood protein adsorption, 2) surface platelet activation, 3) intrinsic pathway studies to mitigate the surface thrombogenesis, and 4) assessing the wide range of biomaterials including zwitterionic polymer, RFGD plasma-polymerized polymer, and their surface analysis. Part of these studies were contribution to the orchestrated efforts toward the development of portable kidney dialysis machine (AKTIV: Ambulatory Kidney To Improve the Vitality). Kyunghoon sees and enjoys science as a tool; the methodology to understand the world, which can improve the understanding and insights of scientific phenomena. This instrumentality has been one of his key characteristics that bringing up the unexpected but new discovery. Besides science, he enjoys swing dancing, photography, racket sports, skiing, playing guitar and piano, drawing, writing, reading, and playing/listening music.